EUROPEAN ORGANISATION FOR NUCLEAR RESEARCH (CERN)

Submitted to: JHEP

CERN-EP-2024-128
3rd June 2024

Search for new particles in events with a hadronically decaying W or Z boson and large missing transverse momentum at $\sqrt{s}$ = 13 TeV using the ATLAS detector

The ATLAS Collaboration

A search is presented for new particles produced in proton–proton collisions at a centre-of-mass energy of 13 TeV that result in final states comprising a massive vector (W or Z) boson that decays hadronically and large missing transverse momentum. The data sample was collected with the ATLAS experiment at the Large Hadron Collider from 2015 to 2018 and corresponds to an integrated luminosity of 140 fb^{-1}. No significant excess over the Standard Model expectation is observed. Model-independent 95% confidence-level limits on the visible cross-section that range from 0.3 fb to 79.5 fb are obtained for non-Standard-Model processes. Exclusion limits are also presented for models with axion-like particles, for two-Higgs-doublet models with a pseudo-scalar mediator between the Standard Model and the dark sector, for the invisible decay of the Higgs boson and for pair-produced weakly interacting dark matter candidates.

Contents

1 Introduction

Many astrophysics measurements [1–3] have indicated the presence of a non-baryonic dark matter (DM) component in the Universe, but the nature of such DM, and how it interacts with normal matter, remain unknown. The discovery of DM particles and their interactions with the Standard Model (SM) particles is one of the main quests in particle physics. At the Large Hadron Collider (LHC) [4], DM particles may be produced in proton–proton collisions and would traverse the detector without interacting. The observational signature of these non-interacting DM particles would be a large missing transverse momentum ($E_{\mathrm{T}}^{\mathrm{miss}}$) recoiling against visible SM particles. Searches for DM candidates can be performed in different final states distinguished by the detected SM particle(s) X ($E_{\mathrm{T}}^{\mathrm{miss}} + X$). In this paper, a search for new particles is performed in final states with a hadronically decaying V (W or Z) boson, missing transverse momentum and no leptons ($E_{\mathrm{T}}^{\mathrm{miss}} + V$).

The $E_{\mathrm{T}}^{\mathrm{miss}} + V$ signature can be used to explore new particles proposed in many theories beyond the SM such as axion-like particles, two-Higgs-doublet models with a pseudoscalar mediator between the Standard Model and the dark sector, the invisible decay of the Higgs boson and pair-produced weakly interacting dark matter candidates.

Axion-like particles (ALPs) are weakly interacting pseudo-scalars. Axions were proposed to solve the charge-parity (CP) symmetry problem in QCD interactions through adding a global U(1) symmetry to the SM [5]. The ALPs model is described with an effective field theory (EFT) that extends the SM Lagrangian using effective operators for the interactions between ordinary matter and the ALPs (a) [6]. The new scale associated with the physics of the ALP (an effective scale (f_a)) regulates the dimension-5 operators built from the SM fields and the ALPs. The analysis reported here uses, for the first time, a model with the ALP generated in association with a V boson as illustrated in Figure 1 (a).

Higgs-related DM models can be tested extensively at the LHC energy frontier and are well motivated after the discovery of the Higgs boson by the the ATLAS and CMS Collaborations in 2012 [7, 8]. A

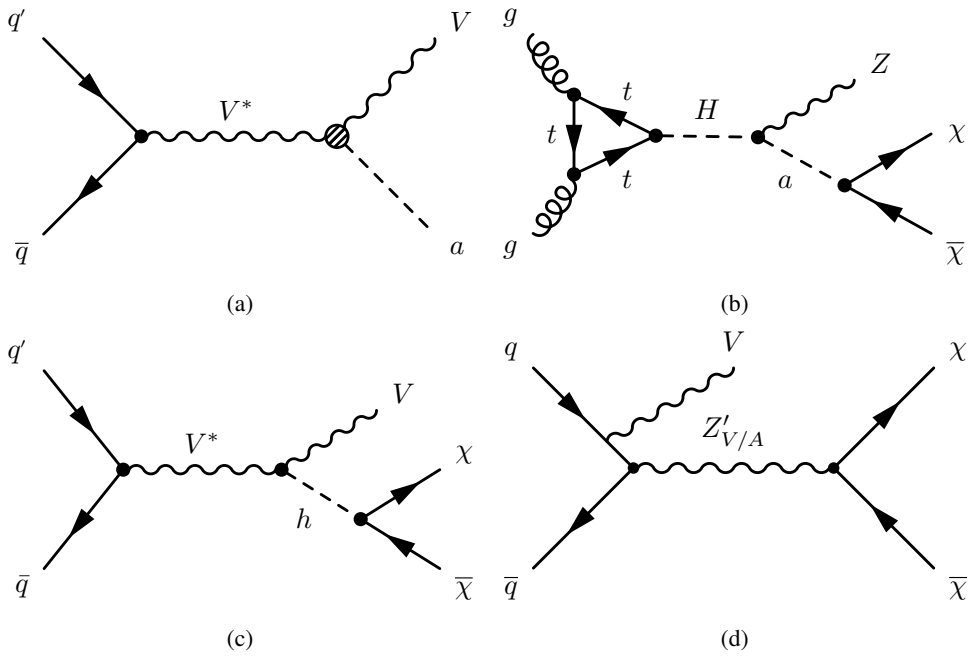

Figure 1: Feynman diagrams for: (a) the production of an ALP a in association with a V boson, (b) the $E_{\mathrm{T}}^{\mathrm{miss}} + Z$ signature production in the 2HDM model with the pseudo-scalar mediator a, (c) the Higgs boson production in association with a V boson in which the Higgs boson decays into DM candidates χ, and (d) the pair production of weakly interacting massive particles χ through a mediator $Z'_{V/A}$ with the emission of a V as initial state radiation.

two-Higgs-doublet model with a pseudo-scalar mediator (2HDM+a) between the SM and the dark sector [9] is hence also explored. In this model, the SM Higgs sector is extended by five physical scalar states in addition to the SM-like Higgs boson h: a scalar (H), pseudo-scalar (A), two charged Higgs bosons ($H^{\pm}$), and the pseudo-scalar mediator (a) that couples to DM particles. The phenomenology of the model is fully determined by 14 independent parameters: the masses of the Higgs bosons (m_H, m_A, and $m_{H^{\pm}}$), the mass of the mediator (m_a), the mass of the DM particle (m_χ), the Yukawa coupling strength between the mediator and the DM particle (g_χ), the electroweak vacuum expectation value (VEV), the ratio of the VEVs of the two Higgs doublets ($\tan\beta$), the mixing angles of the CP-even (α) and CP-odd (θ) weak eigenstates, the quartic coupling (λ_3) of the pure 2HDM potential term and the two quartic couplings of the potential terms connecting the doublet (λ_{P1}) and singlet fields (λ_{P2}). Only the production in association with the Z boson, as shown in Figure 1 (b), is considered for this search, because it can be resonantly produced through the H boson and due to the small interaction cross-section when considering the associated production with the W boson. Results from other ATLAS analyses with complementary final states are combined in Ref. [10].

If kinematically allowed, DM particles may be produced in Higgs boson decays and lead to an invisible final state. In the SM, the Higgs boson decay into undetectable final states occurs via the $ZZ^* \to 4\nu$ process and has a branching fraction below 0.1%. This process can be probed in $E_{\mathrm{T}}^{\mathrm{miss}} + V$ final states through Vh associated production, as shown in Figure 1 (c). In addition, the production of a Higgs boson through gluon–gluon fusion, vector boson fusion and in association with a top-quark pair ($t\bar{t}$) considered in this search to be consistent with the approach of other ATLAS analyses that probe similar models [11]. The most recent experimental results from the ATLAS and CMS Collaborations have set observed (expected) upper limits at 95% confidence level on the branching ratio of the Higgs boson decaying invisibly of 0.107

(0.077) [11] and 0.15 (0.08) [12], respectively.

Weakly interacting massive particles (WIMPs) [13] can naturally produce the right thermal relic density of the universe through the freeze-out mechanism. In this paper, as a minimal extension of the SM, a simplified DM model [14] is used to describe the production of WIMPs through the exchange of a vector boson mediator (Z'_V) or axial-vector boson mediator (Z'_A) in the s-channel. The model postulates a Dirac fermion particle χ and has five free parameters [15]: the mass of the Dirac fermion particle (m_χ), the mediator mass ($m_{Z'}$) and the mediator couplings to quarks (g_q), to all leptons (g_l), and to DM particles (g_χ). In Figure 1 (d) one possible Feynman diagram representing this interaction is shown, where a V boson is radiated in the initial state. The $E_{\mathrm{T}}^{\mathrm{miss}} + X$ signatures have been explored by the ATLAS and CMS Collaborations for the cases where X is a jet [16, 17], photon [18, 19], hadronically decaying V [17, 20] or leptonically decaying Z boson [21, 22], using the proton–proton collision data collected during the LHC Run 2 (2015 – 2018). The ATLAS $E_{\mathrm{T}}^{\mathrm{miss}}$ + jet search sets the strongest bounds in this model, excluding mediator masses up to 2.1 TeV for DM masses of 1 GeV assuming SM initial state radiation production rates.

This paper presents a search for an excess over the SM prediction in the $E_{\mathrm{T}}^{\mathrm{miss}} + V$ signature using proton–proton collision data collected at a centre-of-mass energy of 13 TeV by the ATLAS experiment at the LHC. The data sample corresponds to a total integrated luminosity of 140 fb^{-1} [23], recorded in the period from 2015 to 2018. The sensitivity of this search is enhanced compared with the previous search, which used a partial Run 2 data sample of 36.1 fb^{-1} [20], due to several factors: the increased size of the data and simulated event samples; the use of improved selection criteria for reconstructed objects and reduced associated uncertainties, and improvements in the event selection.

Different analysis strategies are used depending on the boost of the V boson in the final state. At low transverse momentum (p_{T}), the hadrons from the V boson decay can be reconstructed into two well-separated jets with a radius parameter $R = 0.4$ (referred to as the resolved topology). The invariant mass of the dijet system allows discrimination between the dijet background and the resonant decay of a V boson. At higher V transverse momentum, it becomes less likely that the V decay products are identified as individual jets in the resolved topology. In this case, the strategy is based on the identification of large-radius jets in the event, with $R = 1.0$, and the use of jet substructure quantities to select jets with an internal structure consistent with the decay of a W or Z boson (referred to as the merged topology).

The dominant SM background processes considered in this search include $Z(\rightarrow \nu\nu)$+jets, $W(\rightarrow \tau\nu)$+jets with the τ-lepton decaying hadronically or into an unidentified charged lepton and a neutrino, $W(\rightarrow e(\mu)\nu)$+jets where the charged lepton is not identified, $Z(\rightarrow \tau\tau)$+jets with each τ-lepton decaying hadronically or into unidentified charged leptons, $t\bar{t}$ and diboson production. Smaller background processes arise from single top-quark production, triboson production, Higgs boson production in association with a V boson (Vh), $t\bar{t}$ production in association with a vector boson ($t\bar{t}V$), and multijet production. The analysis strategy defines three signal regions and twelve control regions enriched in the dominant background contributions such as V+jets and $t\bar{t}$. A simultaneous likelihood fit in all signal and control regions is used to extract the background and signal estimates using the missing transverse momentum as the discriminating variable. The results are interpreted in the context of ALPs, 2HDM+a, the invisible decay of the Higgs boson and simplified dark matter models.

The paper is organised as follows. A brief introduction to the ATLAS detector is given in Section 2. The data and simulated Monte Carlo samples are described in Section 3. The algorithms for the reconstruction and identification of final state particles are summarized in Section 4. Section 5 describes the criteria for the selection of signal event candidates. The experimental and theoretical systematic uncertainties are

discussed, along with the statistical analysis and results, in Section 6, with their interpretation presented in Section 7. Concluding remarks are given in Section 8.

2 ATLAS detector

The ATLAS detector [24] is a general-purpose detector designed to precisely measure the properties of all particles emerging from proton–proton collisions and covers nearly the entire solid angle around the collision point[1]. It consists of the Inner Detector (ID) surrounded by a thin superconducting solenoid that provides a 2 T axial magnetic field, the calorimeters and the Muon Spectrometer (MS).

The ID system is designed to measure the direction, momentum and charge of electrically charged particles produced in the collisions and to precisely determine the locations of primary and secondary vertices. It has full coverage in a pseudorapidity range $|\eta| < 2.5$ and consists of a silicon pixel detector, a silicon microstrip detector and a transition radiation tracker, arranged in a coaxial geometry around the beam axis. The innermost silicon pixel layer was added to the ID before the start of data-taking in 2015 [25, 26].

The calorimeters lie outside of the ID and measure energies of particles in the pseudorapidity range $|\eta| < 4.9$. The main components of the calorimeter system are the electromagnetic calorimeter, which measures the energy of electrons and photons, and the hadronic calorimeter, which measures energy deposited by hadrons.

The MS is the outermost detector, designed to measure the deflection of muons in a magnetic field generated by three large superconducting toroid magnets with eight coils each. The field integral of the toroids ranges between 2.0 and 6.0 T m across most of the detector. The MS also provides a stand-alone muon trigger. Muons can be measured in the pseudorapidity range $|\eta| < 2.7$, and triggered in the pseudorapidity range $|\eta| < 2.4$.

Events are selected in real-time using a two-level trigger system [27]. The first level provides a hardware-based trigger decision, while the second level makes a trigger decision based on software algorithms.

An extensive software suite [28] is used in data simulation, in the reconstruction and analysis of real and simulated data, in detector operations, and in the trigger and data acquisition systems of the experiment.

3 Data and Monte Carlo simulated events

The analysis uses proton–proton collision data at $\sqrt{s} = 13$ TeV recorded by the ATLAS detector during the data-taking period from 2015 to 2018. Only data in which all subdetectors were functioning well are used. Standard detector quality criteria [29] are applied to reduce the impact of instrumental noise and out-of-time calorimeter energy deposits from cosmic rays and beam backgrounds. The data sample was collected with a bunch crossing interval (bunch spacing) of 25 ns and corresponds to an integrated luminosity of 140 fb^{-1}, with an uncertainty of 0.83% [23], obtained using the LUCID-2 [30] detector

[1] ATLAS uses a right-handed coordinate system with its origin at the nominal interaction point (IP) in the centre of the detector and the z-axis along the beam pipe. The x-axis points from the IP to the centre of the LHC ring, and the y-axis points upwards. Polar coordinates (r, ϕ) are used in the transverse plane, ϕ being the azimuthal angle around the z-axis. The pseudorapidity is defined in terms of the polar angle θ as $\eta = -\ln\tan(\theta/2)$ and is equal to the rapidity $y = \frac{1}{2}\ln\left(\frac{E+p_z c}{E-p_z c}\right)$ in the relativistic limit. Angular distance is measured in units of $\Delta R_y \equiv \sqrt{(\Delta y)^2 + (\Delta\phi)^2}$.

Table 1: The list of the Monte Carlo generators used to simulate the signal and background events.

Process	Matrix element generator	Matrix element PDF	Parton shower and hadronisation	Underlying event model tune	Normalisation order
Signal processes					
Axion-like particles	MadGraph5_aMC@NLO [39]	NNPDF3.0NLO [40]	Pythia 8.235 [41]	A14 [42]	NLO [43]
2HDM with a pseudo-scalar	MadGraph5_aMC@NLO	NNPDF3.0NLO	Pythia 8.306	A14	LO
Invisibly decaying Higgs boson	Powheg-Box v2 [44]	PDF4LHC15NLO [45]	Pythia 8.212	AZNLO [46]	NLO
Simplified Dark Matter model	MadGraph5_aMC@NLO	NNPDF3.0NLO	Pythia 8.235	A14	NLO [43]
Dominant background processes					
Z+jets	Sherpa 2.2.11 [35–37]	NNPDF3.0NNLO	Sherpa 2.2.11	Sherpa Default	NNLO
W+jets	Sherpa 2.2.11	NNPDF3.0NNLO	Sherpa 2.2.11	Sherpa Default	NNLO
$t\bar{t}$	Powheg-Box v2 [44, 47, 48] MadGraph5_aMC@NLO	NNPDF3.0NLO	Pythia 8.230	A14	NNLO+NNLL [49]
Diboson	Sherpa 2.2.1 Sherpa 2.2.2	NNPDF3.0NNLO	Sherpa 2.2.1 Sherpa 2.2.2	Sherpa Default	NLO
Smaller background processes					
Single top-quarks	Powheg-Box v2 [50, 51]	NNPDF3.0NLO	Pythia 8.230	A14	NLO
Triboson	Sherpa 2.2.2	NNPDF3.0NNLO	Sherpa 2.2.2	Sherpa Default	NLO
Vh	Powheg-Box v2	NNPDF3.0NLO	Pythia 8.186	AZNLO	NNLO(QCD)/ NLO (EW)
$t\bar{t}V$	MadGraph5_aMC@NLO	NNPDF3.0NLO	Pythia 8.210	A14	NLO

for the primary luminosity measurements, complemented by measurements using the inner detector and calorimeters.

Monte Carlo (MC) generators are used to simulate the signal and background events needed to compute the detector efficiency and predict the SM background contributions. These samples of events, together with samples generated with alternative generators, are also used to estimate the systematic uncertainties. All simulated event samples were produced with a detailed detector simulation based on the Geant4 [31] package and employed the same particle reconstruction algorithms used on data. Additional proton–proton interactions in the same or neighbouring bunch-crossings (pile-up) were included in the simulation process. These pile-up events were generated using the Pythia 8.186 [32] package with the A3 set of tuned parameters (tune) [33] and the NNPDF2.3LO parton distribution function (PDF) set [34], and are corrected to match the distribution of the average number of interactions per bunch crossing observed in the data. For all simulated event samples, except the samples generated with Sherpa [35–37], the EvtGen 1.2.0 [38] package was used to simulate the decays of b- and c-hadrons. Compared with the previous publication [20], the numbers of simulated events was increased substantially to reduce the statistical uncertainties arising from these samples. A summary of MC samples is shown in Table 1.

Samples of ALP production in association with a V boson are generated by suppressing processes that couple the ALP to photons, gluons or the Higgs boson. The ALP mass is set to 1 MeV and ALP couplings to the V boson ($c_{\tilde{W}}$) up to 1 are considered. Effective scales f_a are explored in the range 1–5 TeV.

The generation of signal samples for 2HDM+a is done separately for the gluon–gluon fusion process and the b-initiated production. The gluon–gluon fusion process is simulated using the 4-flavour scheme, whereas the b-initiated process is calculated using the 5-flavour scheme. The samples are generated using the following parameters: $m_A = m_H = m_{H^\pm}$, $\lambda_{P1} = \lambda_{P2} = \lambda_3 = 3$, $g_\chi = 1$, and in the alignment limit, $\sin(\beta - \alpha) = 1$. The choice of setting $m_H = m_{H^\pm}$ is made to evade the constraints from electroweak precision measurements [9], while the requirement $m_A = m_H$ is introduced to reduce the number of independent model parameters [52]. The nominal samples were produced with $\tan\beta$ of 1 and 10, and $\sin\theta$ of 0.35 and 0.7.

Five benchmark scenarios recommended by the LHC Dark Matter Working Group [52] are used:

- Benchmark scenario 1: 2D scans in the m_a-m_A plane, assuming $\tan\beta = 1.0$ with $\sin\theta = 0.35$ or $\sin\theta = 0.7$,
- Benchmark scenario 2: 2D scans in the m_a-$\tan\beta$ plane, assuming $m_A = 600\,\text{GeV}$ with $\sin\theta = 0.35$ or $\sin\theta = 0.7$,
- Benchmark scenario 3: 2D scans in the m_A-$\tan\beta$ plane, assuming $m_a = 250\,\text{GeV}$ with $\sin\theta = 0.35$ or $\sin\theta = 0.7$,
- Benchmark scenario 4: 1D scans in the $\sin\theta$ range, assuming $\tan\beta = 1.0$ with the fixed masses of $m_A = 600$ (1000) GeV and $m_a = 200$ (350) GeV, and
- Benchmark scenario 5: 1D scan in the m_χ range, assuming $m_A = 1000\,\text{GeV}$, $m_a = 400\,\text{GeV}$, $\tan\beta = 1.0$, and $\sin\theta = 0.35$.

To probe the invisible branching ratio of the Higgs boson, signal samples for all Higgs-boson production modes are generated by forcing the Higgs boson to decay into two Z bosons, which then decay into neutrinos. The Higgs boson mass is set to 125 GeV and the branching ratio to invisible particles is set to 100%. The cross-sections used for the various production processes follow the Higgs cross-section Yellow Report for $m_h = 125\,\text{GeV}$ [53].

The simplified DM model signal samples are generated with vector or axial-vector mediator masses $m_{Z'_{V/A}}$ in the range 100 GeV to 1.7 TeV. The mediator coupling parameters are set to $g_q = 0.25$, $g_l = 0$ and $g_\chi = 1.0$ as recommended by the LHC DM Working Group [54], and the width of the mediator is computed as the minimal width allowed given the couplings and masses. In the on-shell regime, the signal acceptance $\times$ efficiency is constant as a function of the DM mass m_χ for a fixed $m_{Z'_{V/A}}$, and the signal generation is mainly performed for $m_\chi = 1\,\text{GeV}$ which allows a good interpolation of the exclusion limits for other mass points. Signal samples at the diagonal $m_{Z'_{V/A}} = 2m_\chi$ are simulated for each value of $m_{Z'_{V/A}}$ between 100 GeV and 1.2 TeV, and a few additional signal samples are also simulated in the off-shell region of the parameter space with the m_χ and $m_{Z'_{V/A}}$ chosen to be close to the diagonal.

4 Object reconstruction and identification

This section describes the reconstruction and identification of jets and leptons (electrons, muons and τ-leptons) used in the calculation of the missing transverse momentum and the definitions of the signal and control regions. Two types of jets are used to reconstruct the hadronically decaying V boson: small-radius ("small-R") and large-radius ("large-R") jets. Leptons are vetoed in the signal regions, while electrons and muons are used to define the control regions.

Small-R jets are reconstructed by clustering particle-flow objects [55] using the anti-k_t algorithm [56, 57] with a radius parameter $R = 0.4$, and are used to identify a V boson with a relatively low boost. The jets are calibrated using a jet-energy scale derived from $\sqrt{s} = 13\,\text{TeV}$ data and simulation [58]. Small-R jets are required to have transverse momentum $p_\text{T} > 20\,\text{GeV}$ and pseudorapidity $|\eta| < 4.5$ when used in the E_T^miss calculation and $|\eta| < 2.5$ when used in the signal and control regions. Jets with transverse momentum between 20 and 60 GeV and $|\eta| < 2.5$ must satisfy the requirements of the jet vertex tagger (JVT) [59] at the *medium* working point. This suppresses pile-up jets from other proton–proton interactions in the same and neighbouring bunch crossings. Jets containing b-hadrons (b-tagged jets) are identified using the

multivariate b-tagging algorithm (DL1r) [60] with a working point that provides a b-tagging efficiency of 77% on average in simulated $t\bar{t}$ events.

Large-R jets are used for the reconstruction of boosted hadronically decaying vector bosons. These jets are built from topological clusters, which are calibrated to the hadronic scale using the local hadronic cell weighting scheme [61]. They are reconstructed using the anti-k_t algorithm with a radius parameter $R = 1.0$ and groomed with a trimming procedure [62] to reduce the impact of pile-up. The groomed jets are then calibrated to the jet energy scale and jet mass scale following the techniques described in Ref. [63]. Large-R jets are required to satisfy $p_{\mathrm{T}} > 200\,\mathrm{GeV}$ and $|\eta| < 2.0$. In the $E_{\mathrm{T}}^{\mathrm{miss}} + V$ search, the large-R jets are tagged as originating from a hadronic V boson decay using p_{T}-dependent requirements on the jet mass, substructure variable D_2 [64], and number of tracks which are ghost-associated [65] to the ungroomed jet, at a working point with a 50% signal efficiency [66, 67]. Variable-radius track jets [68] are used to identify large-R jets containing b-hadrons and are reconstructed from ID tracks using the anti-k_t algorithm, where only tracks with $p_{\mathrm{T}} > 0.5\,\mathrm{GeV}$ and a longitudinal impact parameter $|z_0 \sin\theta| < 3\,\mathrm{mm}$ are used. The variable-radius track jets are required to satisfy $p_{\mathrm{T}} > 10\,\mathrm{GeV}$ and $|\eta| < 2.5$, and are matched to large-R jets using $\Delta R \equiv \sqrt{\Delta\eta^2 + \Delta\phi^2}$. The DL1r discriminant at the 77% b-tagging efficiency working point is also used for this collection.

Electrons are reconstructed by matching tracks found in the ID to clusters of energy deposited in the electromagnetic calorimeter. They must satisfy the *loose* likelihood criteria with $p_{\mathrm{T}} > 7\,\mathrm{GeV}$ and $|\eta| < 2.47$ [69], with their energy calibrated as described in Ref. [70]. Additional criteria are applied in the control regions defined using electrons; they must satisfy the *medium* likelihood criteria and have a higher threshold of $p_{\mathrm{T}} > 25\,\mathrm{GeV}$. To suppress jets misidentified as electrons, electrons are required to be isolated as defined by two fixed criteria on track- and calorimeter-based isolation variables [71]. The *tight* and *loose* isolation working points are used for electron selection and veto, respectively. In addition, to suppress electrons not originating from the primary vertex, requirements are set on the longitudinal impact parameter, $|z_0 \sin\theta| < 0.5\,\mathrm{mm}$, and the transverse impact parameter significance, $|d_0|/\sigma(d_0) < 5$.

Muons are reconstructed making use of the information from the ID and the MS [72, 73]. All muons must fulfil the *loose* identification criteria with $p_{\mathrm{T}} > 7\,\mathrm{GeV}$ and $|\eta| < 2.7$, and satisfy $|z_0 \sin\theta| < 0.5\,\mathrm{mm}$ and $|d_0|/\sigma(d_0) < 3$. In addition, the muons used to define the control regions must satisfy the *medium* identification working point with $p_{\mathrm{T}} > 25\,\mathrm{GeV}$ and $|\eta| < 2.5$. All muons are required to be isolated using the *loose* working point.

Hadronically decaying τ-lepton candidates are reconstructed by combining information from the ID and calorimeters [74]. The τ-lepton reconstruction algorithm is seeded by reconstructed small-R jets with $p_{\mathrm{T}} > 10\,\mathrm{GeV}$ and $|\eta| < 2.5$, with the reconstructed energies of the τ-lepton candidates corrected to the τ-lepton energy scale [74]. τ-lepton candidates must satisfy the *loose* working point, have $p_{\mathrm{T}} > 20\,\mathrm{GeV}$ and $|\eta| < 2.5$, excluding the transition region between the electromagnetic barrel and endcap calorimeters ($1.37 < |\eta| < 1.52$), and have one or three associated charged tracks.

The ambiguities among objects are resolved by following an overlap removal procedure that uses the geometrical variable ΔR. If two electrons share the same inner-detector track, then only the electron with the higher p_{T} is considered. An electron is rejected if it shares the same inner-detector track with a muon. If a small-R jet and an electron or a τ-lepton have $\Delta R < 0.2$, then the electron or τ-lepton is rejected if the small-R jet is b-tagged; otherwise the overlapping jet is removed. Small-R jets are also discarded if they lie within $\Delta R < 0.2$ of a muon, are not b-tagged and have fewer than three associated tracks with $p_{\mathrm{T}} > 500\,\mathrm{MeV}$. A lepton lying within $\Delta R < 0.4$ of a small-R jet that survived all previous overlap criteria is rejected. If a large-R jet and an electron have $\Delta R < 1.0$, the overlapping jet is removed. A variable-radius

track jet is rejected if a lepton (electron, muon or τ-lepton) lies within the cone defined by its variable radius. Hadronically decaying τ-leptons that lie within $\Delta R < 0.2$ of an electron or muon are rejected, and any remaining jet within $\Delta R < 0.2$ of a hadronically decaying τ-lepton is removed.

The vector missing transverse momentum ($\boldsymbol{E}_{\mathrm{T}}^{\mathbf{miss}}$) is defined as the negative vector sum of the transverse momenta of fully calibrated jets and leptons (electrons, muons and τ-leptons), along with a track soft term [75] that includes other tracks reconstructed in the ID. A closely related quantity, the vector missing transverse momentum with invisible leptons ($\boldsymbol{E}_{\mathrm{T},\ell}^{\mathbf{miss}}$), is defined in the same way but treats leptons as invisible particles. These two quantities are identical for events without leptons. The $E_{\mathrm{T},\ell}^{\mathrm{miss}}$ distribution[2] of V+jets processes that contains a leptonic decay can be used to study the $E_{\mathrm{T}}^{\mathrm{miss}}$ distribution of the V+jet backgrounds in the signal region. In addition, the vector track-based missing transverse momentum ($\boldsymbol{p}_{\mathrm{T}}^{\mathbf{miss}}$) and the vector track-based missing transverse momentum with invisible leptons ($\boldsymbol{p}_{\mathrm{T},\ell}^{\mathbf{miss}}$) follow the same definitions but use only charged tracks.

The definition of $E_{\mathrm{T}}^{\mathrm{miss}}$ significance $\mathcal{S}$ is:

$$\mathcal{S} = \frac{E_{\mathrm{T}}^{\mathrm{miss}}}{[\sigma_L^2(1-\rho_{LT}^2)]^{1/2}}$$

where σ_L^2 is the total standard deviation in the longitudinal direction (parallel to $\boldsymbol{E}_{\mathrm{T}}^{\mathbf{miss}}$), corresponding to the summation of the covariance matrices describing the resolutions of the objects used in the $\boldsymbol{E}_{\mathrm{T}}^{\mathbf{miss}}$ calculation, and ρ_{LT} is the correlation factor of the longitudinal L and transverse T measurements. In this way, $\mathcal{S}$ takes into account the expected resolutions of all the objects that enter the $E_{\mathrm{T}}^{\mathrm{miss}}$ calculation and their directional correlations [76].

5 Event selection

The events considered in this search must satisfy a set of preselection criteria and the requirements of one of the signal regions (SRs) or control regions (CRs).

The selection starts by requiring that the event satisfies one of the unprescaled $E_{\mathrm{T}}^{\mathrm{miss}}$ trigger selections [77] with thresholds between 70 and 110 GeV, depending on the data-taking period, or the lowest unprescaled single electron trigger, depending on the region. The $E_{\mathrm{T}}^{\mathrm{miss}}$ calculation at trigger-level does not include muon information, which is why $E_{\mathrm{T}}^{\mathrm{miss}}$ triggers can be used for signatures containing muons, but not those containing electrons. Data cleaning requirements are applied to reject non-collision backgrounds. Events are required to have a primary vertex with at least two associated tracks with $p_{\mathrm{T}} > 500$ MeV. The hard scatter vertex is selected as the one with the largest sum of the square of the transverse momenta of the associated tracks. To suppress multijet events where significant $E_{\mathrm{T}}^{\mathrm{miss}}$ originates from jet energy mismeasurements in the calorimeters, the azimuthal angles between $\boldsymbol{E}_{\mathrm{T},\ell}^{\mathbf{miss}}$ and all small-R jets (j_i) or $\boldsymbol{p}_{\mathrm{T},\ell}^{\mathbf{miss}}$ need to satisfy $\min_i(\Delta\phi(\boldsymbol{E}_{\mathrm{T},\ell}^{\mathbf{miss}}, j_i)) > 20°$ and $\Delta\phi(\boldsymbol{E}_{\mathrm{T},\ell}^{\mathbf{miss}}, \boldsymbol{p}_{\mathrm{T},\ell}^{\mathbf{miss}}) < 90°$, and $p_{\mathrm{T},\ell}^{\mathrm{miss}}$ must exceed 30 GeV.

The merged topology requires $E_{\mathrm{T},\ell}^{\mathrm{miss}} > 250$ GeV, at least one large-R jet (J) and up to four small-R jets. The upper bound on the number of small-R jets is imposed because this number is expected to be small for the signal models probed. The azimuthal angle between $\boldsymbol{E}_{\mathrm{T},\ell}^{\mathbf{miss}}$ and the leading large-R jet, $\Delta\phi(\boldsymbol{E}_{\mathrm{T},\ell}^{\mathbf{miss}}, J_1)$,

[2] The magnitudes of missing transverse momentum variables are denoted as: $E_{\mathrm{T},\ell}^{\mathrm{miss}} \equiv |\boldsymbol{E}_{\mathrm{T},\ell}^{\mathbf{miss}}|$.

is required to be larger than 120°. To suppress background processes with heavy-flavour jets, events with b-tagged track jets not associated with the leading large-R jet are vetoed. The merged topology event selection is further split into high purity and low purity subsets to enhance the sensitivity, labelled with `MHP` (merged high purity) and `MLP` (merged low purity). Events that satisfy all selection criteria from the V boson tagger for the leading large-R jet are classified into the `MHP` subset. If an event satisfies the requirement on the jet mass but fails the requirements on the substructure variable D_2 or the number of tracks, it is classified into the `MLP` subset.

Events that do not satisfy the merged topology selection are considered for the resolved topology selection. The resolved topology requires $E_{\mathrm{T},\ell}^{\mathrm{miss}} > 200\,\mathrm{GeV}$ and two to four small-R jets, with the leading jet p_{T} larger than 45 GeV and the scalar sum of the transverse momenta of all small-R jets larger than 120 (150) GeV in events with two (more than two) small-R jets. Additionally, the azimuthal angle between $\boldsymbol{E}_{\mathbf{T},\ell}^{\mathbf{miss}}$ and the leading dijet system is required to satisfy $\Delta\phi(\boldsymbol{E}_{\mathbf{T},\ell}^{\mathbf{miss}}, j_1 j_2) > 120°$. To select a dijet system consistent with a hadronic V boson decay, the angles between the two leading small-R jets (j_1, j_2) must satisfy $\Delta\phi(j_1, j_2) < 140°$ and $\Delta R(j_1, j_2) < 1.4$, and the invariant mass of the dijet system must be consistent with a V boson, $65 \leq m_{j_1 j_2} \leq 105\,\mathrm{GeV}$.

In the SRs, a veto is applied on events with electrons, muons or τ-leptons and on events with an $E_{\mathrm{T}}^{\mathrm{miss}}$ significance lower than 8. The signal regions are labelled `SRMHP` for the merged topology with a high purity, `SRMLP` for the merged topology with a low purity, and `SRR` for the resolved topology.

The dominant background contributions, discussed in more details below, are constrained in background-enriched CRs defined using leptons. Four CRs are defined for each SR:

- di-leptonic CRs are required to have two leptons (ee or $\mu\mu$) to estimate the contribution of the Z+jets process, and
- single-leptonic CRs are required to have one muon. They are split using different b-tagged jet multiplicities to distinguish between W+jets and $t\bar{t}$ processes.

The dominant background in the signal regions is Z+jets where the Z boson decays to two neutrinos. This process can be studied using events in which the Z boson decays to muons or electrons. Similarly, irreducible diboson background contributions involving $Z \to \nu\nu$ decays such as $Z(\nu\nu)Z(q\bar{q})$ and $Z(\nu\nu)W(q'\bar{q})$ can be constrained in the di-leptonic CRs through the $Z(ll)V(qq)$ process where the $V(qq)$ decay products fall into the W/Z mass window. The di-leptonic CRs select $Z \to \mu\mu(ee)$ events by requiring exactly two muons (two electrons), an electron (muon) veto and $m_{\mu\mu(ee)} \in [66, 116]$ GeV and are labelled as `CRMHP2mu` (`CRMHP2el`), `CRMLP2mu` (`CRMLP2el`), and `CRR2mu` (`CRR2el`).

The modelling of the $W(\to \mu\nu)$ + jets process is corrected using CRs defined with one muon and zero b-tagged track jets inside the large-R jet (merged) or zero b-tagged small-R jets (resolved) in the merged (labelled as `CRMHP1mu0b` and `CRMLP1mu0b`) and the resolved topologies (labelled as `CRR1mu0b`). These CRs select $W \to \mu\nu$ events by requiring exactly one muon, an electron veto and the transverse mass $m_{\mu\nu}^{\mathrm{T}} \in [30, 100]$ GeV, defined as $m_{\mu\nu}^{\mathrm{T}} = \sqrt{2p_{\mathrm{T}}^{\mu} E_{\mathrm{T}}^{\mathrm{miss}}(1 - \cos(\Delta\phi(\boldsymbol{p}_{\mathbf{T}}^{\boldsymbol{\mu}}, \boldsymbol{E}_{\mathbf{T}}^{\mathbf{miss}})))}$.

The modelling of the $t\bar{t}$ and single top-quark backgrounds is corrected using CRs designed with one muon and at least one b-tagged track jet inside the large-R jet in the merged topology (labelled as `CRMHP1mu1b` and `CRMLP1mu1b`) or at least one b-tagged small-R jet in the resolved topology (labelled as `CRR1mu1b`). They follow the same definition as the previous CRs, except that at least one b-tagged track jet (merged) or at least one b-tagged small-R jet (resolved) is required. The SR and CR selections are summarized in Table 2 for the merged high purity, merged low purity and resolved topologies.

Table 2: Summary of the event selection, with small-R jets (j), large-R jets (J), the number of b-tagged track jets ($n_{b\in J}$) inside the leading large-R jet (J_1), and the number of b-tagged small-R jets (n_b).

	Merged					**Resolved**				
Preselection	Data cleaning Primary vertex with at least two tracks with $p_{\mathrm{T}} > 500\,\mathrm{MeV}$ No τ-leptons $p_{\mathrm{T},\ell}^{\mathrm{miss}} > 30\,\mathrm{GeV}$ $\min_i(\Delta\phi(\boldsymbol{E}_{\mathbf{T},\boldsymbol{\ell}}^{\mathbf{miss}}, j_i)) > 20°$ $\Delta\phi(\boldsymbol{E}_{\mathbf{T},\boldsymbol{\ell}}^{\mathbf{miss}}, \boldsymbol{p}_{\mathbf{T},\boldsymbol{\ell}}^{\mathbf{miss}}) < 90°$									
$\Delta\phi(\boldsymbol{E}_{\mathbf{T},\boldsymbol{\ell}}^{\mathbf{miss}}, V)$	$\Delta\phi(\boldsymbol{E}_{\mathbf{T},\boldsymbol{\ell}}^{\mathbf{miss}}, J_1) > 120°$					$\Delta\phi(\boldsymbol{E}_{\mathbf{T},\boldsymbol{\ell}}^{\mathbf{miss}}, j_1 j_2) > 120°$				
$E_{\mathrm{T},\ell}^{\mathrm{miss}}$	$> 250\,\mathrm{GeV}$					$> 200\,\mathrm{GeV}$				
Jets	$\geq 1J;\ \leq 4j$ $p_{\mathrm{T}}^{J_1} > 200\,\mathrm{GeV}$ b-tagged track jet veto outside J_1					$\geq 2j;\ \leq 4j$ $p_{\mathrm{T}}^{j_1} > 45\,\mathrm{GeV}$ $\sum_i p_{\mathrm{T}}^{j_i} \geq 120\,(150)\,\mathrm{GeV}$ for $2j$ ($\geq 3j$)				
V-tag	**High purity:** mass and substructure **Low purity:** mass and inverted substructure					$\Delta\phi(j_1, j_2) < 140°;\ \Delta R(j_1, j_2) < 1.4$ $m_{j_1 j_2} \in [65, 105]\,\mathrm{GeV}$				
	SR	CR2mu	CR2el	CR1mu0b	CR1mu1b	SR	CR2mu	CR2el	CR1mu0b	CR1mu1b
Trigger	$E_{\mathrm{T}}^{\mathrm{miss}}$	$E_{\mathrm{T}}^{\mathrm{miss}}$	Electron	$E_{\mathrm{T}}^{\mathrm{miss}}$	$E_{\mathrm{T}}^{\mathrm{miss}}$	$E_{\mathrm{T}}^{\mathrm{miss}}$	$E_{\mathrm{T}}^{\mathrm{miss}}$	Electron	$E_{\mathrm{T}}^{\mathrm{miss}}$	$E_{\mathrm{T}}^{\mathrm{miss}}$
e	0	0	2	0	0	0	0	2	0	0
μ	0	2	0	1	1	0	2	0	1	1
$\mathcal{S}$	>8	-	-	-	-	>8	-	-	-	-
$m_{\ell\ell}$ [GeV]	-	$\in [66, 116]$	$\in [66, 116]$	-	-	-	$\in [66, 116]$	$\in [66, 116]$	-	-
$m_{\mu\nu}^{\mathrm{T}}$ [GeV]	-	-	-	$\in [30, 100]$	$\in [30, 100]$	-	-	-	$\in [30, 100]$	$\in [30, 100]$
$n_{b\in J}$	-	-	-	0	≥ 1	-	-	-	-	-
n_b	-	-	-	-	-	-	-	-	0	≥ 1

A set of criteria to suppress the contribution of multijet events is included as mentioned earlier. Due to its low acceptance in the SRs and the challenge of accurately modelling non-Gaussian effects in jet reconstruction and resolution, the residual multijet background in the SRs[3] is estimated using a data-driven approach. A template region enriched in multijets is built by inverting the preselection requirement $\min_i(\Delta\phi(\boldsymbol{E}_{\mathrm{T},\ell}^{\mathbf{miss}}, j_i)) < 20^\circ$. A multijet template of the $E_{\mathrm{T}}^{\mathrm{miss}}$ spectrum for the range $150 < E_{\mathrm{T}}^{\mathrm{miss}} < 600\,\mathrm{GeV}$ is extracted from this sample by subtracting the contribution from other sources of background, as estimated using MC, from data. The normalisation is determined through a fit that uses the V mass upper-sideband region $110 < m_{J/j_1j_2} < 250\,\mathrm{GeV}$ without the $\Delta\phi(\boldsymbol{E}_{\mathrm{T}}^{\mathbf{miss}}, \boldsymbol{p}_{\mathrm{T}}^{\mathbf{miss}}) < 90^\circ$ requirement. The multijet background estimate is small compared with the total MC-based background expectation, and is estimated to be 0.1% in SRMHP, 0.2% in SRMLP and 0.5% in SRR.

6 Statistical analysis, systematic uncertainties and the background-only model results

A binned maximum likelihood fit is used for the background estimation and the interpretation of the results. The fit is performed simultaneously on the $E_{\mathrm{T}}^{\mathrm{miss}}$ distributions in all SRs and on the $E_{\mathrm{T},\ell}^{\mathrm{miss}}$ distributions in all CRs. The fit variable is referred to below as $E_{\mathrm{T},\ell}^{\mathrm{miss}}$ in all regions for simplicity as the two variables are identical in the SRs. The likelihood is built by multiplying the likelihoods obtained in each region:

$$L(\mu, \boldsymbol{\kappa}, \boldsymbol{\theta}) = \prod_r \prod_i \mathrm{Poisson}\left(N_{r,i}^{\mathrm{obs}} \mid N_{r,i}^{\mathrm{sig}}(\mu, \boldsymbol{\theta}) + N_{r,i}^{\mathrm{bkg}}(\boldsymbol{\kappa}, \boldsymbol{\theta})\right) f_{\mathrm{constr}}(\boldsymbol{\theta})$$

where i is the i-th $E_{\mathrm{T},\ell}^{\mathrm{miss}}$ bin considered in the fit, r denotes the regions (SRs and CRs), $N_{r,i}^{\mathrm{obs}}$ is the observed yield in the i-th $E_{\mathrm{T},\ell}^{\mathrm{miss}}$ bin of region r, $N_{r,i}^{\mathrm{sig(bkg)}}$ is the expected yield of the signal (background) in the i-th $E_{\mathrm{T},\ell}^{\mathrm{miss}}$ bin of the region r, $\boldsymbol{\theta}$ is the vector of nuisance parameters including systematic uncertainties in the predicted yield in each region and $E_{\mathrm{T},\ell}^{\mathrm{miss}}$ bin, μ is the scale factor associated with the normalisation of the signal model (signal strength), and $\boldsymbol{\kappa}$ is the vector of the normalisation factors of the main backgrounds (Z+jets, W+jets and $t\bar{t}$). The term f_{constr} represents the product of the Gaussian constraints applied to each of the nuisance parameters. The unconstrainted parameters in the fit are the signal strength μ and the normalisation factors $\boldsymbol{\kappa}$. Separate normalisation factors are assigned to the Z+jets, W+jets and $t\bar{t}$ background normalisations for all three topologies (resolved, merged high purity and merged low purity), resulting in a total of ten normalisation factors, including the signal strength μ. The normalisations of diboson and other electroweak backgrounds are taken from the nominal MC predictions and each is allowed to vary within an assigned uncertainty of 25% [78]. The multijet contributions in the SRs are estimated using a data-driven approach, as described in Section 5.

The uncertainites related to the finite number of simulated events are included using Gaussian constraints in each bin where they are larger than 0.5% of the total number of simulated events in the bin.

As detailed below, systematic uncertainties in the overall normalisation and the $E_{\mathrm{T},\ell}^{\mathrm{miss}}$ shape of the signal and background processes are estimated and implemented in the fit. The systematic uncertainties are correlated across regions and background processes, except the process-specific uncertainties, which are only correlated across regions.

[3] The multijet background in the CRs is negligible.

Experimental uncertainties include the energy scale and resolution of small-R jets [58], large-R jets [63], electrons [70], muons [73] and τ-leptons [74], as well as reconstruction, identification and isolation uncertainties for electrons [71] and muons [72], and pile-up uncertainties for small-R jets [79]. Additional uncertainties regarding the jet mass scale [80] and V-tagging [66, 67] of large-R jets are taken into account, as are b-tagging [81–83] and $E_{\mathrm{T}}^{\mathrm{miss}}$ soft term [75] uncertainties.

Several theoretical modelling uncertainties are considered for the background processes, and affect mostly the shape of the $E_{\mathrm{T},\ell}^{\mathrm{miss}}$ distribution. The uncertainties include the effects from varying QCD renormalisation and factorisation scales, the choice of the PDF set, the variation of the strong coupling constant and the modelling of the parton showers. For V+jets, additional uncertainties from higher-order electroweak corrections and matching scale variation are considered. For $t\bar{t}$, additional uncertainties arise from the A14 tune, hard scatter generation and parton shower matching. For the Wt background, an uncertainty in the scheme to remove overlaps with the $t\bar{t}$ background is included, where *diagram removal* is used for the nominal fit and the difference with *diagram subtraction* [84] is symmetrised and used as the uncertainty. Theoretical uncertainties in the signal yields due to variations of the renormalisation and factorisation scales, uncertainties in the PDFs along with variations of the strong coupling constant, different generator tunes and the modelling of the parton showers, are estimated for all signal models. In addition, the uncertainty in the initial and final state radiation parameters of the parton shower is considered for the invisible decay of the Higgs boson. An uncertainty of 100% in the normalisation of the multijet background is assigned to cover the statistical uncertainty in data, the impact of non-multijet background and the extrapolation from the multijet CR to the SRs.

The impact of a given group of systematic uncertainties on the post-fit signal strength uncertainty is summarised in Table 3. The procedure is done for the invisible Higgs model and one representative point for each of the ALPs, 2HDM+a and simplified DM models together, using Asimov datasets which are constructed as the sum of the background expectations and the respective signal model with a signal strength of $\mu = 1$. The dominant uncertainty groups are those related to large-R jets (which includes the V-tagging uncertainties), muons, V+jets modelling and normalisation (dominated by the diboson normalisation uncertainty). The importance of the uncertainty groups varies for different signal models, depending on the $E_{\mathrm{T}}^{\mathrm{miss}}$ shape of the signal. For example, signals with a harder $E_{\mathrm{T}}^{\mathrm{miss}}$ distribution are more sensitive to V+jets modelling uncertainties and to data statistical uncertainty, since these increase with $E_{\mathrm{T}}^{\mathrm{miss}}$. Lepton uncertainties can also have a large impact as they affect the normalisation factors extracted in the CRs and extrapolated to the SRs.

A background-only fit (μ fixed to zero) including all SRs and CRs is performed and results in the $E_{\mathrm{T},\ell}^{\mathrm{miss}}$ distributions for data and the expected SM backgrounds shown in Figures 2 – 5.

Table 4 shows the best-fit background yields in the SRs from the background-only fit, which reflect the consistency of the background model with the observed data. The normalisation factors of the Z+jets, W+jets, and $t\bar{t}$ backgrounds are listed in Table 5. The $t\bar{t}$ merged high purity normalisation factor is lower than that found in the other regions. This is due to a mismodelling of the number of tracks associated with large-R jets in the $t\bar{t}$ simulation [67]. This mismodelling leads to a smaller (larger) ratio of data versus MC events in the high (low) purity merged regions. Therefore the $t\bar{t}$ merged high (low) purity normalisation factor is found to be below (above) that of the resolved region, which is not affected by this mismodelling. No significant deviation from the SM background expectation is observed in data. Therefore expected and observed upper limits on signal models are presented in the next section.

Table 3: Impact of groups of uncertainties on the post-fit signal strength from a fit to the Asimov dataset with $\mu = 1$. The impact is defined as the square root of the difference between the squares of the total uncertainty and the uncertainty obtained by neglecting the group of systematic uncertainties in question. It is shown for the signal models (a) ALPs with $m_a = 1\,\text{MeV}$, $c_{\tilde{W}} = 0.2$, and $f_a = 3\,\text{TeV}$, (b) 2HDM+a with $\tan\beta = 1$, $\sin\theta = 0.35$, $m_A = 1\,\text{TeV}$, and $m_a = 100\,\text{GeV}$, (c) the invisible decay of the Higgs boson with $\mathcal{B}_{h\to inv}$=100%, and (d) the simplified DM axial-vector model with $m_\chi = 1\,\text{GeV}$ and $m_{Z'_A} = 1\,\text{TeV}$.

Group of uncertainties	Impact on μ uncertainty $\times 100$			
	(a) ALP $c_{\tilde{W}} = 0.2$, $f_a = 3\,\text{TeV}$	(b) 2HDM+a $m_A = 1\,\text{TeV}$ $m_a = 100\,\text{GeV}$	(c) $h \to inv$ $\mathcal{B}_{h\to inv}$=100%	(d) Simplified DM $m_\chi = 1\,\text{GeV}$, $m_{Z'_A} = 1\,\text{TeV}$
Large-R jets	24	13	4	13
Small-R jets	19	6	6	10
b-tagging	2	1	2	1
$E_{\text{T}}^{\text{miss}}$	2	1	4	1
Pile-up	5	2	3	3
Electron	11	4	7	8
Muon	22	7	9	15
τ-lepton	1	<1	<1	<1
Luminosity	2	1	1	1
Normalisation (including $\boldsymbol{\kappa}$)	23	7	7	15
V+jets modelling	32	11	7	18
Diboson modelling	12	4	2	7
$t\bar{t}$ modelling	5	2	1	2
Multijet estimate	1	1	1	1
Single-top modelling	1	1	1	1
Signal modelling	12	1	12	8
Simulated events sample size	23	11	4	11
Statistical	56	20	6	23
Systematic	66	26	19	35
Total	86	33	20	43

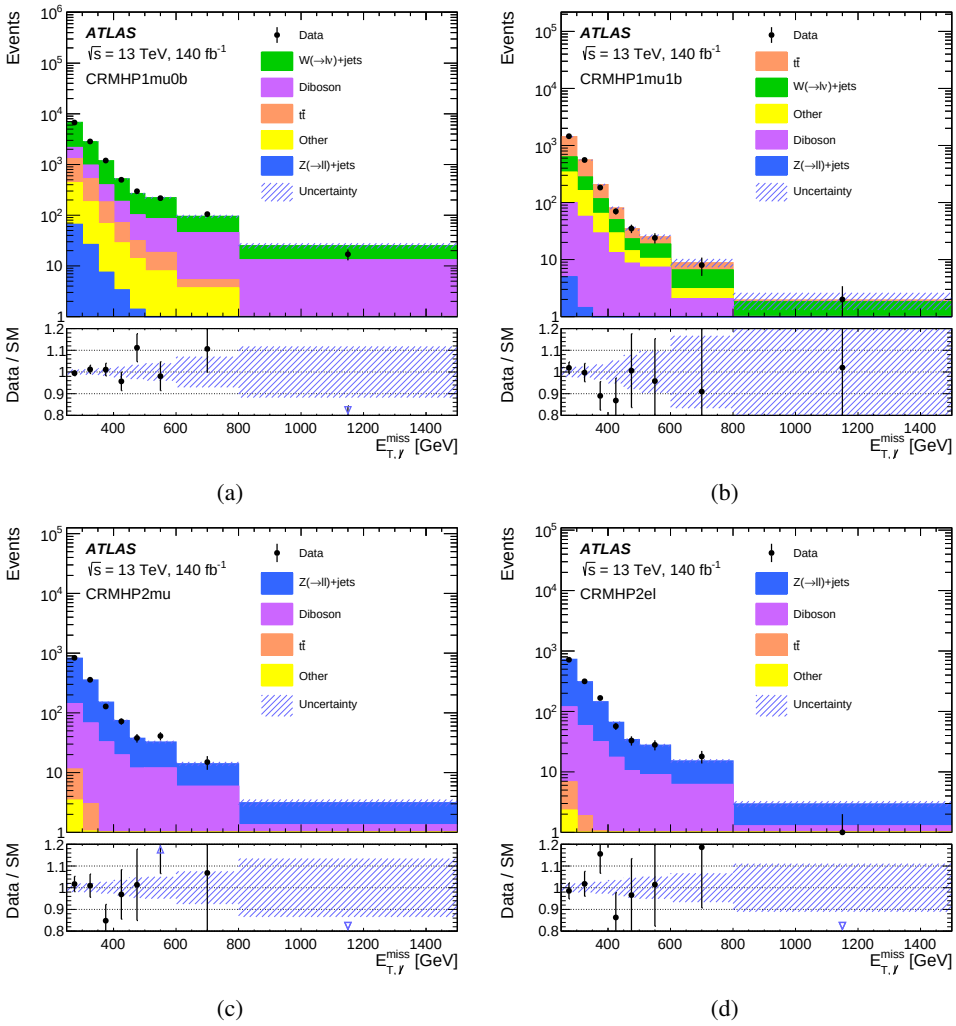

Figure 2: Distribution of $E_{\mathrm{T},\ell}^{\mathrm{miss}}$ after the background-only fit, in the control regions: (a) `CRMHP1mu0b`, (b) `CRMHP1mu1b`, (c) `CRMHP2mu`, and (d) `CRMHP2el`. The total uncertainty in the background is shown as a shaded band and the error bars on the data points represent the statistical uncertainty. Small background contributions such as $t\bar{t}V$, Vh, single-top and triboson processes are grouped into one category and shown as "Other". The last bin contains the overflow.

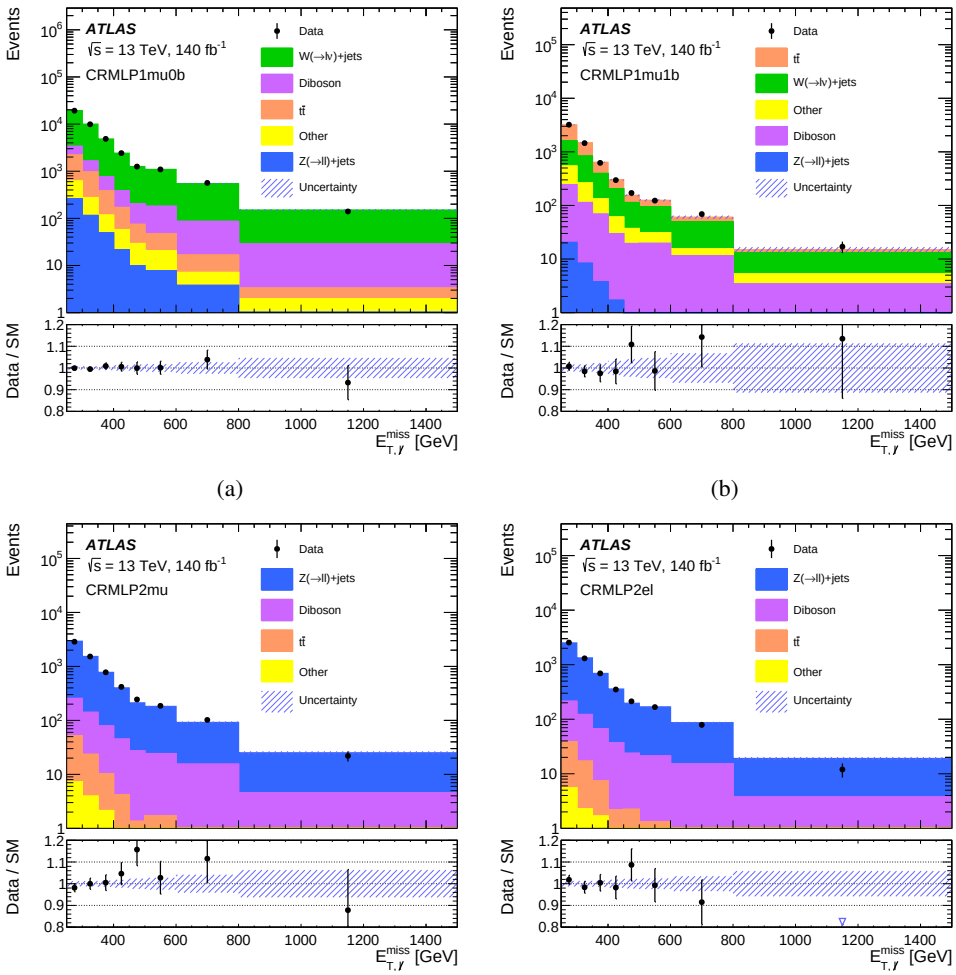

Figure 3: Distribution of $E_{\mathrm{T},\ell}^{\mathrm{miss}}$ after the background-only fit, in the control regions: (a) `CRMLP1mu0b`, (b) `CRMLP1mu1b`, (c) `CRMLP2mu`, and (d) `CRMLP2el`. The total uncertainty in the background is shown as a shaded band and the error bars on the data points represent the statistical uncertainty. Small background contributions such as $t\bar{t}V$, Vh, single-top and triboson processes are grouped into one category and shown as "Other". The last bin contains the overflow.

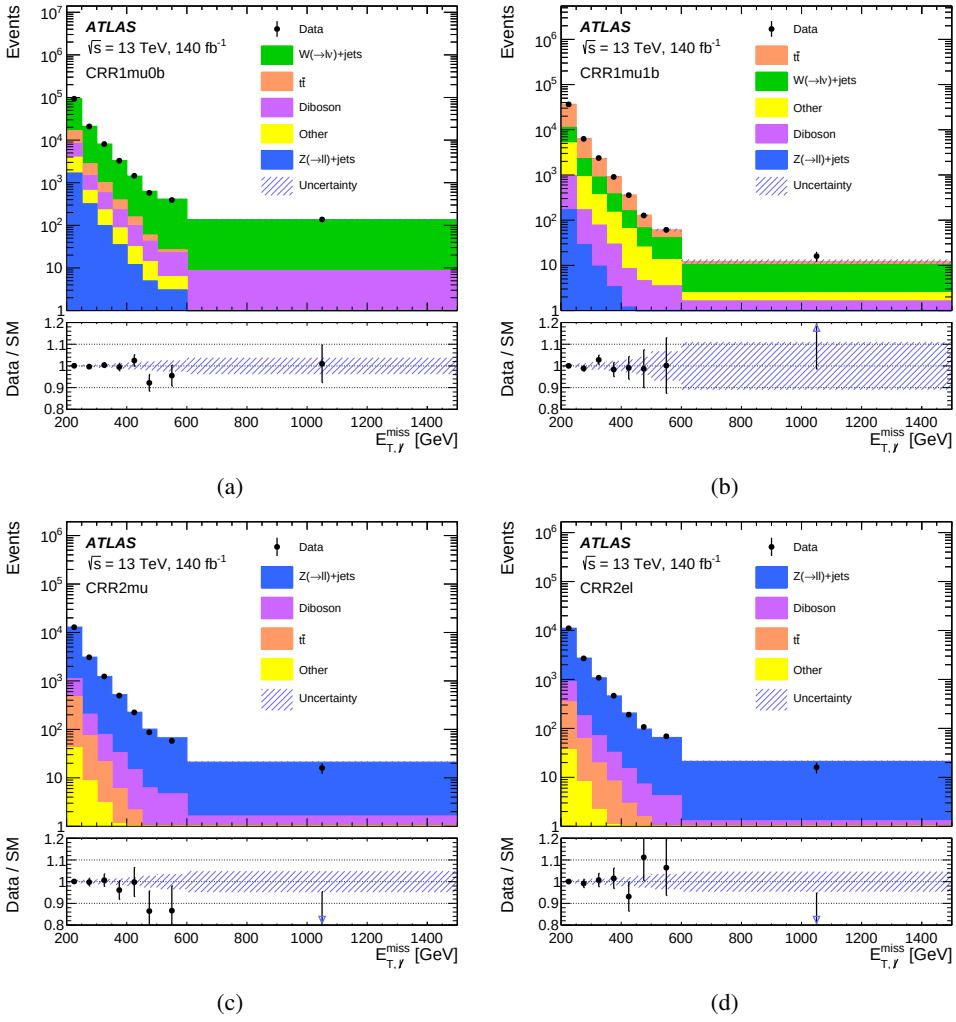

Figure 4: Distribution of $E_{\mathrm{T},\ell}^{\mathrm{miss}}$ after the background-only fit, in the control regions: (a) `CRR1mu0b`, (b) `CRR1mu1b`, (c) `CRR2mu`, and (d) `CRR2el`. The total uncertainty in the background is shown as a shaded band and the error bars on the data points represent the statistical uncertainty. Small background contributions such as $t\bar{t}V$, Vh, single-top and triboson processes are grouped into one category and shown as "Other". The last bin contains the overflow.

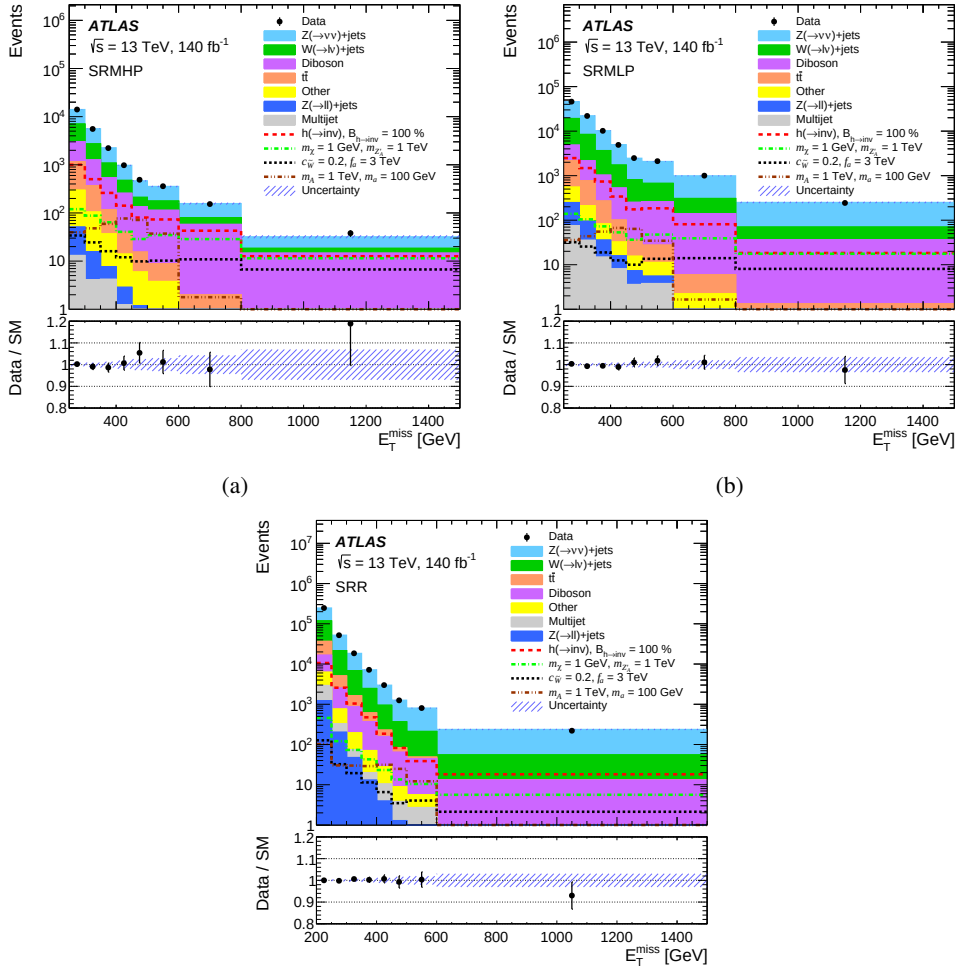

(a) (b)

(c)

Figure 5: Distribution of $E_{\mathrm{T}}^{\mathrm{miss}}$ after the background-only fit, in the signal regions: (a) SRMHP, (b) SRMLP, and (c) SRR. The total uncertainty in the background is shown as a shaded band and the error bars on the data points represent the statistical uncertainty. Small background contributions such as $t\bar{t}V$, Vh, single-top and triboson processes are grouped into one category and shown as "Other". Example signal distributions with their nominal normalisations are shown, from top to bottom: invisible Higgs, simplified DM model with an axial-vector mediator, ALP and 2HDM+a. The last bin contains the overflow.

Table 4: The expected and observed numbers of events shown separately for each signal region. The background yields and uncertainties are shown after the background-only fit to data. The quoted background uncertainties include both statistical and systematic contributions. The uncertainties in the total background can differ from the squared sum of those on individual components due to correlations of nuisance parameters. Small background contributions such as $t\bar{t}V$, Vh, single-top quark and triboson processes are grouped into one category and shown as "Other".

	Signal Regions		
Sample	SRMHP	SRMLP	SRR
$Z(\to \nu\nu)$ + jets	12 200 ± 500	54 100 ± 1200	180 100 ± 2500
$W(\to \ell\nu)$ + jets	6320 ± 330	25 600 ± 700	105 500 ± 2000
Diboson	3700 ± 700	5800 ± 1500	13 100 ± 3000
$t\bar{t}$	1240 ± 130	2470 ± 340	23 600 ± 1300
Other	380 ± 50	490 ± 60	3920 ± 340
$Z(\to \ell\ell)$ + jets	55 ± 6	266 ± 13	1480 ± 40
Multijet	24 ± 18	140 ± 100	1900 ± 1400
Total background	23 870 ± 160	88 880 ± 300	329 500 ± 800
Data	23 861	88 836	329 588

Table 5: The best-fit values of the normalisation factors of the Z+jets, W+jets, and $t\bar{t}$ backgrounds after the background-only fit.

Normalisation factor	Merged high purity	Merged low purity	Resolved
$\kappa_{Z\text{+jets}}$	0.98 ± 0.09	1.03 ± 0.05	0.99 ± 0.05
$\kappa_{W\text{+jets}}$	0.95 ± 0.09	0.93 ± 0.05	0.91 ± 0.05
$\kappa_{t\bar{t}}$	0.68 ± 0.12	1.03 ± 0.21	0.90 ± 0.06

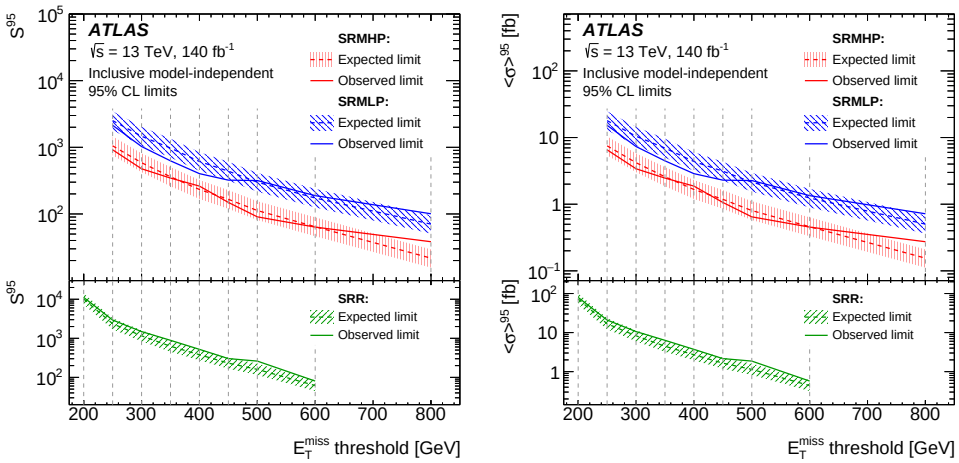

(a) (b)

Figure 6: Observed and expected 95% CL upper limits on (a) the number of signal events, and (b) the visible cross-section for an inclusive model-independent fit. The vertical dashed-grey lines show the starting $E_{\mathrm{T}}^{\mathrm{miss}}$ bin for the range in which the fit is performed.

7 Interpretations of the results

The results are translated into expected and observed upper limits on the presence of new particles using a simultaneous likelihood fit in both the signal and control regions, and the confidence level ($\mathrm{CL_S}$) modified frequentist approach [85].

7.1 Model-independent exclusion limits

The model-independent observed and expected upper limits at 95% CL on the number of signal events, S_{obs}^{95} and S_{exp}^{95}, and on the visible cross-section, $\langle\sigma\rangle_{\mathrm{obs}}^{95}$ and $\langle\sigma\rangle_{\mathrm{exp}}^{95}$, defined as the product of the production cross-section, acceptance and efficiency, $\sigma \times A \times \varepsilon$, are shown in Figure 6. The limits on the visible cross-section are extracted by dividing the 95% CL upper limit on the number of signal events by the integrated luminosity, taking into account the systematic uncertainties in the SM backgrounds and the uncertainty in the integrated luminosity. A fit is performed separately in each SR on the inclusive $E_{\mathrm{T}}^{\mathrm{miss}}$ distribution and is repeated for increasing $E_{\mathrm{T}}^{\mathrm{miss}}$ thresholds indicated by the vertical dashed-grey lines. Values of the visible cross-sections as a function of the $E_{\mathrm{T}}^{\mathrm{miss}}$ threshold that are excluded at 95% CL range from 6.5 to 0.3 fb for SRMHP, from 15.3 to 0.7 fb for SRMLH and from 79.5 to 0.6 fb for SRR.

7.2 Model-dependent exclusion limits

Upper limits at 95% CL are also derived for axion-like particles, the two-Higgs-doublet model with a pseudoscalar, the branching ratio of the Higgs boson to invisible particles, and the simplified DM model with the vector or axial-vector mediator.

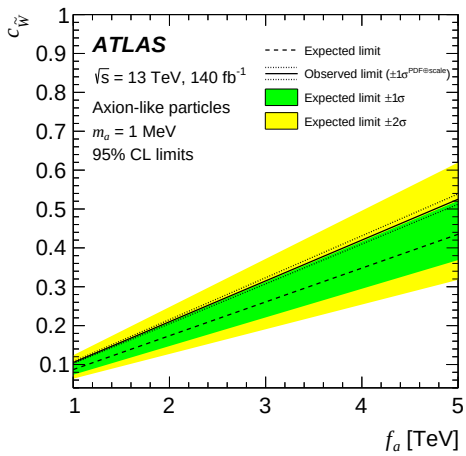

Figure 7: Observed (solid line) and expected (dashed line) exclusion upper limits at 95% CL on the coupling $c_{\tilde{W}}$ as a function of the effective scale f_a for an ALP mass of 1 MeV, with the $\pm1\sigma$ signal theory uncertainties (PDF $\oplus$ scale) in the observed limit and the $\pm1\sigma$ and $\pm2\sigma$ uncertainties in the expected limit (inner and outer shaded bands). The limits are computed with no suppression of events with $\hat{s} > f_a^2$. The area above the line is excluded at 95% CL.

Axion-like particles

In the ALP model, the result is expressed in terms of 95% CL exclusion limits on the model parameters. Figure 7 shows the 95% exclusion contour in the $c_{\tilde{W}}$–f_a plane for a fixed axion mass of 1 MeV. The exclusion limits do not change significantly for axion masses up to at least 1 GeV. Values of the coupling $c_{\tilde{W}}$ above 0.1 are excluded for $f_a = 1$ TeV, and the limit on $c_{\tilde{W}}$ increases linearly with f_a. In terms of the ratio $c_{\tilde{W}}/f_a$, values above 0.11 TeV^{-1} are excluded. The ALP model is an EFT and becomes invalid for $\hat{s} > f_a^2$ (where $\hat{s}$ corresponds to the invariant mass-squared of the partonic collision). The validity of the effective field theory implementation is verified by applying a suppression factor $f_a^4/\hat{s}^2$ [6]. For values of f_a below 2 TeV, the signal yields are reduced by up to 50% for events with $\hat{s} > f_a^2$ when applying this weighting factor. The reduction is about 5% for $f_a = 2$ TeV, while it is negligible for f_a above 3 TeV.

Two-Higgs-doublet model with a pseudoscalar

For the 2HDM+a model, the exclusion limits are derived for all five benchmark scenarios introduced in Section 3. The exclusion contours in the m_A–m_a scans with $\tan\beta = 1.0$ for $\sin\theta = 0.35$ and $\sin\theta = 0.7$, which correspond to Scenario 1 introduced in Section 3, are shown in Figure 8. For $\sin\theta = 0.35$ (0.7), the maximum reach is $m_a = 340$ (420) GeV at $m_A = 900$ GeV, while values between $m_A = 520$ (480) GeV and $m_A = 1100$ (1220) GeV are excluded for $m_a = 100$ GeV.

Figure 9 shows the exclusion limits as a function of $\tan\beta$ and the mass of the pseudo-scalar mediator m_a with $m_A = 600$ GeV for both θ choices: $\sin\theta = 0.35$ and $\sin\theta = 0.7$, which correspond to Scenario 2 introduced in Section 3. This search probes values of m_a up to 195 (270) GeV for $\tan\beta = 0.3$ and $\tan\beta$ up to 12 (2.5) at $m_a = 100$ GeV for $\sin\theta = 0.35$ (0.7).

An exclusion limit is also derived as a function of $\tan\beta$ and the mass of the pseudo-scalar m_A with $m_a = 250$ GeV for both θ choices: $\sin\theta = 0.35$ and $\sin\theta = 0.7$, which correspond to Scenario 3 introduced in Section 3. Figure 10 (a) shows that for $\sin\theta = 0.35$ at $\tan\beta = 20$ masses m_A can be excluded between 600 and 1450 GeV, and for $\tan\beta = 0.3$ between 740 and 1450 GeV as well as a small range around 1.7 TeV.

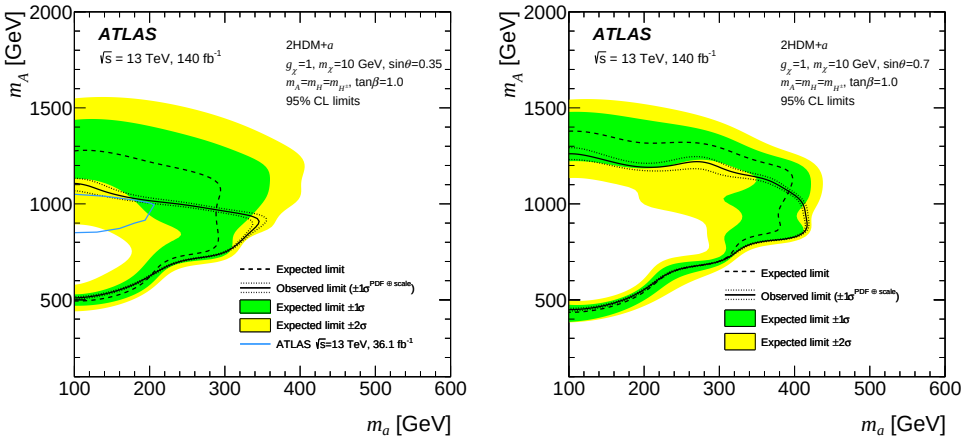

(a) (b)

Figure 8: Observed (solid line) and expected (dashed line) exclusion upper limits at 95% CL in the m_A–m_a plane for the 2HDM+a model, assuming (a) $\sin\theta = 0.35$ and (b) $\sin\theta = 0.7$, with the $\pm1\sigma$ signal theory uncertainties (PDF $\oplus$ scale) in the observed limit and the $\pm1\sigma$ and $\pm2\sigma$ uncertainties in the expected limit (inner and outer shaded bands). The other model parameters are given in the plot legend. The area inside the closed region is excluded at 95% CL. The previous ATLAS observed limit obtained with the $E_{\mathrm{T}}^{\mathrm{miss}} + V$ signature for $\sin\theta = 0.35$ is shown with the lighter solid line [86].

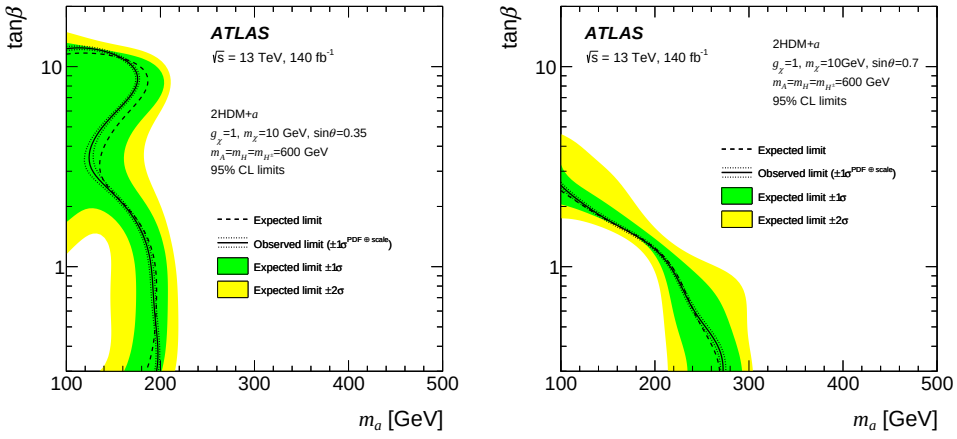

(a) (b)

Figure 9: Observed (solid line) and expected (dashed line) exclusion upper limits at 95% CL in the $\tan\beta$–m_a plane for the 2HDM+a model, assuming (a) $\sin\theta = 0.35$ and (b) $\sin\theta = 0.7$, with the $\pm1\sigma$ signal theory uncertainties (PDF $\oplus$ scale) in the observed limit and the $\pm1\sigma$ and $\pm2\sigma$ uncertainties in the expected limit (inner and outer shaded bands). The other model parameters are given in the plot legend. The area inside the closed region is excluded at 95% CL.

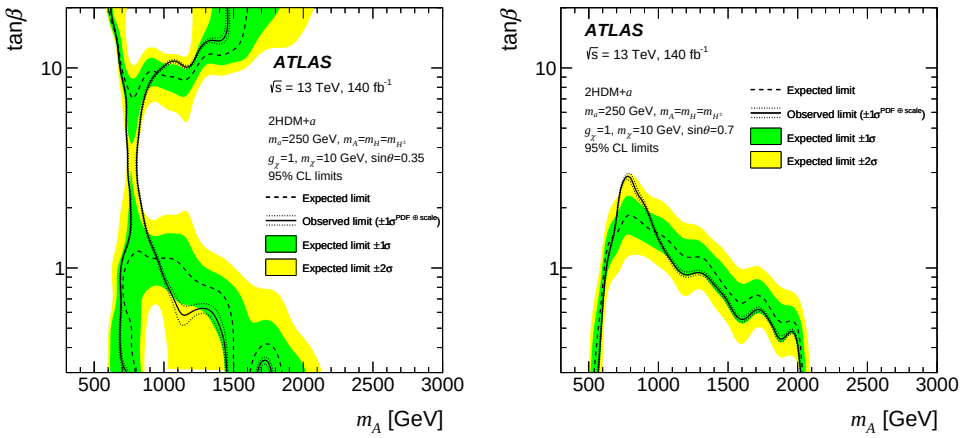

(a) (b)

Figure 10: Observed (solid line) and expected (dashed line) exclusion upper limits at 95% CL in the $\tan\beta$–m_A plane for the 2HDM+a, assuming (a) $\sin\theta = 0.35$ and (b) $\sin\theta = 0.7$, with the $\pm1\sigma$ signal theory uncertainties (PDF $\oplus$ scale) in the observed limit and the $\pm1\sigma$ and $\pm2\sigma$ uncertainties in the expected limit (inner and outer shaded bands). The other model parameters are given on the plots. The area inside the closed region is excluded at 95% CL.

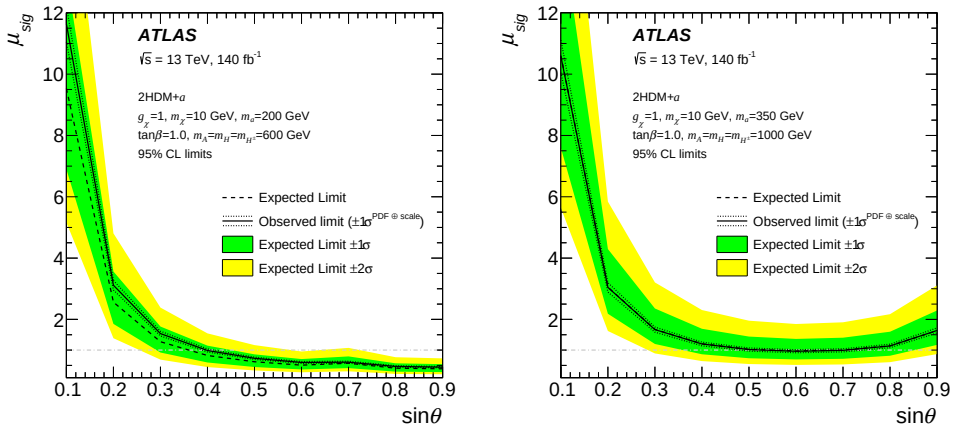

(a) (b)

Figure 11: Observed (solid line) and expected (dashed line) exclusion upper limits on the signal strength μ_{sig} at 95% CL as a function of $\sin\theta$ for the 2HDM+a, with the $\pm1\sigma$ signal theory uncertainties (PDF $\oplus$ scale) in the observed limit and the $\pm1\sigma$ and $\pm2\sigma$ uncertainties in the expected limit (inner and outer shaded bands): (a) the low mass and (b) high mass hypotheses. The model parameters are given on the plots.

The search probes values of m_A in the range between 580 and 2010 GeV at $\tan\beta = 0.3$ for $\sin\theta = 0.7$, as shown in Figure 10 (b).

Figure 11 shows the exclusion limits on the signal strength (μ_{sig}) as a function of $\sin\theta$ for the low mass hypothesis where $m_a = 200\,\text{GeV}$ and $m_A = 600\,\text{GeV}$, and the high mass hypothesis with $m_a = 350\,\text{GeV}$ and $m_A = 1000\,\text{GeV}$, which correspond to Scenario 4 introduced in Section 3. Values down to 0.6 (1.0) of μ_{sig} are excluded for the low (high) mass hypothesis at $\sin\theta = 0.6$.

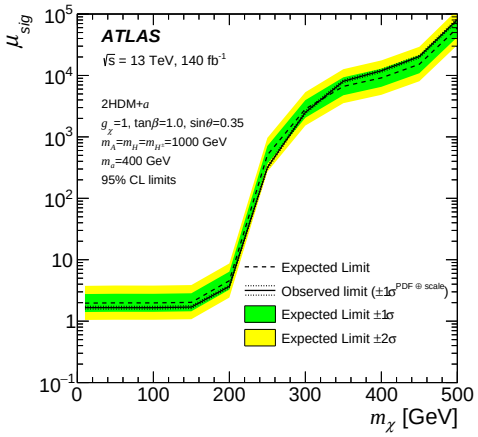

Figure 12: Observed (solid line) and expected (dashed line) exclusion upper limits on the signal strength (μ_{sig}) at 95% CL as a function of m_χ assuming $m_a = 400\,\text{GeV}$, $m_A = 1000\,\text{GeV}$, $\sin\theta = 0.35$ and $\tan\beta = 1.0$, with the $\pm1\sigma$ signal theory uncertainties (PDF $\oplus$ scale) in the observed limit and the $\pm1\sigma$ and $\pm2\sigma$ uncertainties in the expected limit (inner and outer shaded bands).

Table 6: Upper limits at 95% CL on the branching ratio of the Higgs boson decaying invisibly.

Limits on $B_{h\to inv.}$	Expected limit	Observed limit
Merged topology	$0.34^{+0.14}_{-0.09}$	0.38
Resolved topology	$0.54^{+0.23}_{-0.15}$	0.71
Combined	$0.31^{+0.13}_{-0.09}$	0.34

The exclusion limits on μ_{sig} as a function of the DM mass m_χ with $\sin\theta = 0.35$ and $\tan\beta = 1.0$ are shown in Figure 12. The masses of m_a and m_A are fixed to 400 GeV and 1000 GeV, respectively, corresponding to Scenario 5 introduced in Section 3. The result excludes μ_{sig} down to 2.0 for $m_\chi = 100\,\text{GeV}$.

Invisible decaying Higgs boson

In the search for the invisible decay of the Higgs boson, the result is interpreted as a 95% CL upper limit on the branching ratio. The signal yields are dominated by Vh associated production (69.4%) in the SRMHP region. The gluon–gluon fusion production dominates in the SRMLP (65.6%) and SRR (65.2%) regions. As shown in Table 6, an observed (expected) upper limit of 0.34 ($0.31^{+0.13}_{-0.09}$) is obtained at 95% CL on the branching ratio $B_{h\to inv}$. The observed (expected) upper limits are also shown for the merged and resolved topologies obtained by running separate fits only considering the merged and resolved regions, respectively. The merged topology dominates the sensitivity.

Simplified Dark Matter model with a vector or axial-vector mediator

In the simplified DM model with a vector or axial-vector mediator, the exclusion limits on masses of the DM (m_χ) and mediator ($m_{Z'_{V/A}}$) are obtained, assuming Dirac DM with couplings $g_q = 0.25$, $g_\chi = 1.0$ and $g_l = 0$. Figure 13 shows the observed and expected 95% CL exclusion limits for the vector mediator and axial-vector mediator models. The masses of the vector mediator up to 955 GeV are excluded for $m_\chi = 1\,\text{GeV}$. For the axial-vector mediator model, masses up to 965 GeV are excluded for $m_\chi = 1\,\text{GeV}$.

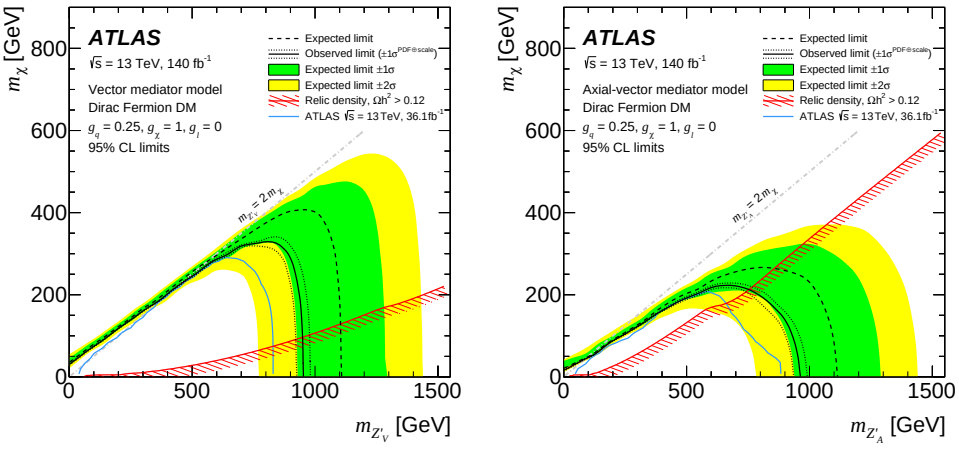

(a) (b)

Figure 13: Exclusion contours at 95% CL on the DM and mediator masses in the simplified DM model with (a) a vector or (b) an axial-vector mediator. The solid (dashed) curve shows the observed (expected) limit, with the $\pm1\sigma$ signal theory uncertainties (PDF $\oplus$ scale) in the observed limit and the $\pm1\sigma$ and $\pm2\sigma$ uncertainties in the expected limit (inner and outer shaded bands). The previous ATLAS observed limit is shown with the lighter solid curve [20, 86]. The hashed curves show the set of points for which the expected relic density is consistent with the Planck and WMAP measurements (i.e. $\Omega h^2 = 0.12$), as computed with MadDM [89]. The area on the hashed side of this curve corresponds to predicted values of the relic density abundance larger than the measured one ($\Omega h^2 > 0.12$).

Both extend the reach of the previous results obtained with an integrated luminosity of 36.1 fb^{-1} [20, 86]. The masses corresponding to the relic density [54] as determined by the Planck [87] and WMAP satellites [88], are also presented which cross the excluded region at $m_{Z'_V} = 950$ GeV and $m_\chi = 97$ GeV for the vector mediator model and $m_{Z'_A} = 750$ GeV and $m_\chi = 210$ GeV for the axial-vector mediator model.

8 Conclusion

A search for new particles has been performed in events with missing transverse momentum and either a large-R jet or a pair of small-R jets compatible with the hadronic decay of a W or Z boson using 140 fb^{-1} of proton–proton collision data at $\sqrt{s} = 13$ TeV recorded with the ATLAS detector at the LHC between 2015 and 2018. In addition to the increased data sample size and the use of improved criteria and reduced uncertainties for reconstructed objects, the analysis implements several improvements in the selection of events, for instance improved b- and V-tagging and the τ-lepton veto, to provide better sensitivity. No significant excess is observed above the expected SM background.

Model-independent upper exclusion limits are derived in the range from 79.5 fb to 0.3 fb at 95% CL for increasing missing transverse momentum thresholds for all the search regions. Exclusion limits are derived for the coupling $c_{\tilde{W}}$ in the ALP model; couplings $c_{\tilde{W}}$ above 0.1 are excluded for $f_a = 1$ TeV. Exclusion limits are also derived for the two-Higgs-doublet model with a pseudo-scalar mediator for all five benchmark scenarios. Masses of the pseudo-scalar mediator m_a are excluded up to 340 (420) GeV for $m_A = 900$ GeV, $\sin\theta = 0.35$ (0.7), and $\tan\beta = 1.0$. The observed upper limit on the branching ratio of the Higgs boson to invisible final states, $B_{h\to inv}$, is found to be 0.34 at 95% CL; the corresponding expected limit is 0.31. The expected limit is a factor of 1.9 better than the previous ATLAS $E_{\mathrm{T}}^{\mathrm{miss}} + V$

search based on 36 fb^{-1}. In the simplified model in which the DM is produced via an s-channel exchange of a vector mediator, mediator masses up to 955 GeV are excluded for a DM mass of 1 GeV and a fixed choice of couplings; in the case of an axial-vector mediator, the exclusion region covers mediator masses up to 965 GeV.

Acknowledgements

We thank CERN for the very successful operation of the LHC and its injectors, as well as the support staff at CERN and at our institutions worldwide without whom ATLAS could not be operated efficiently.

The crucial computing support from all WLCG partners is acknowledged gratefully, in particular from CERN, the ATLAS Tier-1 facilities at TRIUMF/SFU (Canada), NDGF (Denmark, Norway, Sweden), CC-IN2P3 (France), KIT/GridKA (Germany), INFN-CNAF (Italy), NL-T1 (Netherlands), PIC (Spain), RAL (UK) and BNL (USA), the Tier-2 facilities worldwide and large non-WLCG resource providers. Major contributors of computing resources are listed in Ref. [90].

We gratefully acknowledge the support of ANPCyT, Argentina; YerPhI, Armenia; ARC, Australia; BMWFW and FWF, Austria; ANAS, Azerbaijan; CNPq and FAPESP, Brazil; NSERC, NRC and CFI, Canada; CERN; ANID, Chile; CAS, MOST and NSFC, China; Minciencias, Colombia; MEYS CR, Czech Republic; DNRF and DNSRC, Denmark; IN2P3-CNRS and CEA-DRF/IRFU, France; SRNSFG, Georgia; BMBF, HGF and MPG, Germany; GSRI, Greece; RGC and Hong Kong SAR, China; ISF and Benoziyo Center, Israel; INFN, Italy; MEXT and JSPS, Japan; CNRST, Morocco; NWO, Netherlands; RCN, Norway; MNiSW, Poland; FCT, Portugal; MNE/IFA, Romania; MESTD, Serbia; MSSR, Slovakia; ARRS and MIZŠ, Slovenia; DSI/NRF, South Africa; MICINN, Spain; SRC and Wallenberg Foundation, Sweden; SERI, SNSF and Cantons of Bern and Geneva, Switzerland; MOST, Taipei; TENMAK, Türkiye; STFC, United Kingdom; DOE and NSF, United States of America.

Individual groups and members have received support from BCKDF, CANARIE, CRC and DRAC, Canada; CERN-CZ, FORTE and PRIMUS, Czech Republic; COST, ERC, ERDF, Horizon 2020, ICSC-NextGenerationEU and Marie Skłodowska-Curie Actions, European Union; Investissements d'Avenir Labex, Investissements d'Avenir Idex and ANR, France; DFG and AvH Foundation, Germany; Herakleitos, Thales and Aristeia programmes co-financed by EU-ESF and the Greek NSRF, Greece; BSF-NSF and MINERVA, Israel; Norwegian Financial Mechanism 2014-2021, Norway; NCN and NAWA, Poland; La Caixa Banking Foundation, CERCA Programme Generalitat de Catalunya and PROMETEO and GenT Programmes Generalitat Valenciana, Spain; Göran Gustafssons Stiftelse, Sweden; The Royal Society and Leverhulme Trust, United Kingdom.

In addition, individual members wish to acknowledge support from CERN: European Organization for Nuclear Research (CERN PJAS); Chile: Agencia Nacional de Investigación y Desarrollo (FONDECYT 1190886, FONDECYT 1230812, FONDECYT 1230987); China: National Natural Science Foundation of China (NSFC - 12175119, NSFC 12275265, NSFC-12075060); Czech Republic: Czech Science Foundation (GACR - 24-11373S), Ministry of Education Youth and Sports (FORTE CZ.02.01.01/00/22_008/0004632), PRIMUS Research Programme (PRIMUS/21/SCI/017); European Union: European Research Council (ERC - 948254, ERC 101089007), Horizon 2020 Framework Programme (MUCCA - CHIST-ERA-19-XAI-00), European Union, Future Artificial Intelligence Research (FAIR-NextGenerationEU PE00000013), Italian Center for High Performance Computing, Big Data and Quantum Computing (ICSC, NextGenerationEU);

France: Agence Nationale de la Recherche (ANR-20-CE31-0013, ANR-21-CE31-0013, ANR-21-CE31-0022), Investissements d'Avenir Labex (ANR-11-LABX-0012); Germany: Baden-Württemberg Stiftung (BW Stiftung-Postdoc Eliteprogramme), Deutsche Forschungsgemeinschaft (DFG - 469666862, DFG - CR 312/5-2); Italy: Istituto Nazionale di Fisica Nucleare (ICSC, NextGenerationEU); Japan: Japan Society for the Promotion of Science (JSPS KAKENHI JP21H05085, JSPS KAKENHI JP22H01227, JSPS KAKENHI JP22H04944, JSPS KAKENHI JP22KK0227); Netherlands: Netherlands Organisation for Scientific Research (NWO Veni 2020 - VI.Veni.202.179); Norway: Research Council of Norway (RCN-314472); Poland: Polish National Agency for Academic Exchange (PPN/PPO/2020/1/00002/U/00001), Polish National Science Centre (NCN 2021/42/E/ST2/00350, NCN OPUS nr 2022/47/B/ST2/03059, NCN UMO-2019/34/E/ST2/00393, UMO-2020/37/B/ST2/01043, UMO-2021/40/C/ST2/00187, UMO-2022/47/O/ST2/00148, UMO-2023/49/B/ST2/04085); Slovenia: Slovenian Research Agency (ARIS grant J1-3010); Spain: Generalitat Valenciana (Artemisa, FEDER, IDIFEDER/2018/048), Ministry of Science and Innovation (MCIN & NextGenEU PCI2022-135018-2, MICIN & FEDER PID2021-125273NB, RYC2019-028510-I, RYC2020-030254-I, RYC2021-031273-I, RYC2022-038164-I), PROMETEO and GenT Programmes Generalitat Valenciana (CIDEGENT/2019/023, CIDEGENT/2019/027); Sweden: Swedish Research Council (Swedish Research Council 2023-04654, VR 2018-00482, VR 2022-03845, VR 2022-04683, VR 2023-03403, VR grant 2021-03651), Knut and Alice Wallenberg Foundation (KAW 2018.0157, KAW 2018.0458, KAW 2019.0447, KAW 2022.0358); Switzerland: Swiss National Science Foundation (SNSF - PCEFP2_194658); United Kingdom: Leverhulme Trust (Leverhulme Trust RPG-2020-004), Royal Society (NIF-R1-231091); United States of America: U.S. Department of Energy (ECA DE-AC02-76SF00515), Neubauer Family Foundation.

References

[1] G. Bertone, D. Hooper and J. Silk, *Particle dark matter: evidence, candidates and constraints*, Phys. Rept. **405** (2005) 279, arXiv: hep-ph/0404175.

[2] J. L. Feng, *Dark Matter Candidates from Particle Physics and Methods of Detection*, Ann. Rev. Astron. Astrophys. **48** (2010) 495, arXiv: 1003.0904 [astro-ph.CO].

[3] T. A. Porter, R. P. Johnson and P. W. Graham, *Dark Matter Searches with Astroparticle Data*, Ann. Rev. Astron. Astrophys. **49** (2011) 155, arXiv: 1104.2836 [astro-ph.HE].

[4] L. Evans and P. Bryant, *LHC Machine*, JINST **3** (2008) S08001.

[5] R. D. Peccei and H. R. Quinn, CP *Conservation in the Presence of Pseudoparticles*, Phys. Rev. Lett. **38** (1977) 1440.

[6] I. Brivio et al., *ALPs effective field theory and collider signatures*, Eur. Phys. J. C **77** (2017) 572, arXiv: 1701.05379 [hep-ph].

[7] ATLAS Collaboration, *Observation of a new particle in the search for the Standard Model Higgs boson with the ATLAS detector at the LHC*, Phys. Lett. B **716** (2012) 1, arXiv: 1207.7214 [hep-ex].

[8] CMS Collaboration, *Observation of a new boson at a mass of 125 GeV with the CMS experiment at the LHC*, Phys. Lett. B **716** (2012) 30, arXiv: 1207.7235 [hep-ex].

[9] M. Bauer, U. Haisch and F. Kahlhoefer, *Simplified dark matter models with two Higgs doublets: I. Pseudoscalar mediators*, JHEP **05** (2017) 138, arXiv: 1701.07427 [hep-ph].

[10] ATLAS Collaboration, *Combination and summary of ATLAS dark matter searches interpreted in a 2HDM with a pseudo-scalar mediator using* $139\,fb^{-1}$ *of* $\sqrt{s} = 13\,TeV$ pp *collision data*, (2023), arXiv: 2306.00641 [hep-ex].

[11] ATLAS Collaboration, *Combination of searches for invisible decays of the Higgs boson using* $139\,fb^{-1}$ *of proton–proton collision data at* $\sqrt{s} = 13\,TeV$ *collected with the ATLAS experiment*, Phys. Lett. B **842** (2023) 137963, arXiv: 2301.10731 [hep-ex].

[12] CMS Collaboration, *A search for decays of the Higgs boson to invisible particles in events with a top–antitop quark pair or a vector boson in proton–proton collisions at* $\sqrt{s} = 13\,TeV$, Eur. Phys. J. C **83** (2023) 933, arXiv: 2303.01214 [hep-ex].

[13] G. Bertone et al., *Identifying WIMP dark matter from particle and astroparticle data*, JCAP **03** (2018) 026, arXiv: 1712.04793 [hep-ph].

[14] D. Alves et al., *Simplified Models for LHC New Physics Searches*, J. Phys. G **39** (2012) 105005, arXiv: 1105.2838 [hep-ph].

[15] D. Abercrombie et al., *Dark Matter benchmark models for early LHC Run-2 Searches: Report of the ATLAS/CMS Dark Matter Forum*, Physics of the Dark Universe **27** (2020) 100371, arXiv: 1507.00966 [hep-ex].

[16] ATLAS Collaboration, *Search for new phenomena in events with an energetic jet and missing transverse momentum in* pp *collisions at* $\sqrt{s} = 13\,TeV$ *with the ATLAS detector*, Phys. Rev. D **103** (2021) 112006, arXiv: 2102.10874 [hep-ex].

[17] CMS Collaboration, *Search for new particles in events with energetic jets and large missing transverse momentum in proton–proton collisions at* $\sqrt{s} = 13\,TeV$, JHEP **11** (2021) 153, arXiv: 2107.13021 [hep-ex].

[18] ATLAS Collaboration, *Search for dark matter in association with an energetic photon in* pp *collisions at* $\sqrt{s} = 13\,TeV$ *with the ATLAS detector*, JHEP **02** (2021) 226, arXiv: 2011.05259 [hep-ex].

[19] CMS Collaboration, *Search for new physics in final states with a single photon and missing transverse momentum in proton–proton collisions at* $\sqrt{s} = 13\,TeV$, JHEP **02** (2019) 074, arXiv: 1810.00196 [hep-ex].

[20] ATLAS Collaboration, *Search for dark matter in events with a hadronically decaying vector boson and missing transverse momentum in* pp *collisions at* $\sqrt{s} = 13\,TeV$ *with the ATLAS detector*, JHEP **10** (2018) 180, arXiv: 1807.11471 [hep-ex].

[21] ATLAS Collaboration, *Search for associated production of a Z boson with an invisibly decaying Higgs boson or dark matter candidates at* $\sqrt{s} = 13\,TeV$ *with the ATLAS detector*, Phys. Lett. B **829** (2022) 137066, arXiv: 2111.08372 [hep-ex].

[22] CMS Collaboration, *Search for dark matter produced in association with a leptonically decaying Z boson in proton–proton collisions at* $\sqrt{s} = 13\,TeV$, Eur. Phys. J. C **81** (2021) 13, arXiv: 2008.04735 [hep-ex].

[23] ATLAS Collaboration, *Luminosity determination in* pp *collisions at* $\sqrt{s} = 13\,TeV$ *using the ATLAS detector at the LHC*, Eur. Phys. J. C **83** (2023) 982, arXiv: 2212.09379 [hep-ex].

[24] ATLAS Collaboration, *The ATLAS Experiment at the CERN Large Hadron Collider*, JINST **3** (2008) S08003.

[25] ATLAS Collaboration, *ATLAS Insertable B-Layer: Technical Design Report*, ATLAS-TDR-19; CERN-LHCC-2010-013, 2010, URL: https://cds.cern.ch/record/1291633, Addendum: ATLAS-TDR-19-ADD-1; CERN-LHCC-2012-009, 2012, URL: https://cds.cern.ch/record/1451888.

[26] B. Abbott et al., *Production and integration of the ATLAS Insertable B-Layer*, JINST **13** (2018) T05008, arXiv: 1803.00844 [physics.ins-det].

[27] ATLAS Collaboration, *Performance of the ATLAS trigger system in 2015*, Eur. Phys. J. C **77** (2017) 317, arXiv: 1611.09661 [hep-ex].

[28] ATLAS Collaboration, *Software and computing for Run 3 of the ATLAS experiment at the LHC*, (2024), arXiv: 2404.06335 [hep-ex].

[29] ATLAS Collaboration, *ATLAS data quality operations and performance for 2015–2018 data-taking*, JINST **15** (2020) P04003, arXiv: 1911.04632 [physics.ins-det].

[30] G. Avoni et al., *The new LUCID-2 detector for luminosity measurement and monitoring in ATLAS*, JINST **13** (2018) P07017.

[31] S. Agostinelli et al., *GEANT4 – a simulation toolkit*, Nucl. Instrum. Meth. A **506** (2003) 250.

[32] T. Sjöstrand, S. Mrenna and P. Skands, *A brief introduction to PYTHIA 8.1*, Comput. Phys. Commun. **178** (2008) 852, arXiv: 0710.3820 [hep-ph].

[33] ATLAS Collaboration, *The Pythia 8 A3 tune description of ATLAS minimum bias and inelastic measurements incorporating the Donnachie–Landshoff diffractive model*, ATL-PHYS-PUB-2016-017, 2016, URL: https://cds.cern.ch/record/2206965.

[34] NNPDF Collaboration, R. D. Ball et al., *Parton distributions with LHC data*, Nucl. Phys. B **867** (2013) 244, arXiv: 1207.1303 [hep-ph].

[35] T. Gleisberg et al., *Event generation with SHERPA 1.1*, JHEP **02** (2009) 007, arXiv: 0811.4622 [hep-ph].

[36] F. Cascioli, P. Maierhöfer and S. Pozzorini, *Scattering Amplitudes with Open Loops*, Phys. Rev. Lett. **108** (2012) 111601, arXiv: 1111.5206 [hep-ph].

[37] T. Gleisberg and S. Höche, *Comix, a new matrix element generator*, JHEP **12** (2008) 039, arXiv: 0808.3674 [hep-ph].

[38] D. J. Lange, *The EvtGen particle decay simulation package*, Nucl. Instrum. Meth. A **462** (2001) 152.

[39] J. Alwall et al., *The automated computation of tree-level and next-to-leading order differential cross sections, and their matching to parton shower simulations*, JHEP **07** (2014) 079, arXiv: 1405.0301 [hep-ph].

[40] NNPDF Collaboration, R. D. Ball et al., *Parton distributions for the LHC run II*, JHEP **04** (2015) 040, arXiv: 1410.8849 [hep-ph].

[41] T. Sjöstrand et al., *An introduction to PYTHIA 8.2*, Comput. Phys. Commun. **191** (2015) 159, arXiv: 1410.3012 [hep-ph].

[42] ATLAS Collaboration, *ATLAS Pythia 8 tunes to 7 TeV data*, ATL-PHYS-PUB-2014-021, 2014, URL: https://cds.cern.ch/record/1966419.

[43] M. Backović et al., *Higher-order QCD predictions for dark matter production at the LHC in simplified models with s-channel mediators*, Eur. Phys. J. C **75** (2015) 482, arXiv: 1508.05327 [hep-ph].

[44] S. Frixione, G. Ridolfi and P. Nason,
A positive-weight next-to-leading-order Monte Carlo for heavy flavour hadroproduction,
JHEP **09** (2007) 126, arXiv: 0707.3088 [hep-ph].

[45] J. Butterworth et al., *PDF4LHC recommendations for LHC Run II*, J. Phys. G **43** (2016) 023001,
arXiv: 1510.03865 [hep-ph].

[46] ATLAS Collaboration, *Measurement of the Z/γ^* boson transverse momentum distribution in pp collisions at $\sqrt{s} = 7$ TeV with the ATLAS detector*, JHEP **09** (2014) 145,
arXiv: 1406.3660 [hep-ex].

[47] P. Nason, *A new method for combining NLO QCD with shower Monte Carlo algorithms*,
JHEP **11** (2004) 040, arXiv: hep-ph/0409146.

[48] S. Frixione, P. Nason and C. Oleari,
Matching NLO QCD computations with parton shower simulations: the POWHEG method,
JHEP **11** (2007) 070, arXiv: 0709.2092 [hep-ph].

[49] M. Czakon and A. Mitov,
Top++: A program for the calculation of the top-pair cross-section at hadron colliders,
Comput. Phys. Commun. **185** (2014) 2930, arXiv: 1112.5675 [hep-ph].

[50] E. Re, *Single-top Wt-channel production matched with parton showers using the POWHEG method*,
Eur. Phys. J. C **71** (2011) 1547, arXiv: 1009.2450 [hep-ph].

[51] S. Alioli, P. Nason, C. Oleari and E. Re,
NLO single-top production matched with shower in POWHEG: s- and t-channel contributions,
JHEP **09** (2009) 111, arXiv: 0907.4076 [hep-ph], Erratum: JHEP **02** (2010) 011.

[52] T. Abe et al., *LHC Dark Matter Working Group: Next-generation spin-0 dark matter models*,
Physics of the Dark Universe **27** (2020) 100351, arXiv: 1810.09420 [hep-ex].

[53] LHC Higgs Cross Section Working Group,
Handbook of LHC Higgs Cross Sections: 3. Higgs Properties, (2013),
arXiv: 1307.1347 [hep-ph].

[54] A. Boveia et al., *Recommendations on presenting LHC searches for missing transverse energy signals using simplified s-channel models of dark matter*,
Physics of the Dark Universe **27** (2020) 100365, arXiv: 1603.04156 [hep-ex].

[55] ATLAS Collaboration,
Jet reconstruction and performance using particle flow with the ATLAS Detector,
Eur. Phys. J. C **77** (2017) 466, arXiv: 1703.10485 [hep-ex].

[56] M. Cacciari, G. P. Salam and G. Soyez, *The anti-k_t jet clustering algorithm*, JHEP **04** (2008) 063,
arXiv: 0802.1189 [hep-ph].

[57] M. Cacciari, G. P. Salam and G. Soyez, *FastJet user manual*, Eur. Phys. J. C **72** (2012) 1896,
arXiv: 1111.6097 [hep-ph].

[58] ATLAS Collaboration, *Jet energy scale and resolution measured in proton–proton collisions at $\sqrt{s} = 13$ TeV with the ATLAS detector*, Eur. Phys. J. C **81** (2021) 689,
arXiv: 2007.02645 [hep-ex].

[59] ATLAS Collaboration, *Performance of pile-up mitigation techniques for jets in pp collisions at $\sqrt{s} = 8$ TeV using the ATLAS detector*, Eur. Phys. J. C **76** (2016) 581,
arXiv: 1510.03823 [hep-ex].

[60] ATLAS Collaboration, *ATLAS flavour-tagging algorithms for the LHC Run 2 pp collision dataset*, Eur. Phys. J. C **83** (2023) 681, arXiv: 2211.16345 [physics.data-an].

[61] ATLAS Collaboration, *Topological cell clustering in the ATLAS calorimeters and its performance in LHC Run 1*, Eur. Phys. J. C **77** (2017) 490, arXiv: 1603.02934 [hep-ex].

[62] D. Krohn, J. Thaler and L.-T. Wang, *Jet Trimming*, JHEP **02** (2010) 084, arXiv: 0912.1342 [hep-ph].

[63] ATLAS Collaboration, *In situ calibration of large-radius jet energy and mass in 13 TeV proton–proton collisions with the ATLAS detector*, Eur. Phys. J. C **79** (2019) 135, arXiv: 1807.09477 [hep-ex].

[64] A. J. Larkoski, I. Moult and D. Neill, *Power Counting to Better Jet Observables*, JHEP **12** (2014) 009, arXiv: 1409.6298 [hep-ph].

[65] M. Cacciari, G. P. Salam and G. Soyez, *The Catchment Area of Jets*, JHEP **04** (2008) 005, arXiv: 0802.1188 [hep-ph].

[66] ATLAS Collaboration, *Performance of top-quark and W-boson tagging with ATLAS in Run 2 of the LHC*, Eur. Phys. J. C **79** (2019) 375, arXiv: 1808.07858 [hep-ex].

[67] ATLAS Collaboration, *Boosted hadronic vector boson and top quark tagging with ATLAS using Run 2 data*, ATL-PHYS-PUB-2020-017, 2020, URL: https://cds.cern.ch/record/2724149.

[68] ATLAS Collaboration, *Flavor Tagging with Track-Jets in Boosted Topologies with the ATLAS Detector*, ATL-PHYS-PUB-2014-013, 2014, URL: https://cds.cern.ch/record/1750681.

[69] ATLAS Collaboration, *Electron and photon performance measurements with the ATLAS detector using the 2015–2017 LHC proton–proton collision data*, JINST **14** (2019) P12006, arXiv: 1908.00005 [hep-ex].

[70] ATLAS Collaboration, *Electron and photon energy calibration with the ATLAS detector using LHC Run 2 data*, JINST **19** (2023) P02009, arXiv: 2309.05471 [hep-ex].

[71] ATLAS Collaboration, *Electron and photon efficiencies in LHC Run 2 with the ATLAS experiment*, (2023), arXiv: 2308.13362 [hep-ex].

[72] ATLAS Collaboration, *Muon reconstruction and identification efficiency in ATLAS using the full Run 2 pp collision data set at $\sqrt{s} = 13$ TeV*, Eur. Phys. J. C **81** (2021) 578, arXiv: 2012.00578 [hep-ex].

[73] ATLAS Collaboration, *Studies of the muon momentum calibration and performance of the ATLAS detector with pp collisions at $\sqrt{s} = 13$ TeV*, Eur. Phys. J. C **83** (2023) 686, arXiv: 2212.07338 [hep-ex].

[74] ATLAS Collaboration, *Measurement of the tau lepton reconstruction and identification performance in the ATLAS experiment using pp collisions at $\sqrt{s} = 13$ TeV*, ATLAS-CONF-2017-029, 2017, URL: https://cds.cern.ch/record/2261772.

[75] ATLAS Collaboration, *The performance of missing transverse momentum reconstruction and its significance with the ATLAS detector using 140 fb^{-1} of $\sqrt{s} = 13$ TeV pp collisions*, (2024), arXiv: 2402.05858 [hep-ex].

[76] ATLAS Collaboration,
Object-based missing transverse momentum significance in the ATLAS Detector,
ATLAS-CONF-2018-038, 2018, URL: https://cds.cern.ch/record/2630948.

[77] ATLAS Collaboration, *Performance of the missing transverse momentum triggers for the ATLAS detector during Run-2 data taking*, JHEP **08** (2020) 080, arXiv: 2005.09554 [hep-ex].

[78] ATLAS Collaboration, *Evidence for the $H \to b\bar{b}$ decay with the ATLAS detector*,
JHEP **12** (2017) 024, arXiv: 1708.03299 [hep-ex].

[79] ATLAS Collaboration, *Tagging and suppression of pileup jets with the ATLAS detector*,
ATLAS-CONF-2014-018, 2014, URL: https://cds.cern.ch/record/1700870.

[80] ATLAS Collaboration, *Measurement of the ATLAS Detector Jet Mass Response using Forward Folding with 80 fb^{-1} of $\sqrt{s}$ = 13 TeV pp data*, ATLAS-CONF-2020-022, 2020,
URL: https://cds.cern.ch/record/2724442.

[81] ATLAS Collaboration, *ATLAS b-jet identification performance and efficiency measurement with $t\bar{t}$ events in pp collisions at $\sqrt{s}$ = 13 TeV*, Eur. Phys. J. C **79** (2019) 970,
arXiv: 1907.05120 [hep-ex].

[82] ATLAS Collaboration,
Calibration of the light-flavour jet mistagging efficiency of the b-tagging algorithms with Z+jets events using 139 fb^{-1} of ATLAS proton–proton collision data at $\sqrt{s}$ = 13 TeV,
Eur. Phys. J. C **83** (2023) 728, arXiv: 2301.06319 [hep-ex].

[83] ATLAS Collaboration, *Measurement of the c-jet mistagging efficiency in $t\bar{t}$ events using pp collision data at $\sqrt{s}$ = 13 TeV collected with the ATLAS detector*, Eur. Phys. J. C **82** (2022) 95,
arXiv: 2109.10627 [hep-ex].

[84] S. Frixione, E. Laenen, P. Motylinski, C. White and B. R. Webber,
Single-top hadroproduction in association with a W boson, JHEP **07** (2008) 029,
arXiv: 0805.3067 [hep-ph].

[85] A. L. Read, *Presentation of search results: the CL_S technique*, J. Phys. G **28** (2002) 2693.

[86] ATLAS Collaboration, *Constraints on mediator-based dark matter and scalar dark energy models using $\sqrt{s}$ = 13 TeV pp collision data collected by the ATLAS detector*, JHEP **05** (2019) 142,
arXiv: 1903.01400 [hep-ex].

[87] Planck Collaboration, *Planck 2018 results - VI. Cosmological parameters*, A&A **641** (2020) A6,
arXiv: 1807.06209 [astro-ph.CO], Erratum: A&A **652** (2021) C4.

[88] Hinshaw, G. et al., *Nine-year Wilkinson Microwave Anisotropy Probe (WMAP) Observations: Cosmological Parameter Results*, Astrophys. J. Suppl. **208** (2013) 19,
arXiv: 1212.5226 [astro-ph.CO].

[89] M. Backović, A. Martini, O. Mattelaer, K. Kong and G. Mohlabeng,
Direct detection of dark matter with MadDM v.2.0, Physics of the Dark Universe **9-10** (2015) 37,
arXiv: 1505.04190 [hep-ph].

[90] ATLAS Collaboration, *ATLAS Computing Acknowledgements*, ATL-SOFT-PUB-2023-001, 2023,
URL: https://cds.cern.ch/record/2869272.

The ATLAS Collaboration

G. Aad [104], E. Aakvaag [17], B. Abbott [123], S. Abdelhameed [119a], K. Abeling [56], N.J. Abicht [50], S.H. Abidi [30], M. Aboelela [45], A. Aboulhorma [36e], H. Abramowicz [154], H. Abreu [153], Y. Abulaiti [120], B.S. Acharya [70a,70b,k], A. Ackermann [64a], C. Adam Bourdarios [4], L. Adamczyk [87a], S.V. Addepalli [27], M.J. Addison [103], J. Adelman [118], A. Adiguzel [22c], T. Adye [137], A.A. Affolder [139], Y. Afik [40], M.N. Agaras [13], J. Agarwala [74a,74b], A. Aggarwal [102], C. Agheorghiesei [28c], F. Ahmadov [39,x], W.S. Ahmed [106], S. Ahuja [97], X. Ai [63e], G. Aielli [77a,77b], A. Aikot [166], M. Ait Tamlihat [36e], B. Aitbenchikh [36a], M. Akbiyik [102], T.P.A. Åkesson [100], A.V. Akimov [38], D. Akiyama [171], N.N. Akolkar [25], S. Aktas [22a], K. Al Khoury [42], G.L. Alberghi [24b], J. Albert [168], P. Albicocco [54], G.L. Albouy [61], S. Alderweireldt [53], Z.L. Alegria [124], M. Aleksa [37], I.N. Aleksandrov [39], C. Alexa [28b], T. Alexopoulos [10], F. Alfonsi [24b], M. Algren [57], M. Alhroob [170], B. Ali [135], H.M.J. Ali [93], S. Ali [32], S.W. Alibocus [94], M. Aliev [34c], G. Alimonti [72a], W. Alkakhi [56], C. Allaire [67], B.M.M. Allbrooke [149], J.F. Allen [53], C.A. Allendes Flores [140f], P.P. Allport [21], A. Aloisio [73a,73b], F. Alonso [92], C. Alpigiani [141], Z.M.K. Alsolami [93], M. Alvarez Estevez [101], A. Alvarez Fernandez [102], M. Alves Cardoso [57], M.G. Alviggi [73a,73b], M. Aly [103], Y. Amaral Coutinho [84b], A. Ambler [106], C. Amelung[37], M. Amerl [103], C.G. Ames [111], D. Amidei [108], K.J. Amirie [158], S.P. Amor Dos Santos [133a], K.R. Amos [166], S. An[85], V. Ananiev [128], C. Anastopoulos [142], T. Andeen [11], J.K. Anders [37], A.C. Anderson [60], S.Y. Andrean [48a,48b], A. Andreazza [72a,72b], S. Angelidakis [9], A. Angerami [42], A.V. Anisenkov [38], A. Annovi [75a], C. Antel [57], E. Antipov [148], M. Antonelli [54], F. Anulli [76a], M. Aoki [85], T. Aoki [156], M.A. Aparo [149], L. Aperio Bella [49], C. Appelt [19], A. Apyan [27], S.J. Arbiol Val [88], C. Arcangeletti [54], A.T.H. Arce [52], E. Arena [94], J-F. Arguin [110], S. Argyropoulos [55], J.-H. Arling [49], O. Arnaez [4], H. Arnold [148], G. Artoni [76a,76b], H. Asada [113], K. Asai [121], S. Asai [156], N.A. Asbah [37], R.A. Ashby Pickering [170], K. Assamagan [30], R. Astalos [29a], K.S.V. Astrand [100], S. Atashi [162], R.J. Atkin [34a], M. Atkinson[165], H. Atmani[36f], P.A. Atmasiddha [131], K. Augsten [135], S. Auricchio [73a,73b], A.D. Auriol [21], V.A. Austrup [103], G. Avolio [37], K. Axiotis [57], G. Azuelos [110,ac], D. Babal [29b], H. Bachacou [138], K. Bachas [155,o], A. Bachiu [35], F. Backman [48a,48b], A. Badea [40], T.M. Baer [108], P. Bagnaia [76a,76b], M. Bahmani [19], D. Bahner [55], K. Bai [126], J.T. Baines [137], L. Baines [96], O.K. Baker [175], E. Bakos [16], D. Bakshi Gupta [8], L.E. Balabram Filho [84b], V. Balakrishnan [123], R. Balasubramanian [117], E.M. Baldin [38], P. Balek [87a], E. Ballabene [24b,24a], F. Balli [138], L.M. Baltes [64a], W.K. Balunas [33], J. Balz [102], I. Bamwidhi [119b], E. Banas [88], M. Bandieramonte [132], A. Bandyopadhyay [25], S. Bansal [25], L. Barak [154], M. Barakat [49], E.L. Barberio [107], D. Barberis [58b,58a], M. Barbero [104], M.Z. Barel [117], K.N. Barends [34a], T. Barillari [112], M-S. Barisits [37], T. Barklow [146], P. Baron [125], D.A. Baron Moreno [103], A. Baroncelli [63a], G. Barone [30], A.J. Barr [129], J.D. Barr [98], F. Barreiro [101], J. Barreiro Guimarães da Costa [14], U. Barron [154], M.G. Barros Teixeira [133a], S. Barsov [38], F. Bartels [64a], R. Bartoldus [146], A.E. Barton [93], P. Bartos [29a], A. Basan [102], M. Baselga [50], A. Bassalat [67,b], M.J. Basso [159a], S. Bataju [45], R. Bate [167], R.L. Bates [60], S. Batlamous[101], B. Batool [144], M. Battaglia [139], D. Battulga [19], M. Bauce [76a,76b], M. Bauer [80], P. Bauer [25], L.T. Bazzano Hurrell [31], J.B. Beacham [52], T. Beau [130], J.Y. Beaucamp [92], P.H. Beauchemin [161], P. Bechtle [25], H.P. Beck [20,n], K. Becker [170], A.J. Beddall [83], V.A. Bednyakov [39], C.P. Bee [148], L.J. Beemster [16], T.A. Beermann [37], M. Begalli [84d], M. Begel [30], A. Behera [148], J.K. Behr [49], J.F. Beirer [37], F. Beisiegel [25], M. Belfkir [119b], G. Bella [154], L. Bellagamba [24b], A. Bellerive [35], P. Bellos [21], K. Beloborodov [38],

D. Benchekroun [36a], F. Bendebba [36a], Y. Benhammou [154], K.C. Benkendorfer [62], L. Beresford [49], M. Beretta [54], E. Bergeaas Kuutmann [164], N. Berger [4], B. Bergmann [135], J. Beringer [18a], G. Bernardi [5], C. Bernius [146], F.U. Bernlochner [25], F. Bernon [37,104], A. Berrocal Guardia [13], T. Berry [97], P. Berta [136], A. Berthold [51], S. Bethke [112], A. Betti [76a,76b], A.J. Bevan [96], N.K. Bhalla [55], S. Bhatta [148], D.S. Bhattacharya [169], P. Bhattarai [146], K.D. Bhide [55], V.S. Bhopatkar [124], R.M. Bianchi [132], G. Bianco [24b,24a], O. Biebel [111], R. Bielski [126], M. Biglietti [78a], C.S. Billingsley [45], M. Bindi [56], A. Bingul [22b], C. Bini [76a,76b], A. Biondini [94], G.A. Bird [33], M. Birman [172], M. Biros [136], S. Biryukov [149], T. Bisanz [50], E. Bisceglie [44b,44a], J.P. Biswal [137], D. Biswas [144], I. Bloch [49], A. Blue [60], U. Blumenschein [96], J. Blumenthal [102], V.S. Bobrovnikov [38], M. Boehler [55], B. Boehm [169], D. Bogavac [37], A.G. Bogdanchikov [38], C. Bohm [48a], V. Boisvert [97], P. Bokan [37], T. Bold [87a], M. Bomben [5], M. Bona [96], M. Boonekamp [138], C.D. Booth [97], A.G. Borbély [60], I.S. Bordulev [38], H.M. Borecka-Bielska [110], G. Borissov [93], D. Bortoletto [129], D. Boscherini [24b], M. Bosman [13], J.D. Bossio Sola [37], K. Bouaouda [36a], N. Bouchhar [166], L. Boudet [4], J. Boudreau [132], E.V. Bouhova-Thacker [93], D. Boumediene [41], R. Bouquet [58b,58a], A. Boveia [122], J. Boyd [37], D. Boye [30], I.R. Boyko [39], L. Bozianu [57], J. Bracinik [21], N. Brahimi [4], G. Brandt [174], O. Brandt [33], F. Braren [49], B. Brau [105], J.E. Brau [126], R. Brener [172], L. Brenner [117], R. Brenner [164], S. Bressler [172], G. Brianti [79a,79b], D. Britton [60], D. Britzger [112], I. Brock [25], G. Brooijmans [42], E.M. Brooks [159b], E. Brost [30], L.M. Brown [168], L.E. Bruce [62], T.L. Bruckler [129], P.A. Bruckman de Renstrom [88], B. Brüers [49], A. Bruni [24b], G. Bruni [24b], M. Bruschi [24b], N. Bruscino [76a,76b], T. Buanes [17], Q. Buat [141], D. Buchin [112], A.G. Buckley [60], O. Bulekov [38], B.A. Bullard [146], S. Burdin [94], C.D. Burgard [50], A.M. Burger [37], B. Burghgrave [8], O. Burlayenko [55], J. Burleson [165], J.T.P. Burr [33], J.C. Burzynski [145], E.L. Busch [42], V. Büscher [102], P.J. Bussey [60], J.M. Butler [26], C.M. Buttar [60], J.M. Butterworth [98], W. Buttinger [137], C.J. Buxo Vazquez [109], A.R. Buzykaev [38], S. Cabrera Urbán [166], L. Cadamuro [67], D. Caforio [59], H. Cai [132], Y. Cai [14,114c], Y. Cai [114a], V.M.M. Cairo [37], O. Cakir [3a], N. Calace [37], P. Calafiura [18a], G. Calderini [130], P. Calfayan [69], G. Callea [60], L.P. Caloba [84b], D. Calvet [41], S. Calvet [41], M. Calvetti [75a,75b], R. Camacho Toro [130], S. Camarda [37], D. Camarero Munoz [27], P. Camarri [77a,77b], M.T. Camerlingo [73a,73b], D. Cameron [37], C. Camincher [168], M. Campanelli [98], A. Camplani [43], V. Canale [73a,73b], A.C. Canbay [3a], E. Canonero [97], J. Cantero [166], Y. Cao [165], F. Capocasa [27], M. Capua [44b,44a], A. Carbone [72a,72b], R. Cardarelli [77a], J.C.J. Cardenas [8], G. Carducci [44b,44a], T. Carli [37], G. Carlino [73a], J.I. Carlotto [13], B.T. Carlson [132,p], E.M. Carlson [168,159a], J. Carmignani [94], L. Carminati [72a,72b], A. Carnelli [138], M. Carnesale [76a,76b], S. Caron [116], E. Carquin [140f], S. Carrá [72a], G. Carratta [24b,24a], A.M. Carroll [126], T.M. Carter [53], M.P. Casado [13,h], M. Caspar [49], F.L. Castillo [4], L. Castillo Garcia [13], V. Castillo Gimenez [166], N.F. Castro [133a,133e], A. Catinaccio [37], J.R. Catmore [128], T. Cavaliere [4], V. Cavaliere [30], N. Cavalli [24b,24a], L.J. Caviedes Betancourt [23b], Y.C. Cekmecelioglu [49], E. Celebi [83], S. Cella [37], F. Celli [129], M.S. Centonze [71a,71b], V. Cepaitis [57], K. Cerny [125], A.S. Cerqueira [84a], A. Cerri [149], L. Cerrito [77a,77b], F. Cerutti [18a], B. Cervato [144], A. Cervelli [24b], G. Cesarini [54], S.A. Cetin [83], D. Chakraborty [118], J. Chan [18a], W.Y. Chan [156], J.D. Chapman [33], E. Chapon [138], B. Chargeishvili [152b], D.G. Charlton [21], M. Chatterjee [20], C. Chauhan [136], Y. Che [114a], S. Chekanov [6], S.V. Chekulaev [159a], G.A. Chelkov [39,a], A. Chen [108], B. Chen [154], B. Chen [168], H. Chen [114a], H. Chen [30], J. Chen [63c], J. Chen [145], M. Chen [129], S. Chen [156], S.J. Chen [114a], X. Chen [63c,138], X. Chen [15,ab], Y. Chen [63a], C.L. Cheng [173], H.C. Cheng [65a], S. Cheong [146], A. Cheplakov [39], E. Cheremushkina [49], E. Cherepanova [117], R. Cherkaoui El Moursli [36e], E. Cheu [7], K. Cheung [66], L. Chevalier [138], V. Chiarella [54], G. Chiarelli [75a], N. Chiedde [104], G. Chiodini [71a], A.S. Chisholm [21], A. Chitan [28b], M. Chitishvili [166], M.V. Chizhov [39],

K. Choi [11], Y. Chou [141], E.Y.S. Chow [116], K.L. Chu [172], M.C. Chu [65a], X. Chu [14,114c], Z. Chubinidze [54], J. Chudoba [134], J.J. Chwastowski [88], D. Cieri [112], K.M. Ciesla [87a], V. Cindro [95], A. Ciocio [18a], F. Cirotto [73a,73b], Z.H. Citron [172], M. Citterio [72a], D.A. Ciubotaru[28b], A. Clark [57], P.J. Clark [53], N. Clarke Hall [98], C. Clarry [158], J.M. Clavijo Columbie [49], S.E. Clawson [49], C. Clement [48a,48b], Y. Coadou [104], M. Cobal [70a,70c], A. Coccaro [58b], R.F. Coelho Barrue [133a], R. Coelho Lopes De Sa [105], S. Coelli [72a], B. Cole [42], J. Collot [61], P. Conde Muiño [133a,133g], M.P. Connell [34c], S.H. Connell [34c], E.I. Conroy [129], F. Conventi [73a,ad], H.G. Cooke [21], A.M. Cooper-Sarkar [129], F.A. Corchia [24b,24a], A. Cordeiro Oudot Choi [130], L.D. Corpe [41], M. Corradi [76a,76b], F. Corriveau [106,v], A. Cortes-Gonzalez [19], M.J. Costa [166], F. Costanza [4], D. Costanzo [142], B.M. Cote [122], J. Couthures [4], G. Cowan [97], K. Cranmer [173], D. Cremonini [24b,24a], S. Crépé-Renaudin [61], F. Crescioli [130], M. Cristinziani [144], M. Cristoforetti [79a,79b], V. Croft [117], J.E. Crosby [124], G. Crosetti [44b,44a], A. Cueto [101], H. Cui [98], Z. Cui [7], W.R. Cunningham [60], F. Curcio [166], J.R. Curran [53], P. Czodrowski [37], M.M. Czurylo [37], M.J. Da Cunha Sargedas De Sousa [58b,58a], J.V. Da Fonseca Pinto [84b], C. Da Via [103], W. Dabrowski [87a], T. Dado [50], S. Dahbi [151], T. Dai [108], D. Dal Santo [20], C. Dallapiccola [105], M. Dam [43], G. D'amen [30], V. D'Amico [111], J. Damp [102], J.R. Dandoy [35], D. Dannheim [37], M. Danninger [145], V. Dao [148], G. Darbo [58b], S.J. Das [30,ae], F. Dattola [49], S. D'Auria [72a,72b], A. D'avanzo [73a,73b], C. David [34a], T. Davidek [136], I. Dawson [96], H.A. Day-hall [135], K. De [8], R. De Asmundis [73a], N. De Biase [49], S. De Castro [24b,24a], N. De Groot [116], P. de Jong [117], H. De la Torre [118], A. De Maria [114a], A. De Salvo [76a], U. De Sanctis [77a,77b], F. De Santis [71a,71b], A. De Santo [149], J.B. De Vivie De Regie [61], D.V. Dedovich[39], J. Degens [94], A.M. Deiana [45], F. Del Corso [24b,24a], J. Del Peso [101], F. Del Rio [64a], L. Delagrange [130], F. Deliot [138], C.M. Delitzsch [50], M. Della Pietra [73a,73b], D. Della Volpe [57], A. Dell'Acqua [37], L. Dell'Asta [72a,72b], M. Delmastro [4], P.A. Delsart [61], S. Demers [175], M. Demichev [39], S.P. Denisov [38], L. D'Eramo [41], D. Derendarz [88], F. Derue [130], P. Dervan [94], K. Desch [25], C. Deutsch [25], F.A. Di Bello [58b,58a], A. Di Ciaccio [77a,77b], L. Di Ciaccio [4], A. Di Domenico [76a,76b], C. Di Donato [73a,73b], A. Di Girolamo [37], G. Di Gregorio [37], A. Di Luca [79a,79b], B. Di Micco [78a,78b], R. Di Nardo [78a,78b], K.F. Di Petrillo [40], M. Diamantopoulou [35], F.A. Dias [117], T. Dias Do Vale [145], M.A. Diaz [140a,140b], F.G. Diaz Capriles [25], A.R. Didenko[39], M. Didenko [166], E.B. Diehl [108], S. Díez Cornell [49], C. Diez Pardos [144], C. Dimitriadi [164], A. Dimitrievska [21], J. Dingfelder [25], T. Dingley [129], I-M. Dinu [28b], S.J. Dittmeier [64b], F. Dittus [37], M. Divisek [136], F. Djama [104], T. Djobava [152b], C. Doglioni [103,100], A. Dohnalova [29a], J. Dolejsi [136], Z. Dolezal [136], K. Domijan [87a], K.M. Dona [40], M. Donadelli [84d], B. Dong [109], J. Donini [41], A. D'Onofrio [73a,73b], M. D'Onofrio [94], J. Dopke [137], A. Doria [73a], N. Dos Santos Fernandes [133a], P. Dougan [103], M.T. Dova [92], A.T. Doyle [60], M.A. Draguet [129], E. Dreyer [172], I. Drivas-koulouris [10], M. Drnevich [120], M. Drozdova [57], D. Du [63a], T.A. du Pree [117], F. Dubinin [38], M. Dubovsky [29a], E. Duchovni [172], G. Duckeck [111], O.A. Ducu [28b], D. Duda [53], A. Dudarev [37], E.R. Duden [27], M. D'uffizi [103], L. Duflot [67], M. Dührssen [37], I. Duminica [28g], A.E. Dumitriu [28b], M. Dunford [64a], S. Dungs [50], K. Dunne [48a,48b], A. Duperrin [104], H. Duran Yildiz [3a], M. Düren [59], A. Durglishvili [152b], B.L. Dwyer [118], G.I. Dyckes [18a], M. Dyndal [87a], B.S. Dziedzic [37], Z.O. Earnshaw [149], G.H. Eberwein [129], B. Eckerova [29a], S. Eggebrecht [56], E. Egidio Purcino De Souza [130], L.F. Ehrke [57], G. Eigen [17], K. Einsweiler [18a], T. Ekelof [164], P.A. Ekman [100], S. El Farkh [36b], Y. El Ghazali [36b], H. El Jarrari [37], A. El Moussaouy [36a], V. Ellajosyula [164], M. Ellert [164], F. Ellinghaus [174], N. Ellis [37], J. Elmsheuser [30], M. Elsawy [119a], M. Elsing [37], D. Emeliyanov [137], Y. Enari [156], I. Ene [18a], S. Epari [13], P.A. Erland [88], D. Ernani Martins Neto [88], M. Errenst [174], M. Escalier [67], C. Escobar [166], E. Etzion [154],

G. Evans[133a], H. Evans[69], L.S. Evans[97], A. Ezhilov[38], S. Ezzarqtouni[36a], F. Fabbri[24b,24a], L. Fabbri[24b,24a], G. Facini[98], V. Fadeyev[139], R.M. Fakhrutdinov[38], D. Fakoudis[102], S. Falciano[76a], L.F. Falda Ulhoa Coelho[37], F. Fallavollita[112], G. Falsetti[44b,44a], J. Faltova[136], C. Fan[165], Y. Fan[14], Y. Fang[14,114c], M. Fanti[72a,72b], M. Faraj[70a,70b], Z. Farazpay[99], A. Farbin[8], A. Farilla[78a], T. Farooque[109], S.M. Farrington[53], F. Fassi[36e], D. Fassouliotis[9], M. Faucci Giannelli[77a,77b], W.J. Fawcett[33], L. Fayard[67], P. Federic[136], P. Federicova[134], O.L. Fedin[38,a], M. Feickert[173], L. Feligioni[104], D.E. Fellers[126], C. Feng[63b], M. Feng[15], Z. Feng[117], M.J. Fenton[162], L. Ferencz[49], R.A.M. Ferguson[93], S.I. Fernandez Luengo[140f], P. Fernandez Martinez[13], M.J.V. Fernoux[104], J. Ferrando[93], A. Ferrari[164], P. Ferrari[117,116], R. Ferrari[74a], D. Ferrere[57], C. Ferretti[108], D. Fiacco[76a,76b], F. Fiedler[102], P. Fiedler[135], A. Filipčič[95], E.K. Filmer[1], F. Filthaut[116], M.C.N. Fiolhais[133a,133c,c], L. Fiorini[166], W.C. Fisher[109], T. Fitschen[103], P.M. Fitzhugh[138], I. Fleck[144], P. Fleischmann[108], T. Flick[174], M. Flores[34d,z], L.R. Flores Castillo[65a], L. Flores Sanz De Acedo[37], F.M. Follega[79a,79b], N. Fomin[33], J.H. Foo[158], A. Formica[138], A.C. Forti[103], E. Fortin[37], A.W. Fortman[18a], M.G. Foti[18a], L. Fountas[9,i], D. Fournier[67], H. Fox[93], P. Francavilla[75a,75b], S. Francescato[62], S. Franchellucci[57], M. Franchini[24b,24a], S. Franchino[64a], D. Francis[37], L. Franco[116], V. Franco Lima[37], L. Franconi[49], M. Franklin[62], G. Frattari[27], Y.Y. Frid[154], J. Friend[60], N. Fritzsche[51], A. Froch[55], D. Froidevaux[37], J.A. Frost[129], Y. Fu[63a], S. Fuenzalida Garrido[140f], M. Fujimoto[104], K.Y. Fung[65a], E. Furtado De Simas Filho[84e], M. Furukawa[156], J. Fuster[166], A. Gaa[56], A. Gabrielli[24b,24a], A. Gabrielli[158], P. Gadow[37], G. Gagliardi[58b,58a], L.G. Gagnon[18a], S. Gaid[163], S. Galantzan[154], E.J. Gallas[129], B.J. Gallop[137], K.K. Gan[122], S. Ganguly[156], Y. Gao[53], F.M. Garay Walls[140a,140b], B. Garcia[30], C. García[166], A. Garcia Alonso[117], A.G. Garcia Caffaro[175], J.E. García Navarro[166], M. Garcia-Sciveres[18a], G.L. Gardner[131], R.W. Gardner[40], N. Garelli[161], D. Garg[81], R.B. Garg[146], J.M. Gargan[53], C.A. Garner[158], C.M. Garvey[34a], V.K. Gassmann[161], G. Gaudio[74a], V. Gautam[13], P. Gauzzi[76a,76b], J. Gavranovic[95], I.L. Gavrilenko[38], A. Gavrilyuk[38], C. Gay[167], G. Gaycken[126], E.N. Gazis[10], A.A. Geanta[28b], C.M. Gee[139], A. Gekow[122], C. Gemme[58b], M.H. Genest[61], A.D. Gentry[115], S. George[97], W.F. George[21], T. Geralis[47], P. Gessinger-Befurt[37], M.E. Geyik[174], M. Ghani[170], K. Ghorbanian[96], A. Ghosal[144], A. Ghosh[162], A. Ghosh[7], B. Giacobbe[24b], S. Giagu[76a,76b], T. Giani[117], A. Giannini[63a], S.M. Gibson[97], M. Gignac[139], D.T. Gil[87b], A.K. Gilbert[87a], B.J. Gilbert[42], D. Gillberg[35], G. Gilles[117], L. Ginabat[130], D.M. Gingrich[2,ac], M.P. Giordani[70a,70c], P.F. Giraud[138], G. Giugliarelli[70a,70c], D. Giugni[72a], F. Giuli[37], I. Gkialas[9,i], L.K. Gladilin[38], C. Glasman[101], G.R. Gledhill[126], G. Glemža[49], M. Glisic[126], I. Gnesi[44b,e], Y. Go[30], M. Goblirsch-Kolb[37], B. Gocke[50], D. Godin[110], B. Gokturk[22a], S. Goldfarb[107], T. Golling[57], M.G.D. Gololo[34g], D. Golubkov[38], J.P. Gombas[109], A. Gomes[133a,133b], G. Gomes Da Silva[144], A.J. Gomez Delegido[166], R. Gonçalo[133a], L. Gonella[21], A. Gongadze[152c], F. Gonnella[21], J.L. Gonski[146], R.Y. González Andana[53], S. González de la Hoz[166], R. Gonzalez Lopez[94], C. Gonzalez Renteria[18a], M.V. Gonzalez Rodrigues[49], R. Gonzalez Suarez[164], S. Gonzalez-Sevilla[57], L. Goossens[37], B. Gorini[37], E. Gorini[71a,71b], A. Gorišek[95], T.C. Gosart[131], A.T. Goshaw[52], M.I. Gostkin[39], S. Goswami[124], C.A. Gottardo[37], S.A. Gotz[111], M. Gouighri[36b], V. Goumarre[49], A.G. Goussiou[141], N. Govender[34c], I. Grabowska-Bold[87a], K. Graham[35], E. Gramstad[128], S. Grancagnolo[71a,71b], C.M. Grant[1,138], P.M. Gravila[28f], F.G. Gravili[71a,71b], H.M. Gray[18a], M. Greco[71a,71b], M.J. Green[1], C. Grefe[25], A.S. Grefsrud[17], I.M. Gregor[49], K.T. Greif[162], P. Grenier[146], S.G. Grewe[112], A.A. Grillo[139], K. Grimm[32], S. Grinstein[13,r], J.-F. Grivaz[67], E. Gross[172], J. Grosse-Knetter[56], J.C. Grundy[129], L. Guan[108], J.G.R. Guerrero Rojas[166], G. Guerrieri[70a,70c], R. Gugel[102],

J.A.M. Guhit[108], A. Guida[19], E. Guilloton[170], S. Guindon[37], F. Guo[14,114c], J. Guo[63c], L. Guo[49], Y. Guo[108], R. Gupta[132], S. Gurbuz[25], S.S. Gurdasani[55], G. Gustavino[76a,76b], P. Gutierrez[123], L.F. Gutierrez Zagazeta[131], M. Gutsche[51], C. Gutschow[98], C. Gwenlan[129], C.B. Gwilliam[94], E.S. Haaland[128], A. Haas[120], M. Habedank[49], C. Haber[18a], H.K. Hadavand[8], A. Hadef[51], S. Hadzic[112], A.I. Hagan[93], J.J. Hahn[144], E.H. Haines[98], M. Haleem[169], J. Haley[124], J.J. Hall[142], G.D. Hallewell[104], L. Halser[20], K. Hamano[168], M. Hamer[25], G.N. Hamity[53], E.J. Hampshire[97], J. Han[63b], K. Han[63a], L. Han[114a], L. Han[63a], S. Han[18a], Y.F. Han[158], K. Hanagaki[85], M. Hance[139], D.A. Hangal[42], H. Hanif[145], M.D. Hank[131], J.B. Hansen[43], P.H. Hansen[43], K. Hara[160], D. Harada[57], T. Harenberg[174], S. Harkusha[38], M.L. Harris[105], Y.T. Harris[129], J. Harrison[13], N.M. Harrison[122], P.F. Harrison[170], N.M. Hartman[112], N.M. Hartmann[111], R.Z. Hasan[97,137], Y. Hasegawa[143], S. Hassan[17], R. Hauser[109], C.M. Hawkes[21], R.J. Hawkings[37], Y. Hayashi[156], S. Hayashida[113], D. Hayden[109], C. Hayes[108], R.L. Hayes[117], C.P. Hays[129], J.M. Hays[96], H.S. Hayward[94], F. He[63a], M. He[14,114c], Y. He[157], Y. He[49], Y. He[98], N.B. Heatley[96], V. Hedberg[100], A.L. Heggelund[128], N.D. Hehir[96,*], C. Heidegger[55], K.K. Heidegger[55], J. Heilman[35], S. Heim[49], T. Heim[18a], J.G. Heinlein[131], J.J. Heinrich[126], L. Heinrich[112,aa], J. Hejbal[134], A. Held[173], S. Hellesund[17], C.M. Helling[167], S. Hellman[48a,48b], R.C.W. Henderson[93], L. Henkelmann[33], A.M. Henriques Correia[37], H. Herde[100], Y. Hernández Jiménez[148], L.M. Herrmann[25], T. Herrmann[51], G. Herten[55], R. Hertenberger[111], L. Hervas[37], M.E. Hesping[102], N.P. Hessey[159a], M. Hidaoui[36b], N. Hidic[136], E. Hill[158], S.J. Hillier[21], J.R. Hinds[109], F. Hinterkeuser[25], M. Hirose[127], S. Hirose[160], D. Hirschbuehl[174], T.G. Hitchings[103], B. Hiti[95], J. Hobbs[148], R. Hobincu[28e], N. Hod[172], M.C. Hodgkinson[142], B.H. Hodkinson[129], A. Hoecker[37], D.D. Hofer[108], J. Hofer[49], T. Holm[25], M. Holzbock[112], L.B.A.H. Hommels[33], B.P. Honan[103], J.J. Hong[69], J. Hong[63c], T.M. Hong[132], B.H. Hooberman[165], W.H. Hopkins[6], M.C. Hoppesch[165], Y. Horii[113], S. Hou[151], A.S. Howard[95], J. Howarth[60], J. Hoya[6], M. Hrabovsky[125], A. Hrynevich[49], T. Hryn'ova[4], P.J. Hsu[66], S.-C. Hsu[141], T. Hsu[67], M. Hu[18a], Q. Hu[63a], S. Huang[65b], X. Huang[14,114c], Y. Huang[142], Y. Huang[102], Y. Huang[14], Z. Huang[103], Z. Hubacek[135], M. Huebner[25], F. Huegging[25], T.B. Huffman[129], C.A. Hugli[49], M. Huhtinen[37], S.K. Huiberts[17], R. Hulsken[106], N. Huseynov[12], J. Huston[109], J. Huth[62], R. Hyneman[146], G. Iacobucci[57], G. Iakovidis[30], L. Iconomidou-Fayard[67], J.P. Iddon[37], P. Iengo[73a,73b], R. Iguchi[156], Y. Iiyama[156], T. Iizawa[129], Y. Ikegami[85], N. Ilic[158], H. Imam[36a], M. Ince Lezki[57], T. Ingebretsen Carlson[48a,48b], J.M. Inglis[96], G. Introzzi[74a,74b], M. Iodice[78a], V. Ippolito[76a,76b], R.K. Irwin[94], M. Ishino[156], W. Islam[173], C. Issever[19,49], S. Istin[22a,ag], H. Ito[171], R. Iuppa[79a,79b], A. Ivina[172], J.M. Izen[46], V. Izzo[73a], P. Jacka[134], P. Jackson[1], C.S. Jagfeld[111], G. Jain[159a], P. Jain[49], K. Jakobs[55], T. Jakoubek[172], J. Jamieson[60], W. Jang[156], M. Javurkova[105], P. Jawahar[103], L. Jeanty[126], J. Jejelava[152a,y], P. Jenni[55,f], C.E. Jessiman[35], C. Jia[63b], J. Jia[148], X. Jia[62], X. Jia[14,114c], Z. Jia[114a], C. Jiang[53], S. Jiggins[49], J. Jimenez Pena[13], S. Jin[114a], A. Jinaru[28b], O. Jinnouchi[157], P. Johansson[142], K.A. Johns[7], J.W. Johnson[139], D.M. Jones[149], E. Jones[49], P. Jones[33], R.W.L. Jones[93], T.J. Jones[94], H.L. Joos[56,37], R. Joshi[122], J. Jovicevic[16], X. Ju[18a], J.J. Junggeburth[105], T. Junkermann[64a], A. Juste Rozas[13,r], M.K. Juzek[88], S. Kabana[140e], A. Kaczmarska[88], M. Kado[112], H. Kagan[122], M. Kagan[146], A. Kahn[131], C. Kahra[102], T. Kaji[156], E. Kajomovitz[153], N. Kakati[172], I. Kalaitzidou[55], C.W. Kalderon[30], N.J. Kang[139], D. Kar[34g], K. Karava[129], M.J. Kareem[159b], E. Karentzos[55], O. Karkout[117], S.N. Karpov[39], Z.M. Karpova[39], V. Kartvelishvili[93], A.N. Karyukhin[38], E. Kasimi[155], J. Katzy[49], S. Kaur[35], K. Kawade[143], M.P. Kawale[123], C. Kawamoto[89], T. Kawamoto[63a], E.F. Kay[37], F.I. Kaya[161],

S. Kazakos[109], V.F. Kazanin[38], Y. Ke[148], J.M. Keaveney[34a], R. Keeler[168], G.V. Kehris[62], J.S. Keller[35], A.S. Kelly[98], J.J. Kempster[149], P.D. Kennedy[102], O. Kepka[134], B.P. Kerridge[137], S. Kersten[174], B.P. Kerševan[95], L. Keszeghova[29a], S. Ketabchi Haghighat[158], R.A. Khan[132], A. Khanov[124], A.G. Kharlamov[38], T. Kharlamova[38], E.E. Khoda[141], M. Kholodenko[38], T.J. Khoo[19], G. Khoriauli[169], J. Khubua[152b], Y.A.R. Khwaira[130], B. Kibirige[34g], D. Kim[6], D.W. Kim[48a,48b], Y.K. Kim[40], N. Kimura[98], M.K. Kingston[56], A. Kirchhoff[56], C. Kirfel[25], F. Kirfel[25], J. Kirk[137], A.E. Kiryunin[112], C. Kitsaki[10], O. Kivernyk[25], M. Klassen[161], C. Klein[35], L. Klein[169], M.H. Klein[45], S.B. Klein[57], U. Klein[94], P. Klimek[37], A. Klimentov[30], T. Klioutchnikova[37], P. Kluit[117], S. Kluth[112], E. Kneringer[80], T.M. Knight[158], A. Knue[50], R. Kobayashi[89], D. Kobylianskii[172], S.F. Koch[129], M. Kocian[146], P. Kodyš[136], D.M. Koeck[126], P.T. Koenig[25], T. Koffas[35], O. Kolay[51], I. Koletsou[4], T. Komarek[88], K. Köneke[55], A.X.Y. Kong[1], T. Kono[121], N. Konstantinidis[98], P. Kontaxakis[57], B. Konya[100], R. Kopeliansky[42], S. Koperny[87a], K. Korcyl[88], K. Kordas[155,d], A. Korn[98], S. Korn[56], I. Korolkov[13], N. Korotkova[38], B. Kortman[117], O. Kortner[112], S. Kortner[112], W.H. Kostecka[118], V.V. Kostyukhin[144], A. Kotsokechagia[138], A. Kotwal[52], A. Koulouris[37], A. Kourkoumeli-Charalampidi[74a,74b], C. Kourkoumelis[9], E. Kourlitis[112,aa], O. Kovanda[126], R. Kowalewski[168], W. Kozanecki[138], A.S. Kozhin[38], V.A. Kramarenko[38], G. Kramberger[95], P. Kramer[102], M.W. Krasny[130], A. Krasznahorkay[37], A.C. Kraus[118], J.W. Kraus[174], J.A. Kremer[49], T. Kresse[51], L. Kretschmann[174], J. Kretzschmar[94], K. Kreul[19], P. Krieger[158], S. Krishnamurthy[105], M. Krivos[136], K. Krizka[21], K. Kroeninger[50], H. Kroha[112], J. Kroll[134], J. Kroll[131], K.S. Krowpman[109], U. Kruchonak[39], H. Krüger[25], N. Krumnack[82], M.C. Kruse[52], O. Kuchinskaia[38], S. Kuday[3a], S. Kuehn[37], R. Kuesters[55], T. Kuhl[49], V. Kukhtin[39], Y. Kulchitsky[38,a], S. Kuleshov[140d,140b], M. Kumar[34g], N. Kumari[49], P. Kumari[159b], A. Kupco[134], T. Kupfer[50], A. Kupich[38], O. Kuprash[55], H. Kurashige[86], L.L. Kurchaninov[159a], O. Kurdysh[67], Y.A. Kurochkin[38], A. Kurova[38], M. Kuze[157], A.K. Kvam[105], J. Kvita[125], T. Kwan[106], N.G. Kyriacou[108], L.A.O. Laatu[104], C. Lacasta[166], F. Lacava[76a,76b], H. Lacker[19], D. Lacour[130], N.N. Lad[98], E. Ladygin[39], A. Lafarge[41], B. Laforge[130], T. Lagouri[175], F.Z. Lahbabi[36a], S. Lai[56], J.E. Lambert[168], S. Lammers[69], W. Lampl[7], C. Lampoudis[155,d], G. Lamprinoudis[102], A.N. Lancaster[118], E. Lançon[30], U. Landgraf[55], M.P.J. Landon[96], V.S. Lang[55], O.K.B. Langrekken[128], A.J. Lankford[162], F. Lanni[37], K. Lantzsch[25], A. Lanza[74a], J.F. Laporte[138], T. Lari[72a], F. Lasagni Manghi[24b], M. Lassnig[37], V. Latonova[134], A. Laurier[153], S.D. Lawlor[142], Z. Lawrence[103], R. Lazaridou[170], M. Lazzaroni[72a,72b], B. Le[103], E.M. Le Boulicaut[52], L.T. Le Pottier[18a], B. Leban[24b,24a], A. Lebedev[82], M. LeBlanc[103], F. Ledroit-Guillon[61], S.C. Lee[151], S. Lee[48a,48b], T.F. Lee[94], L.L. Leeuw[34c], H.P. Lefebvre[97], M. Lefebvre[168], C. Leggett[18a], G. Lehmann Miotto[37], M. Leigh[57], W.A. Leight[105], W. Leinonen[116], A. Leisos[155,q], M.A.L. Leite[84c], C.E. Leitgeb[19], R. Leitner[136], K.J.C. Leney[45], T. Lenz[25], S. Leone[75a], C. Leonidopoulos[53], A. Leopold[147], R. Les[109], C.G. Lester[33], M. Levchenko[38], J. Levêque[4], L.J. Levinson[172], G. Levrini[24b,24a], M.P. Lewicki[88], C. Lewis[141], D.J. Lewis[4], A. Li[5], B. Li[63b], C. Li[63a], C-Q. Li[112], H. Li[63a], H. Li[63b], H. Li[114a], H. Li[15], H. Li[63b], J. Li[63c], K. Li[141], L. Li[63c], M. Li[14,114c], S. Li[14,114c], S. Li[63d,63c], T. Li[5], X. Li[106], Z. Li[129], Z. Li[156], Z. Li[14,114c], S. Liang[14,114c], Z. Liang[14], M. Liberatore[138], B. Liberti[77a], K. Lie[65c], J. Lieber Marin[84e], H. Lien[69], H. Lin[108], K. Lin[109], R.E. Lindley[7], J.H. Lindon[2], J. Ling[62], E. Lipeles[131], A. Lipniacka[17], A. Lister[167], J.D. Little[69], B. Liu[14], B.X. Liu[114b], D. Liu[63d,63c], E.H.L. Liu[21], J.B. Liu[63a], J.K.K. Liu[33], K. Liu[63d], K. Liu[63d,63c], M. Liu[63a], M.Y. Liu[63a], P. Liu[14], Q. Liu[63d,141,63c], X. Liu[63a], X. Liu[63b], Y. Liu[114b,114c], Y.L. Liu[63b], Y.W. Liu[63a],

J. Llorente Merino[145], S.L. Lloyd[96], E.M. Lobodzinska[49], P. Loch[7], T. Lohse[19], K. Lohwasser[142], E. Loiacono[49], M. Lokajicek[134,*], J.D. Lomas[21], J.D. Long[165], I. Longarini[162], R. Longo[165], I. Lopez Paz[68], A. Lopez Solis[49], N. Lorenzo Martinez[4], A.M. Lory[111], M. Losada[119a], G. Löschcke Centeno[149], O. Loseva[38], X. Lou[48a,48b], X. Lou[14,114c], A. Lounis[67], P.A. Love[93], G. Lu[14,114c], M. Lu[67], S. Lu[131], Y.J. Lu[66], H.J. Lubatti[141], C. Luci[76a,76b], F.L. Lucio Alves[114a], F. Luehring[69], I. Luise[148], O. Lukianchuk[67], O. Lundberg[147], B. Lund-Jensen[147,*], N.A. Luongo[6], M.S. Lutz[37], A.B. Lux[26], D. Lynn[30], R. Lysak[134], E. Lytken[100], V. Lyubushkin[39], T. Lyubushkina[39], M.M. Lyukova[148], M.Firdaus M. Soberi[53], H. Ma[30], K. Ma[63a], L.L. Ma[63b], W. Ma[63a], Y. Ma[124], J.C. MacDonald[102], P.C. Machado De Abreu Farias[84e], R. Madar[41], T. Madula[98], J. Maeda[86], T. Maeno[30], H. Maguire[142], V. Maiboroda[138], A. Maio[133a,133b,133d], K. Maj[87a], O. Majersky[49], S. Majewski[126], N. Makovec[67], V. Maksimovic[16], B. Malaescu[130], Pa. Malecki[88], V.P. Maleev[38], F. Malek[61,m], M. Mali[95], D. Malito[97], U. Mallik[81], S. Maltezos[10], S. Malyukov[39], J. Mamuzic[13], G. Mancini[54], M.N. Mancini[27], G. Manco[74a,74b], J.P. Mandalia[96], S.S. Mandarry[149], I. Mandić[95], L. Manhaes de Andrade Filho[84a], I.M. Maniatis[172], J. Manjarres Ramos[91], D.C. Mankad[172], A. Mann[111], S. Manzoni[37], L. Mao[63c], X. Mapekula[34c], A. Marantis[155,q], G. Marchiori[5], M. Marcisovsky[134], C. Marcon[72a], M. Marinescu[21], S. Marium[49], M. Marjanovic[123], A. Markhoos[55], M. Markovitch[67], E.J. Marshall[93], Z. Marshall[18a], S. Marti-Garcia[166], J. Martin[98], T.A. Martin[137], V.J. Martin[53], B. Martin dit Latour[17], L. Martinelli[76a,76b], M. Martinez[13,r], P. Martinez Agullo[166], V.I. Martinez Outschoorn[105], P. Martinez Suarez[13], S. Martin-Haugh[137], G. Martinovicova[136], V.S. Martoiu[28b], A.C. Martyniuk[98], A. Marzin[37], D. Mascione[79a,79b], L. Masetti[102], T. Mashimo[156], J. Masik[103], A.L. Maslennikov[38], P. Massarotti[73a,73b], P. Mastrandrea[75a,75b], A. Mastroberardino[44b,44a], T. Masubuchi[156], T. Mathisen[164], J. Matousek[136], N. Matsuzawa[156], J. Maurer[28b], A.J. Maury[67], B. Maček[95], D.A. Maximov[38], A.E. May[103], R. Mazini[151], I. Maznas[118], M. Mazza[109], S.M. Mazza[139], E. Mazzeo[72a,72b], C. Mc Ginn[30], J.P. Mc Gowan[168], S.P. Mc Kee[108], C.C. McCracken[167], E.F. McDonald[107], A.E. McDougall[117], J.A. Mcfayden[149], R.P. McGovern[131], R.P. Mckenzie[34g], T.C. Mclachlan[49], D.J. Mclaughlin[98], S.J. McMahon[137], C.M. Mcpartland[94], R.A. McPherson[168,v], S. Mehlhase[111], A. Mehta[94], D. Melini[166], B.R. Mellado Garcia[34g], A.H. Melo[56], F. Meloni[49], A.M. Mendes Jacques Da Costa[103], H.Y. Meng[158], L. Meng[93], S. Menke[112], M. Mentink[37], E. Meoni[44b,44a], G. Mercado[118], S. Merianos[155], C. Merlassino[70a,70c], L. Merola[73a,73b], C. Meroni[72a,72b], J. Metcalfe[6], A.S. Mete[6], E. Meuser[102], C. Meyer[69], J-P. Meyer[138], R.P. Middleton[137], L. Mijović[53], G. Mikenberg[172], M. Mikestikova[134], M. Mikuž[95], H. Mildner[102], A. Milic[37], D.W. Miller[40], E.H. Miller[146], L.S. Miller[35], A. Milov[172], D.A. Milstead[48a,48b], T. Min[114a], A.A. Minaenko[38], I.A. Minashvili[152b], L. Mince[60], A.I. Mincer[120], B. Mindur[87a], M. Mineev[39], Y. Mino[89], L.M. Mir[13], M. Miralles Lopez[60], M. Mironova[18a], A. Mishima[156], M.C. Missio[116], A. Mitra[170], V.A. Mitsou[166], Y. Mitsumori[113], O. Miu[158], P.S. Miyagawa[96], T. Mkrtchyan[64a], M. Mlinarevic[98], T. Mlinarevic[98], M. Mlynarikova[37], S. Mobius[20], P. Mogg[111], M.H. Mohamed Farook[115], A.F. Mohammed[14,114c], S. Mohapatra[42], G. Mokgatitswane[34g], L. Moleri[172], B. Mondal[144], S. Mondal[135], K. Mönig[49], E. Monnier[104], L. Monsonis Romero[166], J. Montejo Berlingen[13], M. Montella[122], F. Montereali[78a,78b], F. Monticelli[92], S. Monzani[70a,70c], N. Morange[67], A.L. Moreira De Carvalho[49], M. Moreno Llácer[166], C. Moreno Martinez[57], P. Morettini[58b], S. Morgenstern[37], M. Morii[62], M. Morinaga[156], F. Morodei[76a,76b], L. Morvaj[37], P. Moschovakos[37], B. Moser[37], M. Mosidze[152b], T. Moskalets[45], P. Moskvitina[116],

J. Moss [32,j], P. Moszkowicz [87a], A. Moussa [36d], E.J.W. Moyse [105], O. Mtintsilana [34g], S. Muanza [104], J. Mueller [132], D. Muenstermann [93], R. Müller [37], G.A. Mullier [164], A.J. Mullin[33], J.J. Mullin[131], D.P. Mungo [158], D. Munoz Perez [166], F.J. Munoz Sanchez [103], M. Murin [103], W.J. Murray [170,137], M. Muškinja [95], C. Mwewa [30], A.G. Myagkov [38,a], A.J. Myers [8], G. Myers [108], M. Myska [135], B.P. Nachman [18a], O. Nackenhorst [50], K. Nagai [129], K. Nagano [85], J.L. Nagle [30,ae], E. Nagy [104], A.M. Nairz [37], Y. Nakahama [85], K. Nakamura [85], K. Nakkalil [5], H. Nanjo [127], E.A. Narayanan [115], I. Naryshkin [38], L. Nasella [72a,72b], M. Naseri [35], S. Nasri [119b], C. Nass [25], G. Navarro [23a], J. Navarro-Gonzalez [166], R. Nayak [154], A. Nayaz [19], P.Y. Nechaeva [38], S. Nechaeva [24b,24a], F. Nechansky [49], L. Nedic [129], T.J. Neep [21], A. Negri [74a,74b], M. Negrini [24b], C. Nellist [117], C. Nelson [106], K. Nelson [108], S. Nemecek [134], M. Nessi [37,g], M.S. Neubauer [165], F. Neuhaus [102], J. Neundorf [49], P.R. Newman [21], C.W. Ng [132], Y.W.Y. Ng [49], B. Ngair [119a], H.D.N. Nguyen [110], R.B. Nickerson [129], R. Nicolaidou [138], J. Nielsen [139], M. Niemeyer [56], J. Niermann [56], N. Nikiforou [37], V. Nikolaenko [38,a], I. Nikolic-Audit [130], K. Nikolopoulos [21], P. Nilsson [30], I. Ninca [49], G. Ninio [154], A. Nisati [76a], N. Nishu [2], R. Nisius [112], J-E. Nitschke [51], E.K. Nkadimeng [34g], T. Nobe [156], T. Nommensen [150], M.B. Norfolk [142], B.J. Norman [35], M. Noury [36a], J. Novak [95], T. Novak [95], L. Novotny [135], R. Novotny [115], L. Nozka [125], K. Ntekas [162], N.M.J. Nunes De Moura Junior [84b], J. Ocariz [130], A. Ochi [86], I. Ochoa [133a], S. Oerdek [49,s], J.T. Offermann [40], A. Ogrodnik [136], A. Oh [103], C.C. Ohm [147], H. Oide [85], R. Oishi [156], M.L. Ojeda [49], Y. Okumura [156], L.F. Oleiro Seabra [133a], I. Oleksiyuk [57], S.A. Olivares Pino [140d], G. Oliveira Correa [13], D. Oliveira Damazio [30], D. Oliveira Goncalves [84a], J.L. Oliver [162], Ö.O. Öncel [55], A.P. O'Neill [20], A. Onofre [133a,133e], P.U.E. Onyisi [11], M.J. Oreglia [40], G.E. Orellana [92], D. Orestano [78a,78b], N. Orlando [13], R.S. Orr [158], L.M. Osojnak [131], R. Ospanov [63a], G. Otero y Garzon [31], H. Otono [90], P.S. Ott [64a], G.J. Ottino [18a], M. Ouchrif [36d], F. Ould-Saada [128], T. Ovsiannikova [141], M. Owen [60], R.E. Owen [137], V.E. Ozcan [22a], F. Ozturk [88], N. Ozturk [8], S. Ozturk [83], H.A. Pacey [129], A. Pacheco Pages [13], C. Padilla Aranda [13], G. Padovano [76a,76b], S. Pagan Griso [18a], G. Palacino [69], A. Palazzo [71a,71b], J. Pampel [25], J. Pan [175], T. Pan [65a], D.K. Panchal [11], C.E. Pandini [117], J.G. Panduro Vazquez [137], H.D. Pandya [1], H. Pang [15], P. Pani [49], G. Panizzo [70a,70c], L. Panwar [130], L. Paolozzi [57], S. Parajuli [165], A. Paramonov [6], C. Paraskevopoulos [54], D. Paredes Hernandez [65b], A. Pareti [74a,74b], K.R. Park [42], T.H. Park [158], M.A. Parker [33], F. Parodi [58b,58a], E.W. Parrish [118], V.A. Parrish [53], J.A. Parsons [42], U. Parzefall [55], B. Pascual Dias [110], L. Pascual Dominguez [101], E. Pasqualucci [76a], S. Passaggio [58b], F. Pastore [97], P. Patel [88], U.M. Patel [52], J.R. Pater [103], T. Pauly [37], C.I. Pazos [161], J. Pearkes [146], M. Pedersen [128], R. Pedro [133a], S.V. Peleganchuk [38], O. Penc [37], E.A. Pender [53], G.D. Penn [175], K.E. Penski [111], M. Penzin [38], B.S. Peralva [84d], A.P. Pereira Peixoto [141], L. Pereira Sanchez [146], D.V. Perepelitsa [30,ae], G. Perera [105], E. Perez Codina [159a], M. Perganti [10], H. Pernegger [37], S. Perrella [76a,76b], O. Perrin [41], K. Peters [49], R.F.Y. Peters [103], B.A. Petersen [37], T.C. Petersen [43], E. Petit [104], V. Petousis [135], C. Petridou [155,d], T. Petru [136], A. Petrukhin [144], M. Pettee [18a], A. Petukhov [38], K. Petukhova [37], R. Pezoa [140f], L. Pezzotti [37], G. Pezzullo [175], T.M. Pham [173], T. Pham [107], P.W. Phillips [137], G. Piacquadio [148], E. Pianori [18a], F. Piazza [126], R. Piegaia [31], D. Pietreanu [28b], A.D. Pilkington [103], M. Pinamonti [70a,70c], J.L. Pinfold [2], B.C. Pinheiro Pereira [133a], A.E. Pinto Pinoargote [138,138], L. Pintucci [70a,70c], K.M. Piper [149], A. Pirttikoski [57], D.A. Pizzi [35], L. Pizzimento [65b], A. Pizzini [117], M.-A. Pleier [30], V. Pleskot [136], E. Plotnikova[39], G. Poddar [96], R. Poettgen [100], L. Poggioli [130], I. Pokharel [56], S. Polacek [136], G. Polesello [74a], A. Poley [145,159a], A. Polini [24b], C.S. Pollard [170], Z.B. Pollock [122], E. Pompa Pacchi [76a,76b], N.I. Pond [98], D. Ponomarenko [116], L. Pontecorvo [37], S. Popa [28a], G.A. Popeneciu [28d],

A. Poreba[37], D.M. Portillo Quintero[159a], S. Pospisil[135], M.A. Postill[142], P. Postolache[28c], K. Potamianos[170], P.A. Potepa[87a], I.N. Potrap[39], C.J. Potter[33], H. Potti[150], J. Poveda[166], M.E. Pozo Astigarraga[37], A. Prades Ibanez[166], J. Pretel[55], D. Price[103], M. Primavera[71a], M.A. Principe Martin[101], R. Privara[125], T. Procter[60], M.L. Proffitt[141], N. Proklova[131], K. Prokofiev[65c], G. Proto[112], J. Proudfoot[6], M. Przybycien[87a], W.W. Przygoda[87b], A. Psallidas[47], J.E. Puddefoot[142], D. Pudzha[55], D. Pyatiizbyantseva[38], J. Qian[108], D. Qichen[103], Y. Qin[13], T. Qiu[53], A. Quadt[56], M. Queitsch-Maitland[103], G. Quetant[57], R.P. Quinn[167], G. Rabanal Bolanos[62], D. Rafanoharana[55], F. Raffaeli[77a,77b], F. Ragusa[72a,72b], J.L. Rainbolt[40], J.A. Raine[57], S. Rajagopalan[30], E. Ramakoti[38], I.A. Ramirez-Berend[35], K. Ran[49,114c], N.P. Rapheeha[34g], H. Rasheed[28b], V. Raskina[130], D.F. Rassloff[64a], A. Rastogi[18a], S. Rave[102], S. Ravera[58b,58a], B. Ravina[56], I. Ravinovich[172], M. Raymond[37], A.L. Read[128], N.P. Readioff[142], D.M. Rebuzzi[74a,74b], G. Redlinger[30], A.S. Reed[112], K. Reeves[27], J.A. Reidelsturz[174], D. Reikher[154], A. Rej[50], C. Rembser[37], M. Renda[28b], F. Renner[49], A.G. Rennie[162], A.L. Rescia[49], S. Resconi[72a], M. Ressegotti[58b,58a], S. Rettie[37], J.G. Reyes Rivera[109], E. Reynolds[18a], O.L. Rezanova[38], P. Reznicek[136], H. Riani[36d], N. Ribaric[93], E. Ricci[79a,79b], R. Richter[112], S. Richter[48a,48b], E. Richter-Was[87b], M. Ridel[130], S. Ridouani[36d], P. Rieck[120], P. Riedler[37], E.M. Riefel[48a,48b], J.O. Rieger[117], M. Rijssenbeek[148], M. Rimoldi[37], L. Rinaldi[24b,24a], P. Rincke[56,164], T.T. Rinn[30], M.P. Rinnagel[111], G. Ripellino[164], I. Riu[13], J.C. Rivera Vergara[168], F. Rizatdinova[124], E. Rizvi[96], B.R. Roberts[18a], S.H. Robertson[106,v], D. Robinson[33], C.M. Robles Gajardo[140f], M. Robles Manzano[102], A. Robson[60], A. Rocchi[77a,77b], C. Roda[75a,75b], S. Rodriguez Bosca[37], Y. Rodriguez Garcia[23a], A. Rodriguez Rodriguez[55], A.M. Rodríguez Vera[118], S. Roe[37], J.T. Roemer[37], A.R. Roepe-Gier[139], O. Røhne[128], R.A. Rojas[105], C.P.A. Roland[130], J. Roloff[30], A. Romaniouk[38], E. Romano[74a,74b], M. Romano[24b], A.C. Romero Hernandez[165], N. Rompotis[94], L. Roos[130], S. Rosati[76a], B.J. Rosser[40], E. Rossi[129], E. Rossi[73a,73b], L.P. Rossi[62], L. Rossini[55], R. Rosten[122], M. Rotaru[28b], B. Rottler[55], C. Rougier[91], D. Rousseau[67], D. Rousso[49], A. Roy[165], S. Roy-Garand[158], A. Rozanov[104], Z.M.A. Rozario[60], Y. Rozen[153], A. Rubio Jimenez[166], A.J. Ruby[94], V.H. Ruelas Rivera[19], T.A. Ruggeri[1], A. Ruggiero[129], A. Ruiz-Martinez[166], A. Rummler[37], Z. Rurikova[55], N.A. Rusakovich[39], H.L. Russell[168], G. Russo[76a,76b], J.P. Rutherfoord[7], S. Rutherford Colmenares[33], M. Rybar[136], E.B. Rye[128], A. Ryzhov[45], J.A. Sabater Iglesias[57], P. Sabatini[166], H.F-W. Sadrozinski[139], F. Safai Tehrani[76a], B. Safarzadeh Samani[137], S. Saha[1], M. Sahinsoy[112], A. Saibel[166], M. Saimpert[138], M. Saito[156], T. Saito[156], A. Sala[72a,72b], D. Salamani[37], A. Salnikov[146], J. Salt[166], A. Salvador Salas[154], D. Salvatore[44b,44a], F. Salvatore[149], A. Salzburger[37], D. Sammel[55], E. Sampson[93], D. Sampsonidis[155,d], D. Sampsonidou[126], J. Sánchez[166], V. Sanchez Sebastian[166], H. Sandaker[128], C.O. Sander[49], J.A. Sandesara[105], M. Sandhoff[174], C. Sandoval[23b], L. Sanfilippo[64a], D.P.C. Sankey[137], T. Sano[89], A. Sansoni[54], L. Santi[37,76b], C. Santoni[41], H. Santos[133a,133b], A. Santra[172], E. Sanzani[24b,24a], K.A. Saoucha[163], J.G. Saraiva[133a,133d], J. Sardain[7], O. Sasaki[85], K. Sato[160], C. Sauer[64b], E. Sauvan[4], P. Savard[158,ac], R. Sawada[156], C. Sawyer[137], L. Sawyer[99], C. Sbarra[24b], A. Sbrizzi[24b,24a], T. Scanlon[98], J. Schaarschmidt[141], U. Schäfer[102], A.C. Schaffer[67,45], D. Schaile[111], R.D. Schamberger[148], C. Scharf[19], M.M. Schefer[20], V.A. Schegelsky[38], D. Scheirich[136], M. Schernau[162], C. Scheulen[56], C. Schiavi[58b,58a], M. Schioppa[44b,44a], B. Schlag[146,l], K.E. Schleicher[55], S. Schlenker[37], J. Schmeing[174], M.A. Schmidt[174], K. Schmieden[102], C. Schmitt[102], N. Schmitt[102], S. Schmitt[49], L. Schoeffel[138], A. Schoening[64b], P.G. Scholer[35], E. Schopf[129], M. Schott[25], J. Schovancova[37], S. Schramm[57], T. Schroer[57], H-C. Schultz-Coulon[64a], M. Schumacher[55],

B.A. Schumm[139], Ph. Schune[138], A.J. Schuy[141], H.R. Schwartz[139], A. Schwartzman[146], T.A. Schwarz[108], Ph. Schwemling[138], R. Schwienhorst[109], F.G. Sciacca[20], A. Sciandra[30], G. Sciolla[27], F. Scuri[75a], C.D. Sebastiani[94], K. Sedlaczek[118], S.C. Seidel[115], A. Seiden[139], B.D. Seidlitz[42], C. Seitz[49], J.M. Seixas[84b], G. Sekhniaidze[73a], L. Selem[61], N. Semprini-Cesari[24b,24a], D. Sengupta[57], V. Senthilkumar[166], L. Serin[67], M. Sessa[77a,77b], H. Severini[123], F. Sforza[58b,58a], A. Sfyrla[57], Q. Sha[14], E. Shabalina[56], A.H. Shah[33], R. Shaheen[147], J.D. Shahinian[131], D. Shaked Renous[172], L.Y. Shan[14], M. Shapiro[18a], A. Sharma[37], A.S. Sharma[167], P. Sharma[81], P.B. Shatalov[38], K. Shaw[149], S.M. Shaw[103], Q. Shen[63c], D.J. Sheppard[145], P. Sherwood[98], L. Shi[98], X. Shi[14], C.O. Shimmin[175], J.D. Shinner[97], I.P.J. Shipsey[129], S. Shirabe[90], M. Shiyakova[39,t], M.J. Shochet[40], J. Shojaii[107], D.R. Shope[128], B. Shrestha[123], S. Shrestha[122,af], M.J. Shroff[168], P. Sicho[134], A.M. Sickles[165], E. Sideras Haddad[34g], A.C. Sidley[117], A. Sidoti[24b], F. Siegert[51], Dj. Sijacki[16], F. Sili[92], J.M. Silva[53], I. Silva Ferreira[84b], M.V. Silva Oliveira[30], S.B. Silverstein[48a], S. Simion[67], R. Simoniello[37], E.L. Simpson[103], H. Simpson[149], L.R. Simpson[108], N.D. Simpson[100], S. Simsek[83], S. Sindhu[56], P. Sinervo[158], S. Singh[158], S. Sinha[49], S. Sinha[103], M. Sioli[24b,24a], I. Siral[37], E. Sitnikova[49], J. Sjölin[48a,48b], A. Skaf[56], E. Skorda[21], P. Skubic[123], M. Slawinska[88], V. Smakhtin[172], B.H. Smart[137], S.Yu. Smirnov[38], Y. Smirnov[38], L.N. Smirnova[38,a], O. Smirnova[100], A.C. Smith[42], D.R. Smith[162], E.A. Smith[40], H.A. Smith[129], J.L. Smith[103], R. Smith[146], M. Smizanska[93], K. Smolek[135], A.A. Snesarev[38], S.R. Snider[158], H.L. Snoek[117], S. Snyder[30], R. Sobie[168,v], A. Soffer[154], C.A. Solans Sanchez[37], E.Yu. Soldatov[38], U. Soldevila[166], A.A. Solodkov[38], S. Solomon[27], A. Soloshenko[39], K. Solovieva[55], O.V. Solovyanov[41], P. Sommer[37], A. Sonay[13], W.Y. Song[159b], A. Sopczak[135], A.L. Sopio[98], F. Sopkova[29b], J.D. Sorenson[115], I.R. Sotarriva Alvarez[157], V. Sothilingam[64a], O.J. Soto Sandoval[140c,140b], S. Sottocornola[69], R. Soualah[163], Z. Soumaimi[36e], D. South[49], N. Soybelman[172], S. Spagnolo[71a,71b], M. Spalla[112], D. Sperlich[55], G. Spigo[37], S. Spinali[93], B. Spisso[73a,73b], D.P. Spiteri[60], M. Spousta[136], E.J. Staats[35], R. Stamen[64a], A. Stampekis[21], M. Standke[25], E. Stanecka[88], W. Stanek-Maslouska[49], M.V. Stange[51], B. Stanislaus[18a], M.M. Stanitzki[49], B. Stapf[49], E.A. Starchenko[38], G.H. Stark[139], J. Stark[91], P. Staroba[134], P. Starovoitov[64a], S. Stärz[106], R. Staszewski[88], G. Stavropoulos[47], P. Steinberg[30], B. Stelzer[145,159a], H.J. Stelzer[132], O. Stelzer-Chilton[159a], H. Stenzel[59], T.J. Stevenson[149], G.A. Stewart[37], J.R. Stewart[124], M.C. Stockton[37], G. Stoicea[28b], M. Stolarski[133a], S. Stonjek[112], A. Straessner[51], J. Strandberg[147], S. Strandberg[48a,48b], M. Stratmann[174], M. Strauss[123], T. Strebler[104], P. Strizenec[29b], R. Ströhmer[169], D.M. Strom[126], R. Stroynowski[45], A. Strubig[48a,48b], S.A. Stucci[30], B. Stugu[17], J. Stupak[123], N.A. Styles[49], D. Su[146], S. Su[63a], W. Su[63d], X. Su[63a], D. Suchy[29a], K. Sugizaki[156], V.V. Sulin[38], M.J. Sullivan[94], D.M.S. Sultan[129], L. Sultanaliyeva[38], S. Sultansoy[3b], T. Sumida[89], S. Sun[173], O. Sunneborn Gudnadottir[164], N. Sur[104], M.R. Sutton[149], H. Suzuki[160], M. Svatos[134], M. Swiatlowski[159a], T. Swirski[169], I. Sykora[29a], M. Sykora[136], T. Sykora[136], D. Ta[102], K. Tackmann[49,s], A. Taffard[162], R. Tafirout[159a], J.S. Tafoya Vargas[67], Y. Takubo[85], M. Talby[104], A.A. Talyshev[38], K.C. Tam[65b], N.M. Tamir[154], A. Tanaka[156], J. Tanaka[156], R. Tanaka[67], M. Tanasini[148], Z. Tao[167], S. Tapia Araya[140f], S. Tapprogge[102], A. Tarek Abouelfadl Mohamed[109], S. Tarem[153], K. Tariq[14], G. Tarna[28b], G.F. Tartarelli[72a], M.J. Tartarin[91], P. Tas[136], M. Tasevsky[134], E. Tassi[44b,44a], A.C. Tate[165], G. Tateno[156], Y. Tayalati[36e,u], G.N. Taylor[107], W. Taylor[159b], R. Teixeira De Lima[146], P. Teixeira-Dias[97], J.J. Teoh[158], K. Terashi[156], J. Terron[101], S. Terzo[13], M. Testa[54], R.J. Teuscher[158,v], A. Thaler[80], O. Theiner[57], N. Themistokleous[53], T. Theveneaux-Pelzer[104], O. Thielmann[174], D.W. Thomas[97],

J.P. Thomas [21], E.A. Thompson [18a], P.D. Thompson [21], E. Thomson [131], R.E. Thornberry [45], C. Tian [63a], Y. Tian [56], V. Tikhomirov [38,a], Yu.A. Tikhonov [38], S. Timoshenko[38], D. Timoshyn [136], E.X.L. Ting [1], P. Tipton [175], A. Tishelman-Charny [30], S.H. Tlou [34g], K. Todome [157], S. Todorova-Nova [136], S. Todt[51], L. Toffolin [70a,70c], M. Togawa [85], J. Tojo [90], S. Tokár [29a], K. Tokushuku [85], O. Toldaiev [69], R. Tombs [33], M. Tomoto [85,113], L. Tompkins [146,l], K.W. Topolnicki [87b], E. Torrence [126], H. Torres [91], E. Torró Pastor [166], M. Toscani [31], C. Tosciri [40], M. Tost [11], D.R. Tovey [142], I.S. Trandafir [28b], T. Trefzger [169], A. Tricoli [30], I.M. Trigger [159a], S. Trincaz-Duvoid [130], D.A. Trischuk [27], B. Trocmé [61], A. Tropina[39], L. Truong [34c], M. Trzebinski [88], A. Trzupek [88], F. Tsai [148], M. Tsai [108], A. Tsiamis [155,d], P.V. Tsiareshka[38], S. Tsigaridas [159a], A. Tsirigotis [155,q], V. Tsiskaridze [158], E.G. Tskhadadze [152a], M. Tsopoulou [155], Y. Tsujikawa [89], I.I. Tsukerman [38], V. Tsulaia [18a], S. Tsuno [85], K. Tsuri [121], D. Tsybychev [148], Y. Tu [65b], A. Tudorache [28b], V. Tudorache [28b], A.N. Tuna [62], S. Turchikhin [58b,58a], I. Turk Cakir [3a], R. Turra [72a], T. Turtuvshin [39,w], P.M. Tuts [42], S. Tzamarias [155,d], E. Tzovara [102], F. Ukegawa [160], P.A. Ulloa Poblete [140c,140b], E.N. Umaka [30], G. Unal [37], A. Undrus [30], G. Unel [162], J. Urban [29b], P. Urrejola [140a], G. Usai [8], R. Ushioda [157], M. Usman [110], Z. Uysal [83], V. Vacek [135], B. Vachon [106], T. Vafeiadis [37], A. Vaitkus [98], C. Valderanis [111], E. Valdes Santurio [48a,48b], M. Valente [159a], S. Valentinetti [24b,24a], A. Valero [166], E. Valiente Moreno [166], A. Vallier [91], J.A. Valls Ferrer [166], D.R. Van Arneman [117], T.R. Van Daalen [141], A. Van Der Graaf [50], P. Van Gemmeren [6], M. Van Rijnbach [37], S. Van Stroud [98], I. Van Vulpen [117], P. Vana [136], M. Vanadia [77a,77b], W. Vandelli [37], E.R. Vandewall [124], D. Vannicola [154], L. Vannoli [54], R. Vari [76a], E.W. Varnes [7], C. Varni [18b], T. Varol [151], D. Varouchas [67], L. Varriale [166], K.E. Varvell [150], M.E. Vasile [28b], L. Vaslin[85], G.A. Vasquez [168], A. Vasyukov [39], L.M. Vaughan [124], R. Vavricka[102], T. Vazquez Schroeder [37], J. Veatch [32], V. Vecchio [103], M.J. Veen [105], I. Veliscek [30], L.M. Veloce [158], F. Veloso [133a,133c], S. Veneziano [76a], A. Ventura [71a,71b], S. Ventura Gonzalez [138], A. Verbytskyi [112], M. Verducci [75a,75b], C. Vergis [96], M. Verissimo De Araujo [84b], W. Verkerke [117], J.C. Vermeulen [117], C. Vernieri [146], M. Vessella [105], M.C. Vetterli [145,ac], A. Vgenopoulos [102], N. Viaux Maira [140f], T. Vickey [142], O.E. Vickey Boeriu [142], G.H.A. Viehhauser [129], L. Vigani [64b], M. Villa [24b,24a], M. Villaplana Perez [166], E.M. Villhauer[53], E. Vilucchi [54], M.G. Vincter [35], A. Visibile[117], C. Vittori [37], I. Vivarelli [24b,24a], E. Voevodina [112], F. Vogel [111], J.C. Voigt [51], P. Vokac [135], Yu. Volkotrub [87b], J. Von Ahnen [49], E. Von Toerne [25], B. Vormwald [37], V. Vorobel [136], K. Vorobev [38], M. Vos [166], K. Voss [144], M. Vozak [117], L. Vozdecky [123], N. Vranjes [16], M. Vranjes Milosavljevic [16], M. Vreeswijk [117], N.K. Vu [63d,63c], R. Vuillermet [37], O. Vujinovic [102], I. Vukotic [40], S. Wada [160], C. Wagner[105], J.M. Wagner [18a], W. Wagner [174], S. Wahdan [174], H. Wahlberg [92], M. Wakida [113], J. Walder [137], R. Walker [111], W. Walkowiak [144], A. Wall [131], E.J. Wallin [100], T. Wamorkar [6], A.Z. Wang [139], C. Wang [102], C. Wang [11], H. Wang [18a], J. Wang [65c], P. Wang [98], R. Wang [62], R. Wang [6], S.M. Wang [151], S. Wang [63b], S. Wang [14], T. Wang [63a], W.T. Wang [81], W. Wang [14], X. Wang [114a], X. Wang [165], X. Wang [63c], Y. Wang [63d], Y. Wang [114a], Y. Wang [63a], Z. Wang [108], Z. Wang [63d,52,63c], Z. Wang [108], A. Warburton [106], R.J. Ward [21], N. Warrack [60], S. Waterhouse [97], A.T. Watson [21], H. Watson [60], M.F. Watson [21], E. Watton [60,137], G. Watts [141], B.M. Waugh [98], J.M. Webb [55], C. Weber [30], H.A. Weber [19], M.S. Weber [20], S.M. Weber [64a], C. Wei [63a], Y. Wei [55], A.R. Weidberg [129], E.J. Weik [120], J. Weingarten [50], C. Weiser [55], C.J. Wells [49], T. Wenaus [30], B. Wendland [50], T. Wengler [37], N.S. Wenke[112], N. Wermes [25], M. Wessels [64a], A.M. Wharton [93], A.S. White [62], A. White [8], M.J. White [1], D. Whiteson [162], L. Wickremasinghe [127], W. Wiedenmann [173], M. Wielers [137], C. Wiglesworth [43], D.J. Wilbern[123], H.G. Wilkens [37], J.J.H. Wilkinson [33], D.M. Williams [42], H.H. Williams[131], S. Williams [33], S. Willocq [105],

B.J. Wilson[103], P.J. Windischhofer[40], F.I. Winkel[31], F. Winklmeier[126], B.T. Winter[55], J.K. Winter[103], M. Wittgen[146], M. Wobisch[99], T. Wojtkowski[61], Z. Wolffs[117], J. Wollrath[162], M.W. Wolter[88], H. Wolters[133a,133c], M.C. Wong[139], E.L. Woodward[42], S.D. Worm[49], B.K. Wosiek[88], K.W. Woźniak[88], S. Wozniewski[56], K. Wraight[60], C. Wu[21], M. Wu[114b], M. Wu[116], S.L. Wu[173], X. Wu[57], Y. Wu[63a], Z. Wu[4], J. Wuerzinger[112,aa], T.R. Wyatt[103], B.M. Wynne[53], S. Xella[43], L. Xia[114a], M. Xia[15], M. Xie[63a], S. Xin[14,114c], A. Xiong[126], J. Xiong[18a], D. Xu[14], H. Xu[63a], L. Xu[63a], R. Xu[131], T. Xu[108], Y. Xu[15], Z. Xu[53], Z. Xu[114a], B. Yabsley[150], S. Yacoob[34a], Y. Yamaguchi[157], E. Yamashita[156], H. Yamauchi[160], T. Yamazaki[18a], Y. Yamazaki[86], J. Yan[63c], S. Yan[60], Z. Yan[105], H.J. Yang[63c,63d], H.T. Yang[63a], S. Yang[63a], T. Yang[65c], X. Yang[37], X. Yang[14], Y. Yang[45], Y. Yang[63a], Z. Yang[63a], W-M. Yao[18a], H. Ye[114a], H. Ye[56], J. Ye[14], S. Ye[30], X. Ye[63a], Y. Yeh[98], I. Yeletskikh[39], B.K. Yeo[18b], M.R. Yexley[98], T.P. Yildirim[129], P. Yin[42], K. Yorita[171], S. Younas[28b], C.J.S. Young[37], C. Young[146], C. Yu[14,114c], Y. Yu[63a], J. Yuan[14,114c], M. Yuan[108], R. Yuan[63d,63c], L. Yue[98], M. Zaazoua[63a], B. Zabinski[88], E. Zaid[53], Z.K. Zak[88], T. Zakareishvili[166], S. Zambito[57], J.A. Zamora Saa[140d,140b], J. Zang[156], D. Zanzi[55], O. Zaplatilek[135], C. Zeitnitz[174], H. Zeng[14], J.C. Zeng[165], D.T. Zenger Jr[27], O. Zenin[38], T. Ženiš[29a], S. Zenz[96], S. Zerradi[36a], D. Zerwas[67], M. Zhai[14,114c], D.F. Zhang[142], J. Zhang[63b], J. Zhang[6], K. Zhang[14,114c], L. Zhang[63a], L. Zhang[114a], P. Zhang[14,114c], R. Zhang[173], S. Zhang[108], S. Zhang[91], T. Zhang[156], X. Zhang[63c], X. Zhang[63b], Y. Zhang[63c], Y. Zhang[98], Y. Zhang[114a], Z. Zhang[18a], Z. Zhang[63b], Z. Zhang[67], H. Zhao[141], T. Zhao[63b], Y. Zhao[139], Z. Zhao[63a], Z. Zhao[63a], A. Zhemchugov[39], J. Zheng[114a], K. Zheng[165], X. Zheng[63a], Z. Zheng[146], D. Zhong[165], B. Zhou[108], H. Zhou[7], N. Zhou[63c], Y. Zhou[15], Y. Zhou[114a], Y. Zhou[7], C.G. Zhu[63b], J. Zhu[108], X. Zhu[63d], Y. Zhu[63c], Y. Zhu[63a], X. Zhuang[14], K. Zhukov[38], N.I. Zimine[39], J. Zinsser[64b], M. Ziolkowski[144], L. Živković[16], A. Zoccoli[24b,24a], K. Zoch[62], T.G. Zorbas[142], O. Zormpa[47], W. Zou[42], L. Zwalinski[37].

[1]Department of Physics, University of Adelaide, Adelaide; Australia.
[2]Department of Physics, University of Alberta, Edmonton AB; Canada.
[3(a)]Department of Physics, Ankara University, Ankara;[(b)]Division of Physics, TOBB University of Economics and Technology, Ankara; Türkiye.
[4]LAPP, Université Savoie Mont Blanc, CNRS/IN2P3, Annecy; France.
[5]APC, Université Paris Cité, CNRS/IN2P3, Paris; France.
[6]High Energy Physics Division, Argonne National Laboratory, Argonne IL; United States of America.
[7]Department of Physics, University of Arizona, Tucson AZ; United States of America.
[8]Department of Physics, University of Texas at Arlington, Arlington TX; United States of America.
[9]Physics Department, National and Kapodistrian University of Athens, Athens; Greece.
[10]Physics Department, National Technical University of Athens, Zografou; Greece.
[11]Department of Physics, University of Texas at Austin, Austin TX; United States of America.
[12]Institute of Physics, Azerbaijan Academy of Sciences, Baku; Azerbaijan.
[13]Institut de Física d'Altes Energies (IFAE), Barcelona Institute of Science and Technology, Barcelona; Spain.
[14]Institute of High Energy Physics, Chinese Academy of Sciences, Beijing; China.
[15]Physics Department, Tsinghua University, Beijing; China.
[16]Institute of Physics, University of Belgrade, Belgrade; Serbia.
[17]Department for Physics and Technology, University of Bergen, Bergen; Norway.
[18(a)]Physics Division, Lawrence Berkeley National Laboratory, Berkeley CA;[(b)]University of California,

Berkeley CA; United States of America.
[19]Institut für Physik, Humboldt Universität zu Berlin, Berlin; Germany.
[20]Albert Einstein Center for Fundamental Physics and Laboratory for High Energy Physics, University of Bern, Bern; Switzerland.
[21]School of Physics and Astronomy, University of Birmingham, Birmingham; United Kingdom.
[22(a)]Department of Physics, Bogazici University, Istanbul;[(b)]Department of Physics Engineering, Gaziantep University, Gaziantep;[(c)]Department of Physics, Istanbul University, Istanbul; Türkiye.
[23(a)]Facultad de Ciencias y Centro de Investigaciónes, Universidad Antonio Nariño, Bogotá;[(b)]Departamento de Física, Universidad Nacional de Colombia, Bogotá; Colombia.
[24(a)]Dipartimento di Fisica e Astronomia A. Righi, Università di Bologna, Bologna;[(b)]INFN Sezione di Bologna; Italy.
[25]Physikalisches Institut, Universität Bonn, Bonn; Germany.
[26]Department of Physics, Boston University, Boston MA; United States of America.
[27]Department of Physics, Brandeis University, Waltham MA; United States of America.
[28(a)]Transilvania University of Brasov, Brasov;[(b)]Horia Hulubei National Institute of Physics and Nuclear Engineering, Bucharest;[(c)]Department of Physics, Alexandru Ioan Cuza University of Iasi, Iasi;[(d)]National Institute for Research and Development of Isotopic and Molecular Technologies, Physics Department, Cluj-Napoca;[(e)]National University of Science and Technology Politechnica, Bucharest;[(f)]West University in Timisoara, Timisoara;[(g)]Faculty of Physics, University of Bucharest, Bucharest; Romania.
[29(a)]Faculty of Mathematics, Physics and Informatics, Comenius University, Bratislava;[(b)]Department of Subnuclear Physics, Institute of Experimental Physics of the Slovak Academy of Sciences, Kosice; Slovak Republic.
[30]Physics Department, Brookhaven National Laboratory, Upton NY; United States of America.
[31]Universidad de Buenos Aires, Facultad de Ciencias Exactas y Naturales, Departamento de Física, y CONICET, Instituto de Física de Buenos Aires (IFIBA), Buenos Aires; Argentina.
[32]California State University, CA; United States of America.
[33]Cavendish Laboratory, University of Cambridge, Cambridge; United Kingdom.
[34(a)]Department of Physics, University of Cape Town, Cape Town;[(b)]iThemba Labs, Western Cape;[(c)]Department of Mechanical Engineering Science, University of Johannesburg, Johannesburg;[(d)]National Institute of Physics, University of the Philippines Diliman (Philippines);[(e)]University of South Africa, Department of Physics, Pretoria;[(f)]University of Zululand, KwaDlangezwa;[(g)]School of Physics, University of the Witwatersrand, Johannesburg; South Africa.
[35]Department of Physics, Carleton University, Ottawa ON; Canada.
[36(a)]Faculté des Sciences Ain Chock, Réseau Universitaire de Physique des Hautes Energies - Université Hassan II, Casablanca;[(b)]Faculté des Sciences, Université Ibn-Tofail, Kénitra;[(c)]Faculté des Sciences Semlalia, Université Cadi Ayyad, LPHEA-Marrakech;[(d)]LPMR, Faculté des Sciences, Université Mohamed Premier, Oujda;[(e)]Faculté des sciences, Université Mohammed V, Rabat;[(f)]Institute of Applied Physics, Mohammed VI Polytechnic University, Ben Guerir; Morocco.
[37]CERN, Geneva; Switzerland.
[38]Affiliated with an institute covered by a cooperation agreement with CERN.
[39]Affiliated with an international laboratory covered by a cooperation agreement with CERN.
[40]Enrico Fermi Institute, University of Chicago, Chicago IL; United States of America.
[41]LPC, Université Clermont Auvergne, CNRS/IN2P3, Clermont-Ferrand; France.
[42]Nevis Laboratory, Columbia University, Irvington NY; United States of America.
[43]Niels Bohr Institute, University of Copenhagen, Copenhagen; Denmark.
[44(a)]Dipartimento di Fisica, Università della Calabria, Rende;[(b)]INFN Gruppo Collegato di Cosenza, Laboratori Nazionali di Frascati; Italy.

[45]Physics Department, Southern Methodist University, Dallas TX; United States of America.
[46]Physics Department, University of Texas at Dallas, Richardson TX; United States of America.
[47]National Centre for Scientific Research "Demokritos", Agia Paraskevi; Greece.
[48(a)]Department of Physics, Stockholm University;[(b)]Oskar Klein Centre, Stockholm; Sweden.
[49]Deutsches Elektronen-Synchrotron DESY, Hamburg and Zeuthen; Germany.
[50]Fakultät Physik , Technische Universität Dortmund, Dortmund; Germany.
[51]Institut für Kern- und Teilchenphysik, Technische Universität Dresden, Dresden; Germany.
[52]Department of Physics, Duke University, Durham NC; United States of America.
[53]SUPA - School of Physics and Astronomy, University of Edinburgh, Edinburgh; United Kingdom.
[54]INFN e Laboratori Nazionali di Frascati, Frascati; Italy.
[55]Physikalisches Institut, Albert-Ludwigs-Universität Freiburg, Freiburg; Germany.
[56]II. Physikalisches Institut, Georg-August-Universität Göttingen, Göttingen; Germany.
[57]Département de Physique Nucléaire et Corpusculaire, Université de Genève, Genève; Switzerland.
[58(a)]Dipartimento di Fisica, Università di Genova, Genova;[(b)]INFN Sezione di Genova; Italy.
[59]II. Physikalisches Institut, Justus-Liebig-Universität Giessen, Giessen; Germany.
[60]SUPA - School of Physics and Astronomy, University of Glasgow, Glasgow; United Kingdom.
[61]LPSC, Université Grenoble Alpes, CNRS/IN2P3, Grenoble INP, Grenoble; France.
[62]Laboratory for Particle Physics and Cosmology, Harvard University, Cambridge MA; United States of America.
[63(a)]Department of Modern Physics and State Key Laboratory of Particle Detection and Electronics, University of Science and Technology of China, Hefei;[(b)]Institute of Frontier and Interdisciplinary Science and Key Laboratory of Particle Physics and Particle Irradiation (MOE), Shandong University, Qingdao;[(c)]School of Physics and Astronomy, Shanghai Jiao Tong University, Key Laboratory for Particle Astrophysics and Cosmology (MOE), SKLPPC, Shanghai;[(d)]Tsung-Dao Lee Institute, Shanghai;[(e)]School of Physics and Microelectronics, Zhengzhou University; China.
[64(a)]Kirchhoff-Institut für Physik, Ruprecht-Karls-Universität Heidelberg, Heidelberg;[(b)]Physikalisches Institut, Ruprecht-Karls-Universität Heidelberg, Heidelberg; Germany.
[65(a)]Department of Physics, Chinese University of Hong Kong, Shatin, N.T., Hong Kong;[(b)]Department of Physics, University of Hong Kong, Hong Kong;[(c)]Department of Physics and Institute for Advanced Study, Hong Kong University of Science and Technology, Clear Water Bay, Kowloon, Hong Kong; China.
[66]Department of Physics, National Tsing Hua University, Hsinchu; Taiwan.
[67]IJCLab, Université Paris-Saclay, CNRS/IN2P3, 91405, Orsay; France.
[68]Centro Nacional de Microelectrónica (IMB-CNM-CSIC), Barcelona; Spain.
[69]Department of Physics, Indiana University, Bloomington IN; United States of America.
[70(a)]INFN Gruppo Collegato di Udine, Sezione di Trieste, Udine;[(b)]ICTP, Trieste;[(c)]Dipartimento Politecnico di Ingegneria e Architettura, Università di Udine, Udine; Italy.
[71(a)]INFN Sezione di Lecce;[(b)]Dipartimento di Matematica e Fisica, Università del Salento, Lecce; Italy.
[72(a)]INFN Sezione di Milano;[(b)]Dipartimento di Fisica, Università di Milano, Milano; Italy.
[73(a)]INFN Sezione di Napoli;[(b)]Dipartimento di Fisica, Università di Napoli, Napoli; Italy.
[74(a)]INFN Sezione di Pavia;[(b)]Dipartimento di Fisica, Università di Pavia, Pavia; Italy.
[75(a)]INFN Sezione di Pisa;[(b)]Dipartimento di Fisica E. Fermi, Università di Pisa, Pisa; Italy.
[76(a)]INFN Sezione di Roma;[(b)]Dipartimento di Fisica, Sapienza Università di Roma, Roma; Italy.
[77(a)]INFN Sezione di Roma Tor Vergata;[(b)]Dipartimento di Fisica, Università di Roma Tor Vergata, Roma; Italy.
[78(a)]INFN Sezione di Roma Tre;[(b)]Dipartimento di Matematica e Fisica, Università Roma Tre, Roma; Italy.
[79(a)]INFN-TIFPA;[(b)]Università degli Studi di Trento, Trento; Italy.

[80]Universität Innsbruck, Department of Astro and Particle Physics, Innsbruck; Austria.
[81]University of Iowa, Iowa City IA; United States of America.
[82]Department of Physics and Astronomy, Iowa State University, Ames IA; United States of America.
[83]Istinye University, Sariyer, Istanbul; Türkiye.
[84(a)]Departamento de Engenharia Elétrica, Universidade Federal de Juiz de Fora (UFJF), Juiz de Fora;[(b)]Universidade Federal do Rio De Janeiro COPPE/EE/IF, Rio de Janeiro;[(c)]Instituto de Física, Universidade de São Paulo, São Paulo;[(d)]Rio de Janeiro State University, Rio de Janeiro;[(e)]Federal University of Bahia, Bahia; Brazil.
[85]KEK, High Energy Accelerator Research Organization, Tsukuba; Japan.
[86]Graduate School of Science, Kobe University, Kobe; Japan.
[87(a)]AGH University of Krakow, Faculty of Physics and Applied Computer Science, Krakow;[(b)]Marian Smoluchowski Institute of Physics, Jagiellonian University, Krakow; Poland.
[88]Institute of Nuclear Physics Polish Academy of Sciences, Krakow; Poland.
[89]Faculty of Science, Kyoto University, Kyoto; Japan.
[90]Research Center for Advanced Particle Physics and Department of Physics, Kyushu University, Fukuoka ; Japan.
[91]L2IT, Université de Toulouse, CNRS/IN2P3, UPS, Toulouse; France.
[92]Instituto de Física La Plata, Universidad Nacional de La Plata and CONICET, La Plata; Argentina.
[93]Physics Department, Lancaster University, Lancaster; United Kingdom.
[94]Oliver Lodge Laboratory, University of Liverpool, Liverpool; United Kingdom.
[95]Department of Experimental Particle Physics, Jožef Stefan Institute and Department of Physics, University of Ljubljana, Ljubljana; Slovenia.
[96]School of Physics and Astronomy, Queen Mary University of London, London; United Kingdom.
[97]Department of Physics, Royal Holloway University of London, Egham; United Kingdom.
[98]Department of Physics and Astronomy, University College London, London; United Kingdom.
[99]Louisiana Tech University, Ruston LA; United States of America.
[100]Fysiska institutionen, Lunds universitet, Lund; Sweden.
[101]Departamento de Física Teorica C-15 and CIAFF, Universidad Autónoma de Madrid, Madrid; Spain.
[102]Institut für Physik, Universität Mainz, Mainz; Germany.
[103]School of Physics and Astronomy, University of Manchester, Manchester; United Kingdom.
[104]CPPM, Aix-Marseille Université, CNRS/IN2P3, Marseille; France.
[105]Department of Physics, University of Massachusetts, Amherst MA; United States of America.
[106]Department of Physics, McGill University, Montreal QC; Canada.
[107]School of Physics, University of Melbourne, Victoria; Australia.
[108]Department of Physics, University of Michigan, Ann Arbor MI; United States of America.
[109]Department of Physics and Astronomy, Michigan State University, East Lansing MI; United States of America.
[110]Group of Particle Physics, University of Montreal, Montreal QC; Canada.
[111]Fakultät für Physik, Ludwig-Maximilians-Universität München, München; Germany.
[112]Max-Planck-Institut für Physik (Werner-Heisenberg-Institut), München; Germany.
[113]Graduate School of Science and Kobayashi-Maskawa Institute, Nagoya University, Nagoya; Japan.
[114(a)]Department of Physics, Nanjing University, Nanjing;[(b)]School of Science, Shenzhen Campus of Sun Yat-sen University;[(c)]University of Chinese Academy of Science (UCAS), Beijing; China.
[115]Department of Physics and Astronomy, University of New Mexico, Albuquerque NM; United States of America.
[116]Institute for Mathematics, Astrophysics and Particle Physics, Radboud University/Nikhef, Nijmegen; Netherlands.

[117]Nikhef National Institute for Subatomic Physics and University of Amsterdam, Amsterdam; Netherlands.
[118]Department of Physics, Northern Illinois University, DeKalb IL; United States of America.
[119(a)]New York University Abu Dhabi, Abu Dhabi;[(b)]United Arab Emirates University, Al Ain; United Arab Emirates.
[120]Department of Physics, New York University, New York NY; United States of America.
[121]Ochanomizu University, Otsuka, Bunkyo-ku, Tokyo; Japan.
[122]Ohio State University, Columbus OH; United States of America.
[123]Homer L. Dodge Department of Physics and Astronomy, University of Oklahoma, Norman OK; United States of America.
[124]Department of Physics, Oklahoma State University, Stillwater OK; United States of America.
[125]Palacký University, Joint Laboratory of Optics, Olomouc; Czech Republic.
[126]Institute for Fundamental Science, University of Oregon, Eugene, OR; United States of America.
[127]Graduate School of Science, Osaka University, Osaka; Japan.
[128]Department of Physics, University of Oslo, Oslo; Norway.
[129]Department of Physics, Oxford University, Oxford; United Kingdom.
[130]LPNHE, Sorbonne Université, Université Paris Cité, CNRS/IN2P3, Paris; France.
[131]Department of Physics, University of Pennsylvania, Philadelphia PA; United States of America.
[132]Department of Physics and Astronomy, University of Pittsburgh, Pittsburgh PA; United States of America.
[133(a)]Laboratório de Instrumentação e Física Experimental de Partículas - LIP, Lisboa;[(b)]Departamento de Física, Faculdade de Ciências, Universidade de Lisboa, Lisboa;[(c)]Departamento de Física, Universidade de Coimbra, Coimbra;[(d)]Centro de Física Nuclear da Universidade de Lisboa, Lisboa;[(e)]Departamento de Física, Universidade do Minho, Braga;[(f)]Departamento de Física Teórica y del Cosmos, Universidad de Granada, Granada (Spain);[(g)]Departamento de Física, Instituto Superior Técnico, Universidade de Lisboa, Lisboa; Portugal.
[134]Institute of Physics of the Czech Academy of Sciences, Prague; Czech Republic.
[135]Czech Technical University in Prague, Prague; Czech Republic.
[136]Charles University, Faculty of Mathematics and Physics, Prague; Czech Republic.
[137]Particle Physics Department, Rutherford Appleton Laboratory, Didcot; United Kingdom.
[138]IRFU, CEA, Université Paris-Saclay, Gif-sur-Yvette; France.
[139]Santa Cruz Institute for Particle Physics, University of California Santa Cruz, Santa Cruz CA; United States of America.
[140(a)]Departamento de Física, Pontificia Universidad Católica de Chile, Santiago;[(b)]Millennium Institute for Subatomic physics at high energy frontier (SAPHIR), Santiago;[(c)]Instituto de Investigación Multidisciplinario en Ciencia y Tecnología, y Departamento de Física, Universidad de La Serena;[(d)]Universidad Andres Bello, Department of Physics, Santiago;[(e)]Instituto de Alta Investigación, Universidad de Tarapacá, Arica;[(f)]Departamento de Física, Universidad Técnica Federico Santa María, Valparaíso; Chile.
[141]Department of Physics, University of Washington, Seattle WA; United States of America.
[142]Department of Physics and Astronomy, University of Sheffield, Sheffield; United Kingdom.
[143]Department of Physics, Shinshu University, Nagano; Japan.
[144]Department Physik, Universität Siegen, Siegen; Germany.
[145]Department of Physics, Simon Fraser University, Burnaby BC; Canada.
[146]SLAC National Accelerator Laboratory, Stanford CA; United States of America.
[147]Department of Physics, Royal Institute of Technology, Stockholm; Sweden.
[148]Departments of Physics and Astronomy, Stony Brook University, Stony Brook NY; United States of

America.
[149]Department of Physics and Astronomy, University of Sussex, Brighton; United Kingdom.
[150]School of Physics, University of Sydney, Sydney; Australia.
[151]Institute of Physics, Academia Sinica, Taipei; Taiwan.
[152(a)]E. Andronikashvili Institute of Physics, Iv. Javakhishvili Tbilisi State University, Tbilisi;[(b)]High Energy Physics Institute, Tbilisi State University, Tbilisi;[(c)]University of Georgia, Tbilisi; Georgia.
[153]Department of Physics, Technion, Israel Institute of Technology, Haifa; Israel.
[154]Raymond and Beverly Sackler School of Physics and Astronomy, Tel Aviv University, Tel Aviv; Israel.
[155]Department of Physics, Aristotle University of Thessaloniki, Thessaloniki; Greece.
[156]International Center for Elementary Particle Physics and Department of Physics, University of Tokyo, Tokyo; Japan.
[157]Department of Physics, Tokyo Institute of Technology, Tokyo; Japan.
[158]Department of Physics, University of Toronto, Toronto ON; Canada.
[159(a)]TRIUMF, Vancouver BC;[(b)]Department of Physics and Astronomy, York University, Toronto ON; Canada.
[160]Division of Physics and Tomonaga Center for the History of the Universe, Faculty of Pure and Applied Sciences, University of Tsukuba, Tsukuba; Japan.
[161]Department of Physics and Astronomy, Tufts University, Medford MA; United States of America.
[162]Department of Physics and Astronomy, University of California Irvine, Irvine CA; United States of America.
[163]University of Sharjah, Sharjah; United Arab Emirates.
[164]Department of Physics and Astronomy, University of Uppsala, Uppsala; Sweden.
[165]Department of Physics, University of Illinois, Urbana IL; United States of America.
[166]Instituto de Física Corpuscular (IFIC), Centro Mixto Universidad de Valencia - CSIC, Valencia; Spain.
[167]Department of Physics, University of British Columbia, Vancouver BC; Canada.
[168]Department of Physics and Astronomy, University of Victoria, Victoria BC; Canada.
[169]Fakultät für Physik und Astronomie, Julius-Maximilians-Universität Würzburg, Würzburg; Germany.
[170]Department of Physics, University of Warwick, Coventry; United Kingdom.
[171]Waseda University, Tokyo; Japan.
[172]Department of Particle Physics and Astrophysics, Weizmann Institute of Science, Rehovot; Israel.
[173]Department of Physics, University of Wisconsin, Madison WI; United States of America.
[174]Fakultät für Mathematik und Naturwissenschaften, Fachgruppe Physik, Bergische Universität Wuppertal, Wuppertal; Germany.
[175]Department of Physics, Yale University, New Haven CT; United States of America.
[a] Also Affiliated with an institute covered by a cooperation agreement with CERN.
[b] Also at An-Najah National University, Nablus; Palestine.
[c] Also at Borough of Manhattan Community College, City University of New York, New York NY; United States of America.
[d] Also at Center for Interdisciplinary Research and Innovation (CIRI-AUTH), Thessaloniki; Greece.
[e] Also at Centro Studi e Ricerche Enrico Fermi; Italy.
[f] Also at CERN, Geneva; Switzerland.
[g] Also at Département de Physique Nucléaire et Corpusculaire, Université de Genève, Genève; Switzerland.
[h] Also at Departament de Fisica de la Universitat Autonoma de Barcelona, Barcelona; Spain.
[i] Also at Department of Financial and Management Engineering, University of the Aegean, Chios; Greece.
[j] Also at Department of Physics, California State University, Sacramento; United States of America.
[k] Also at Department of Physics, King's College London, London; United Kingdom.

[l] Also at Department of Physics, Stanford University, Stanford CA; United States of America.
[m] Also at Department of Physics, Stellenbosch University; South Africa.
[n] Also at Department of Physics, University of Fribourg, Fribourg; Switzerland.
[o] Also at Department of Physics, University of Thessaly; Greece.
[p] Also at Department of Physics, Westmont College, Santa Barbara; United States of America.
[q] Also at Hellenic Open University, Patras; Greece.
[r] Also at Institucio Catalana de Recerca i Estudis Avancats, ICREA, Barcelona; Spain.
[s] Also at Institut für Experimentalphysik, Universität Hamburg, Hamburg; Germany.
[t] Also at Institute for Nuclear Research and Nuclear Energy (INRNE) of the Bulgarian Academy of Sciences, Sofia; Bulgaria.
[u] Also at Institute of Applied Physics, Mohammed VI Polytechnic University, Ben Guerir; Morocco.
[v] Also at Institute of Particle Physics (IPP); Canada.
[w] Also at Institute of Physics and Technology, Mongolian Academy of Sciences, Ulaanbaatar; Mongolia.
[x] Also at Institute of Physics, Azerbaijan Academy of Sciences, Baku; Azerbaijan.
[y] Also at Institute of Theoretical Physics, Ilia State University, Tbilisi; Georgia.
[z] Also at National Institute of Physics, University of the Philippines Diliman (Philippines); Philippines.
[aa] Also at Technical University of Munich, Munich; Germany.
[ab] Also at The Collaborative Innovation Center of Quantum Matter (CICQM), Beijing; China.
[ac] Also at TRIUMF, Vancouver BC; Canada.
[ad] Also at Università di Napoli Parthenope, Napoli; Italy.
[ae] Also at University of Colorado Boulder, Department of Physics, Colorado; United States of America.
[af] Also at Washington College, Chestertown, MD; United States of America.
[ag] Also at Yeditepe University, Physics Department, Istanbul; Türkiye.
[*] Deceased